

CASE FILE
COPY

FABRICATION OF ALUMINUM-CARBON COMPOSITES

by R. C. Novak

FINAL REPORT

Prepared for

NASA - Lewis Research Center
Contract NAS3-15704

United Aircraft
Research Laboratories



EAST HARTFORD, CONNECTICUT 06108

1. Report No. NASA CR-121266		2. Government Accession No.		3. Recipient's Catalog No.	
4. Title and Subtitle FABRICATION OF ALUMINUM-CARBON COMPOSITES				5. Report Date August 1973	
				6. Performing Organization Code	
7. Author(s) R. C. Novak				8. Performing Organization Report No. M911326-13	
9. Performing Organization Name and Address United Aircraft Research Laboratories East Hartford, Connecticut				10. Work Unit No.	
				11. Contract or Grant No. NAS3-15704	
12. Sponsoring Agency Name and Address National Aeronautics and Space Administration Washington, D.C. 20546				13. Type of Report and Period Covered Contractor Report	
				14. Sponsoring Agency Code	
15. Supplementary Notes Project Manager, David L. McDanel, NASA Lewis Research Center, Cleveland, Ohio					
16. Abstract A program of screening, optimization, and evaluation of unidirectional carbon-aluminum composites was conducted. During the screening phase both large diameter monofilament and small diameter multifilament reinforcements were utilized to determine optimum precursor tape making and consolidation techniques. Difficulty was encountered in impregnating and consolidating the multifiber reinforcements. Large diameter monofilament reinforcement was found easier to fabricate into composites and was selected to carry into the optimization phase in which the hot pressing parameters were refined and the size of the fabricated panels was scaled up. After process optimization the mechanical properties of the carbon-aluminum composites were characterized in tension, stress-rupture and creep, mechanical fatigue, thermal fatigue, thermal aging, thermal expansion, and impact.					
17. Key Words (Suggested by Author(s)) Composites Carbon-aluminum Fabrication Mechanical properties			18. Distribution Statement Unclassified - unlimited		
19. Security Classif. (of this report) Unclassified		20. Security Classif. (of this page) Unclassified		21. No. of Pages 95	
				22. Price* \$3.00	

ABSTRACT

A program of screening, optimization, and evaluation of unidirectional carbon-aluminum composites was conducted. During the screening phase both large diameter monofilament and small diameter multifilament reinforcements were utilized to determine optimum precursor tape making and consolidation techniques. Difficulty was encountered in impregnating and consolidating the multifiber reinforcements. Large diameter monofilament reinforcement was found easier to fabricate into composites and was selected to carry into the optimization phase in which the hot pressing parameters were refined and the size of the fabricated panels was scaled up. After process optimization the mechanical properties of the carbon-aluminum composites were characterized in tension, stress-rupture and creep, mechanical fatigue, thermal fatigue, thermal aging, thermal expansion, and impact.

Report M911326-13

Fabrication of Aluminum-Carbon Composites

TABLE OF CONTENTS

SUMMARY	
I. INTRODUCTION	1
II. MATERIALS	3
III. TASK I - PRELIMINARY SCREENING OF FIBER-MATRIX COMBINATIONS AND FABRICATION METHODS	7
3.1 Experimental Procedure	7
3.2 Results and Discussion	8
3.2.1 Multifilament Composites	8
3.2.1.1 Thornel 75	8
3.2.1.2 Type HM	11
3.2.1.3 Thornel 50	16
3.2.2 Monofilament Composites	16
3.2.2.1 Filament Strength Characterization	18
3.2.2.2 Styrene Bonded Precursor Tape Composites	18
3.2.2.3 Slurry Precursor Tape Composites	24
3.2.2.4 Plasma Spray Precursor Tape Composites	28
IV. TASK II - COMPOSITE OPTIMIZATION AND SCALE-UP	34
4.1 Experimental Procedure	34
4.2 Results and Discussion	34
4.2.1 Filament Strength Characterization	34
4.2.2 Composite Optimization	34
4.2.3 Composite Scale-Up	39
V. TASK III - FABRICATION AND CHARACTERIZATION OF COMPOSITES	43
5.1 Filament Strength Characterization	43
5.2 Tension Testing	43

TABLE OF CONTENTS (Cont'd)

5.3	Stress-Rupture and Creep	59
5.3.1	Experimental Procedure	59
5.3.2	Results and Discussion	59
5.4	Mechanical Fatigue	62
5.4.1	Experimental Procedure	62
5.4.2	Results and Discussion	66
5.5	Thermal Fatigue	66
5.5.1	Experimental Procedure	66
5.5.2	Results and Discussion	69
5.6	Thermal Aging	80
5.6.1	Experimental Procedure	80
5.6.2	Results and Discussion	80
5.7	Thermal Expansion	84
5.8	Impact	84
5.8.1	Experimental Procedure	84
5.8.2	Results and Discussion	84
VI.	CONCLUSIONS	94
VII.	REFERENCES	95

LIST OF TABLES

<u>No.</u>		<u>Page</u>
I	T-75 Multifilament Graphite/Aluminum Composites - Slurry Precursor Process	9
II	HM Multifilament Graphite/Aluminum Composites - Slurry Precursor Process	13
III	Task I - Tensile Strength of NASA-Hough Carbon Base Monofilament	19
IV	Task I - Hough Monofilament/2024 Aluminum Composites - Styrene Bonding Precursor Process	20
V	Task I - Hough Monofilament/2024 Aluminum Composites - Slurry Precursor Process	25
VI	Task I - Hough Monofilament/2024 Aluminum Composites - Plasma Spray Precursor Process	29
VII	Task II - Tensile Strength of NASA-Hough Carbon Base Monofilament	35
VIII	Task II - NASA-Hough Monofilament/2024 Aluminum Composites - Plasma Spray Precursor Process	36
IX	Task II - NASA-Hough Monofilament/2024 Aluminum Composites - Composite Scale-Up	42
X	Task III - Tensile Strength of Carbon Base Monofilaments	44
XI	Task III - Longitudinal Tensile Properties - Room Temperature	46
XII	Task III - Longitudinal Tensile Properties - Elevated Temperature	55
XIII	Task III - Transverse Tensile Properties - Room Temperature	57
XIV	Task III - Transverse Tensile Properties - Elevated Temperature	58
XV	Creep Test Data - NASA-Hough Monofilament/2024 Aluminum	64
XVI	Izod Impact - NASA-Hough/2024	86

LIST OF ILLUSTRATIONS

<u>Figure No.</u>		<u>Page</u>
1	NASA-Hough Carbon Base Monofilament	4
2	NASA-Hough Carbon Base Monofilament	5
3	UARL Carbon base monofilament	6
4	Thornel 75 - Pure Aluminum Slurry Impregnated Tape	10
5	Type HM - Pure Aluminum Slurry Impregnated Tape	12
6	Thornel 50/526 Aluminum Aerospace Liquid Infiltration	17
7	Hough Monofilament - 2024 Aluminum Styrene Bonded Precursor Tape	22
8	NASA-Hough Monofilament/2024 Aluminum Tensile Fracture Surface	23
9	Hough Monofilament - 2024 Aluminum Slurry Precursor Tape	26
10	NASA-Hough Monofilament/2024 Aluminum Tensile Fracture Surface	27
11	NASA-Hough Monofilament/2024 Aluminum Tensile Fracture Surface	31
12	Hough Monofilament - 2024 Aluminum Plasma Spray Precursor Tape	32
13	Transverse Tensile Fracture Surface NASA-Hough Monofilament/2024	40
14	Longitudinal Tensile Fracture Surface NASA-Hough Monofilament/2024	48
15	Filament Volume Fraction Variation Study NASA-Hough/2024	49
16	UARL Monofilament/2024	51
17	UARL Monofilament Composite No. 1963	52

LIST OF ILLUSTRATIONS (Cont'd)

<u>Figure No.</u>		<u>Page</u>
18	Longitudinal Tensile Fracture Surface UARL Mono-filament/2024	53
19	Longitudinal Tension Fracture Surface	56
20	Stress-Rupture NASA-Hough Carbon/2024 Aluminum	60
21	Stress-Rupture NASA-Hough Carbon/2024 Aluminum	61
22	NASA-Hough/2024 Stress-Rupture	63
23	Creep NASA-Hough Carbon/2024 Aluminum	65
24	Bending Fatigue NASA-Hough Carbon/2024 Aluminum	67
25	Bending Fatigue NASA-Hough Carbon/2024 Aluminum	68
26	Thermal Fatigue NASA-Hough/2024 Composite	70
27	Thermal Fatigue NASA-Hough/2024 Transverse Reinforcement	71
28	Thermal Fatigue	73
29	Thermal Fatigue Specimens 50 v/o NASA-Hough/2024	74
30	UARL/2024 Untested Composite No. 1951	75
31	Thermal Fatigue UARL/2024	77
32	Thermal Fatigue	78
33	UARL/2024 Composite 1964 Used for Thermal Fatigue	79
34	Thermal Aging Longitudinal Tension	81
35	Thermal Aging	82
36	Thermal Aging Transverse Tension	83
37	Thermal Expansion NASA-Hough Carbon/-2024 Aluminum	85

LIST OF ILLUSTRATIONS (Cont'd)

<u>Figure No.</u>		<u>Page</u>
38	NASA-Hough/2024 Izod Impact Specimen	87
39	Izod Impact Specimen NASA-Hough/2024 Composite 1944	88
40	Izod Impact NASA-Hough Carbon/2024 Aluminum	90
41	Impact Energy vs $V_f d_f \sigma_f^2 / 24 \tau_{my}$	91
42	Izod Impact Microstructure of Composite 1943	92

SUMMARY

The objectives of this work were to develop, then to optimize fabrication techniques for unidirectional carbon-aluminum composites, and to characterize the thermo-mechanical behavior of the material. Both large diameter carbon-base monofilaments (NASA-Hough and UARL) and small diameter carbon multifilaments (Thornel 75 and 50, Hercules HM) were investigated as reinforcement. Three techniques were evaluated for making monofilament precursor tape: plasma spray, slurry coating, and styrene bonding. Plasma spraying was found to produce the most uniform and reproducible material. The best conditions for diffusion bonding the precursor tapes having 2024 as the matrix were 450°C, 69 MN/m² (10 ksi), for 30 minutes in an argon atmosphere.

Slurry infiltration followed by diffusion bonding was investigated as a fabrication technique for multifilament composites. It was found that composite strength was limited by fiber breakage or poorly consolidated matrix and work on the multifilaments was terminated with the exception of the Thornel 50 which was prepared by a liquid infiltration technique.

Scale-up of the fabrication process to produce larger panels reinforced with monofilament was readily accomplished using precursor tape techniques and hot pressing conditions developed during the initial screening study.

In general, the mechanical property characterization showed that the tensile properties of the monofilament could be translated into the composite. The transverse properties were poor due to a poor filament-matrix bond. The elevated temperature potential of the NASA-Hough monofilament was demonstrated through good retention of room temperature tensile properties at temperatures as high as 427°C, and resistance to thermal aging, thermal fatigue and stress-rupture. The UARL monofilament composites were somewhat more affected by elevated temperatures, probably as a result of the higher boron content of the filament. Mechanical fatigue tests (fully reversed bending) revealed that some form of internal damage, which occurred prior to total fracture, resulted in reductions in composite stiffness. Impact testing of NASA-Hough composites resulted in better energy absorption per unit area than measured in state-of-the-art BORSIC[®]-aluminum. However, further improvements in the material behavior are required and this calls for stronger, larger filament and/or a better interfacial bond strength.

Thornel 50 multifilament composites exhibited lower strength than expected, but did show resistance to thermal aging and thermal cycling.

I. INTRODUCTION

The field of fiber reinforced composites is a continuously expanding one in which new combinations of fiber and matrix are sought in order to improve strength, stiffness, temperature capability, etc. Carbon reinforced aluminum is a particularly interesting composite material because the carbon filaments offer excellent specific strength and stiffness over a large temperature range while the aluminum matrix has an upper temperature capability in excess of state-of-the-art resin composites, and exhibits elastic-plastic behavior which is beneficial from a fracture standpoint.

Until recently carbon reinforcement was available only as the multifilament yarn or tow widely used in resin matrix composites. The theoretical properties of aluminum matrix composites reinforced with carbon yarn can be shown to be superior to those of state of metal matrix composites such as boron-aluminum and the cost of multifilament has become relatively low. However, due to carbon filament size, wettability, reactivity, and infiltration considerations, serious problems exist which have prevented those theoretical properties from being realized.

In order to reduce the fabrication problems inherent with small-diameter multifiber yarns and tows, NASA-Lewis awarded several contracts to develop large-diameter carbon monofilaments, and within the past two years two such carbon-base monofilaments have become available. Both monofilaments, NASA-Hough and United Aircraft Research Laboratories (UARL), consist of a carbon-boron alloy vapor deposited on a carbon substrate. Monofilament diameter is approximately 0.0081 cm (.0032 in.).

The objective of this program was to develop fabrication techniques for unidirectional carbon-aluminum and to measure certain mechanical properties of the composites utilizing both multifilament and monofilament as the reinforcement. The program was divided into five tasks as outlined below:

- Task I - Preliminary Screening of Fiber-Matrix Combinations and Fabrication Methods
- Task II - Composite Size Scale-Up and Optimization
- Task III - Fabrication and Characterization of Composites
- Task IV - Fabrication of Panels for Delivery to NASA
- Task V - Reports

During Task I, methods for making precursor tapes of carbon-aluminum were to be evaluated as well as hot pressing parameters for consolidation of the tapes into 2.54 cm x 7.62 cm (1 in. x 3 in.) composites. The term "precursor tape" refers to the initial combining of reinforcing fiber with unconsolidated aluminum matrix, much as fibers and resins are combined into uncured "prepregs" which are later processed into cured composites. Multifilament tapes were to be made by a slurry infiltration technique while monofilament tapes were to be made by slurry coating, styrene bonding, and plasma spraying. The primary criterion for judging the fabrication variables was to be the tensile strength of the composite.

Task II was to involve an optimization of the best precursor tape and consolidation techniques, then a scale-up of the process to produce large composites approximately 30 cm x 30 cm x .050 cm (12 in. x 12 in. x .020 in.).

During Task III large panels were to be fabricated, then tested to provide a broad understanding of the mechanical behavior of unidirectional carbon-aluminum composites. These tests were to include: tension, stress-rupture and creep, mechanical fatigue, thermal fatigue, thermal aging, thermal expansion, and impact.

The following sections of this report describe the work conducted during each of the three technical tasks.

II. MATERIALS

The multifilaments evaluated in the program were Type HM, Thornel 75, and Thornel 50. The Type HM and Thornel 75 were purchased from commercial sources in untreated (no surface treatment) form. The Thornel 50 was supplied by NASA-Lewis in the form of aluminum-infiltrated rods having eight graphite yarn bundles per rod. The infiltration of the graphite yarn was done by Aerospace Corp.

No property measurements were made on the multifilament graphite. Nominal properties of these fibers as supplied by the manufacturers are:

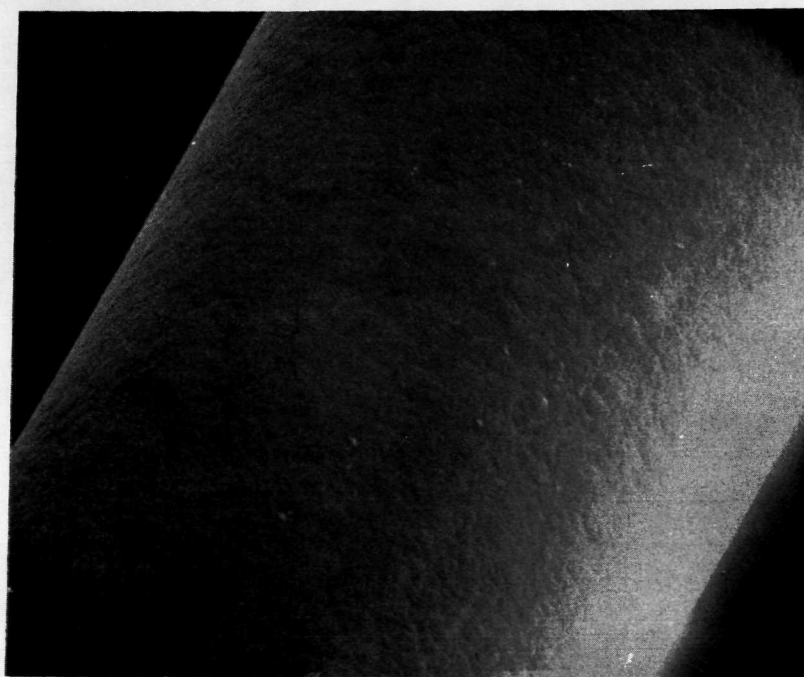
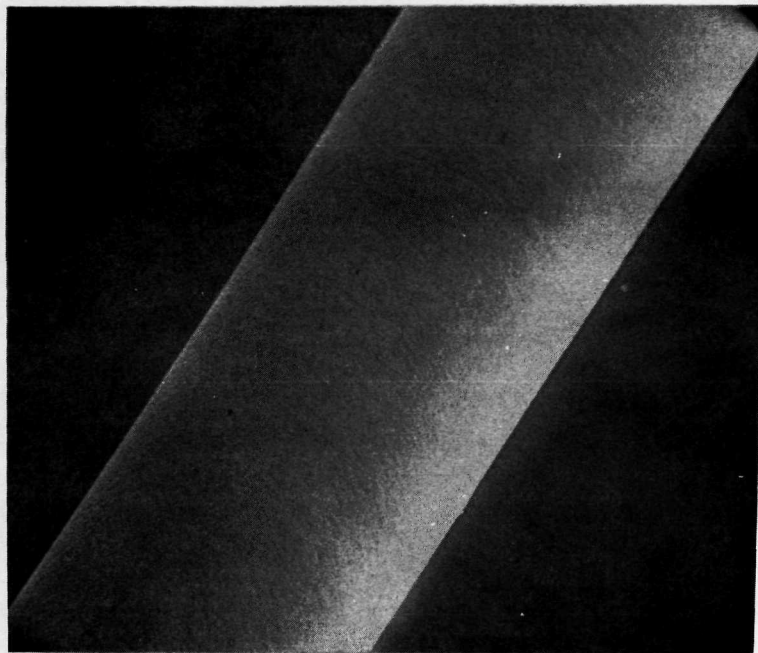
<u>Fiber</u>	<u>Tensile Modulus</u>		<u>Tensile Strength</u>		<u>Density</u>
	<u>GN/m²</u>	<u>(10⁶ psi)</u>	<u>GN/m²</u>	<u>(10³ psi)</u>	
HM	365-407	53-59	2.07	300	1.89
T-75	545	79	2.38	345	1.82
T-50	393	57	1.97	285	1.67

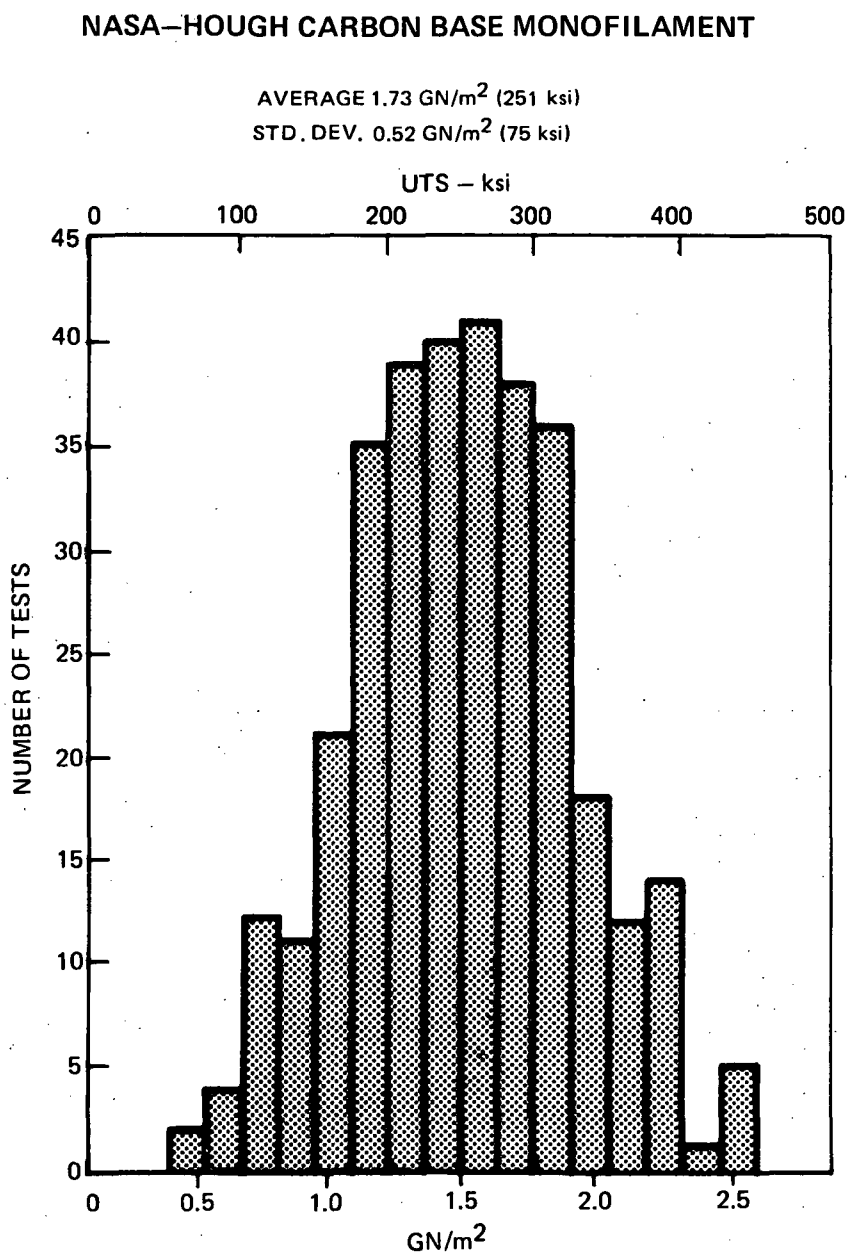
Two types of carbon-base monofilament were investigated as reinforcement: NASA-Hough and UARL. Both filaments are made by chemical vapor deposition of carbon and boron on a small diameter carbon substrate. The processes for making the filaments differ somewhat in that the NASA-Hough is produced in a multiple stage reactor using a gas consisting of hydrocarbon, borane, and hydrogen in an argon carrier (Ref. 1) while the UARL process involves a single stage reactor with a gas consisting of hydrocarbon, boron trichloride, and hydrogen (Ref. 2). The composition of the NASA-Hough filament is approximately 73 wt % C, 27 wt % B, while the UARL is 33 wt % C, 66 wt % B. Figure 1 presents a scanning electron micrograph (SEM) of the NASA-Hough monofilament, showing that the surface of the filament is much smoother than the "corncob" structure of boron filament.

During the course of the program a large number of tensile tests were conducted on both types of monofilaments. The results of these tests, all carried out at a 2.54 cm (1 in.) gage length, are presented in histogram form in Figs. 2 and 3. Further comment regarding the average values and the scatter in strength will be made in subsequent sections of this report.

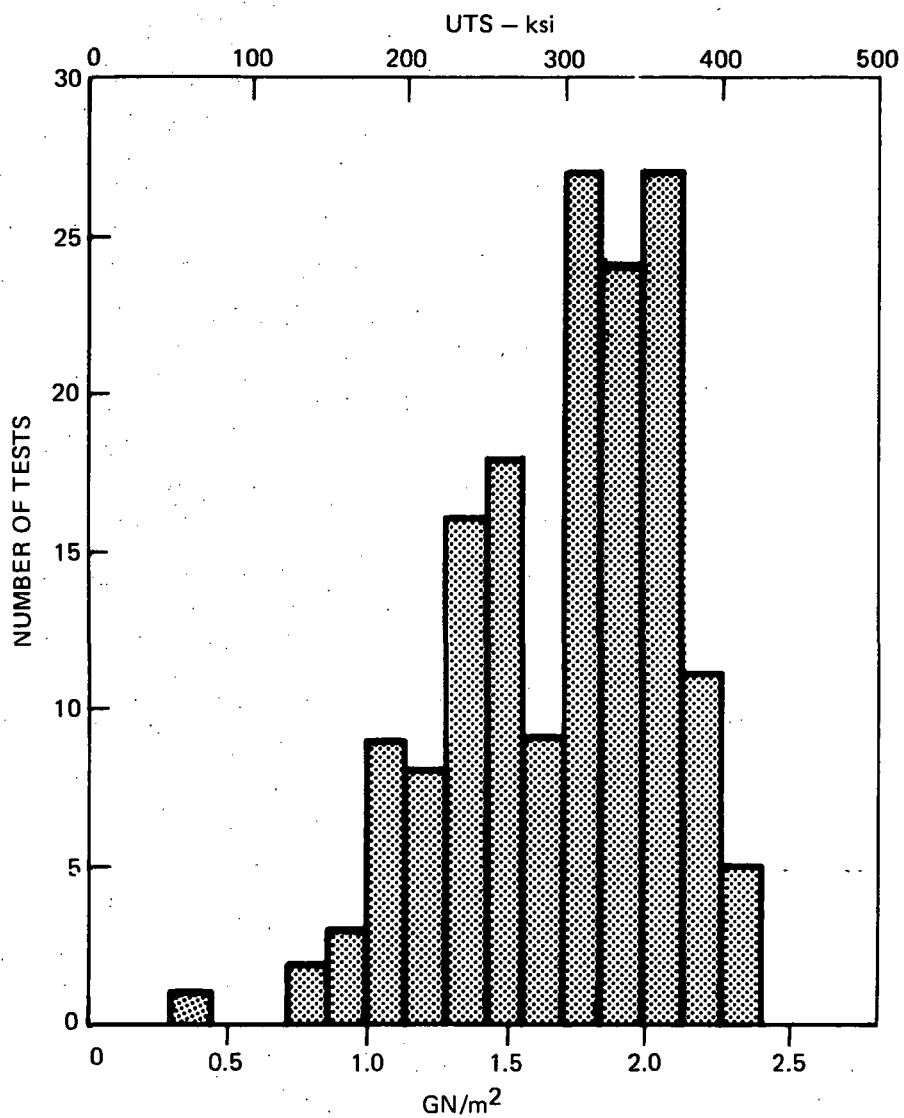
Aluminum matrices utilized in the program included 2024 powder and foil with monofilament composites and submicron 40xd pure aluminum powder and 1145 foil as well as -400 mesh Al-7.7% Si alloy powder (528) and Al-Si alloy foil (713) with multifilament composites.

NASA-HOUGH CARBON BASE MONOFILAMENT





UARL CARBON BASE MONOFILAMENT

AVERAGE 2.18 GN/m^2 (315 ksi)STD. DEV. 0.47 GN/m^2 (68.3 ksi)

III. TASK I - PRELIMINARY SCREENING OF FIBER-MATRIX COMBINATIONS AND FABRICATION METHODS

3.1 Experimental Procedure

Precursor tape was prepared with multifilament carbon by infiltrating the fiber bundle with a dilute slurry of aluminum powder, the technique being similar to that employed in the wet winding of resin matrix composite tapes. Fiber was continuously unwound from the roll, passed through a dilute slurry of aluminum powder/binder/solvent, and wound on a take-up drum which was wrapped with aluminum foil. The general formulation for the slurry was:

60g aluminum powder
5g polystyrene
5g camphene
190 ml toluene

The polystyrene served as a binder to hold the fiber bundles together and to adhere them to the aluminum foil. Camphene was included to act as a wetting agent. The fiber was wound at a spacing such that the bundles were just touching.

Another multifilament precursor produced by Aerospace Corp. was also evaluated. The precursor fabrication process is proprietary to Aerospace but involves a chemical cleaning of the fiber to allow it to be wetted by liquid aluminum (Ref. 3). The surface treated graphite is then immersed in liquid aluminum, generally an Al-Si alloy, and infiltrated. The entire process is carried out under inert conditions to preserve the surface treatment.

Three techniques were evaluated for producing monofilament precursor tapes: styrene bonding, slurry, and plasma spraying. In the styrene bonding process the monofilament was wound onto a rotating drum covered with one mil thick 2024 foil, then coated with a solution of polystyrene in toluene in order to bond the fibers to the foil and permit easy handling of the tape. The slurry process consisted of winding filament on the foil covered drum then brushing on a slurry of aluminum powder to fill the interstices between the filaments. The slurry contained 60g 2024 powder (-400 mesh), 4g polystyrene, and 196 ml toluene. The brushing was repeated until the desired amount of powder was deposited. In the plasma spray process the filament was wound on the foil covered drum as before. The drum was then passed by a plasma spray torch under controlled rotation and traverse speeds to produce a uniform coating of plasma sprayed aluminum powder on the tape. The amount of aluminum deposited was controlled through the powder feed rate, drum speed, and number of passes.

Both monofilament and multifilament precursor tapes were consolidated into composites by hot pressing under an argon atmosphere. With the exception of the Aerospace material, all hot pressing was carried out in the solid state (diffusion bonding). The Aerospace material was consolidated at a temperature between the matrix alloy solidus and liquidus (melt bonding).

The primary means of evaluating the fabrication variables was a composite tensile test which was conducted on a straight sided specimen, 7.6 cm x .63 cm x .051 cm (3 in. x 1/4 in. x .020 in.). Aluminum doublers were adhesively bonded to both ends of the specimen leaving a 2.54 cm (1 in.) gage length. All tests were conducted at a crosshead speed of 0.0254 cm/min (0.01 in./min). Specimen elongation was measured using two strain gages, one being bonded to each side to eliminate bending effects.

3.2 Results and Discussion

3.2.1 Multifilament Composites

Several composites were fabricated from slurry infiltrated tapes reinforced with Hercules HM fiber and Thornel 75. Work under this program demonstrated that the most difficult problem in fabricating composites from slurry infiltrated tapes was to achieve consolidation during hot pressing yet avoid excessive fiber breakage. Since the fibers were not treated to be wettable by aluminum, hot pressing was done with the aluminum in the solid state. Consequently the possibility existed for the small carbon fibers to be broken while being pressed in the presence of the aluminum particles. The line of investigation to overcome this problem was to minimize the consolidation pressure and to maximize the temperature to permit good consolidation.

3.2.1.1 Thornel 75

Composites which were fabricated with Thornel 75 as the reinforcement are listed in Table I along with the tensile data. The nature of the Thornel 75 yarn (2 ply twisted bundle) made uniform infiltration of the aluminum powder very difficult. The relatively large size of the 528 Al-Si alloy (37 μ) made infiltration with that powder particularly difficult. Reasonable success was achieved with the submicron 40xd flake, however the composite cross section photomicrograph in Fig. 4 shows that even in that case the bundle was not totally penetrated.

In addition to the infiltration problems, 40xd itself was found to be unsuitable as a matrix material. Due to the small particle size the oxide content in the matrix was quite high and the matrix had very little ductility. Pure 40xd was hot pressed at 640°C at 34.5 MN/m² (5000 psi) then tested in tension at

Table I
T-75 Multifilament Graphite/Aluminum Composites
Slurry Precursor Process

No.	Matrix Powder	Matrix Foil	Fabrication Conditions			Data					
			Temp (°C)	Pressure $\frac{\text{MN}}{\text{m}^2}$ (ksi)	Time (min)	Modulus $\frac{\text{GN}}{\text{m}^2}$ (msi)	UTS $\frac{\text{GN}}{\text{m}^2}$ (ksi)	Failure Strain (%)			
1665	40xd	1145	650	11.5	1.67	30	Poor release from mold - no test				
1666	40xd	1145	650	11.5	1.67	30	Poor release from mold - no test				
1702	40xd	1145	650	5.8	0.84	30	253	36.7	.283	41.2	.12
1703	40xd	1145	655	5.8	0.84	60	266	38.5	.280	40.5	.101
							232	33.7	.292	42.3	.126
1714	40xd	1145	655	2.9	0.42	60	219	31.8	.233	33.8	.108
							238	34.5	.239	34.7	.106
1687	528	713	570	11.5	1.67	30	146	21.2	.166	24.0	.15
							171	24.7	.216	31.2	.16

THORNEL 75 – PURE ALUMINUM SLURRY IMPREGNATED TAPE



C-1714

100 μ

FABRICATION: 655°C, 2.9 MN/m² (420 PSI), 60 MIN

room temperature. The strength of the matrix was found to be 276 MN/m^2 (40 ksi) while the strain to failure was only 0.5 percent. When used as a composite matrix some of this strain capacity would be used up during the fabrication process due to the residual stresses which result from the differential thermal contraction between the filaments and the matrix. Thus the tensile behavior of the composite might very well be limited by the strain capacity of the matrix. These problems were compounded by the fact that the high fabrication temperatures required to achieve reasonable matrix consolidation at low pressure tended to favor a reaction between the graphite fibers and the aluminum matrix to form a carbide, Al_4C_3 . The evidence of this carbide formation was a strong methane odor which resulted from the reaction of $\text{Al} + \text{C}$ with moisture. The carbide formation would be expected to degrade the fiber strength.

The composite strength measurements in Table I indicate the difficulty which the above-mentioned problems presented. Filament volume fractions were in the 40-50 percent range which should have produced composites with strengths well in excess of $.69 \text{ GN/m}^2$ (100 ksi). As a result of this screening, Thornel 75 composites were dropped from further evaluation.

3.2.1.2 Type HM

Infiltration of the untwisted HM tow was much more readily accomplished and as shown in Fig. 5 it was possible to produce composites prepared from the infiltrated tows which exhibited very uniform fiber distribution with a minimum of voids. The HM reinforced composites which were fabricated and the results of the tensile tests which were performed are summarized in Table II. These trials were performed concurrently with the T-75 composites and several of the initial composites utilized 40xd powder as the matrix. The strengths of these composites were quite low, and for the reasons discussed previously 40xd was excluded from the latter portions of the screening program. The highest strength measured was $.52 \text{ GN/m}^2$ (75 ksi) on composite 1734. The fabrication variable which received the most attention was pressure, the intent being to fabricate under as low a pressure as possible in order to minimize fiber breakage during hot pressing. The temperature was as close to the solidus as possible. The series of composites fabricated at 6.9 MN/m^2 (1000 psi) or less generally exhibited poor consolidation. This was partially due to the fact that the yarn was not always uniformly infiltrated with the aluminum slurry. Several techniques of infiltrating the fiber bundle with the slurry were evaluated including continuously hand drawing the yarn through the slurry, allowing the yarn to soak for one minute then withdrawing it, soaking the yarn then withdrawing it through two glass rods set 0.063 cm (0.025 in.) apart, and spreading the fiber then painting it. Composites were made from yarn infiltrated by each technique and examined. The first two techniques produced generally good results in terms of uniform infiltration, but in both cases some of the yarn bundles still showed

TYPE HM – PURE ALUMINUM SLURRY IMPREGNATED TAPE



C-1704

100 μ

FABRICATION: 658°C, 5.8 MN/m² (840 PSI), 60 MIN

Table II
HM Multifilament Graphite/Aluminum Composites
Slurry Precursor Process

No.	Matrix Powder	Matrix Foil	Fabrication Conditions			Data					
			Temp (°C)	Pressure $\frac{\text{MN}}{\text{m}^2}$ (ksi)	Time (min)	Modulus $\frac{\text{GN}}{\text{m}^2}$ (msi)		UTS $\frac{\text{GN}}{\text{m}^2}$ (ksi)	Failure Strain (%)		
1674	40xd	1145	650	11.5	1.67	30	Poor release from mold, extracted fibers broken - no test				
1701	40xd	1145	650	5.8	0.84	30	114	16.5	.189	27.4	0.17
							154	22.3	.220	31.9	0.14
1704	40xd	1145	658	5.8	0.84	60	164	23.8	.272	39.4	0.18
							192	27.9	.268	38.8	0.15
1713	40xd	1145	655	2.9	0.42	60	162	23.5	.117	16.9	0.08
							155	22.5	.154	22.3	0.115
1686	528	713	570	11.5	1.67	30	120	17.4	.445	64.5	0.38
							134	19.5	.394	57.0	0.34
1712	528	713	570	8.6	1.25	60	126	18.3	.413	59.9	0.38
							130	18.9	.400	58.0	0.48
1727	528	713	570	3.5	0.50	60	Poor consolidation - no test				
1730	528	713	573	5.2	0.75	60	Poor consolidation, poor release from mold - no test				

Table II (Cont'd)

No.	Matrix Powder	Matrix Foil	Fabrication Conditions				Data			
			Temp (°C)	Pressure $\frac{\text{MN}}{\text{m}^2}$ (ksi)	Time (min)		Modulus $\frac{\text{GN}}{\text{m}^2}$ (msi)	UTS $\frac{\text{GN}}{\text{m}^2}$ (ksi)		Failure Strain (%)
1733	528	713	572	5.2	0.75	60	Poor consolidation, poor release from mold - no test			
1734	528	713	570	6.9	1.00	60	290	42.0	.518	75.2
							233	33.7	.341	49.5
1764	528	713	570	6.9	1.00	60	Poor consolidation - no test			
1765	528	713	570	5.5	0.80	120	Poor consolidation - no test			
1766	528	713	570	5.5	0.80	240	Poor consolidation - no test			
1768	528	713	590	6.9	1.00	30	Poor consolidation - no test			
1771	528	713	570	6.9	1.00	30	Fair consolidation - no test			
1772	528	713	570	6.9	1.00	30	Fair consolidation - no test			

aluminum-poor regions in their centers. Drawing the fiber through the glass rods and the painting technique were less satisfactory in that poor infiltration was more general.

Another problem was the degree of consolidation of the matrix under the pressures being used in composite consolidation. It was found that the strain to failure of pure 528 powder when pressed at 570°C, 6.9 MN/m² (1 ksi), 30 minutes was only 0.3 percent, indicating that the powder was not fully consolidated. This explained the fact that composites consolidated under those conditions did not exhibit full strength. Composites and unreinforced 528 powder specimens were then prepared at a series of pressures, all at 570°C for 30 minutes to determine if a set of hot press conditions existed which would result in good matrix consolidation and not cause breakage of the composites. The 528 matrix specimens were tested in tension and the composites were dissolved in nitric acid in order to extract the fibers and examine them for breakage. In all cases the fiber bundles were infiltrated by a batch process hand drawing technique in which little or no tension was applied to the bundle while it was being pulled through the aluminum powder slurry. The results of these tests are summarized below.

Pressure		528 Tensile	HM-528 Composites
<u>MN/m²</u>	<u>(psi)</u>	<u>Failure Strain</u> <u>(%)</u>	<u>Fiber Breakage</u>
5.8	835	-	very little
6.9	1000	0.3	none
8.6	1250	-	none
10.4	1500	0.6	no data
11.7	1700	-	extensive
13.8	2000	1.1	no data
17.3	2500	5.2	no data

The data on the pure matrix material indicated that a consolidation pressure of at least 13.8 MN/m² (2000 psi) was necessary in order to achieve a reasonable strain to failure in the matrix, i.e., one that was somewhat higher than that of the fibers. A pressure of 2500 psi would probably be more desirable since it produced much more ductility in the alloy. The examination of extracted filaments revealed that breakage occurred at approximately 10.4 MN/m² (1500 psi) thus producing a dilemma in that the minimum pressure required to produce matrix consolidation was in excess of that which caused filament breakage. Two possibilities existed for reducing the pressure required to achieve matrix consolidation: increase the hot press temperature and/or increase the hot press time. It was felt that the temperature could not be increased significantly without running the risk of heating the matrix above the solidus (578°C) and

causing some dewetting of the matrix. A trial was made with composite 1768 but it resulted in poor consolidation. The alternative of longer hot press times was investigated (composites 1765 and 1766) but consolidation was poor.

As a result of these investigations it was determined that the slurry infiltrated multifilament yarn approach did not demonstrate sufficient promise to be investigated in the subsequent tasks of the program. Consequently, work on the system was discontinued.

3.2.1.3 Thornel 50

The remaining multifilament system screened during Task I was Thornel 50 infiltrated with 526 alloy supplied by Aerospace Corp. The initial batch of material received for evaluation was considered by the vendor to be of low quality, and was used primarily to gain experience in working with the material.

Hot pressing trials were carried out under the following conditions in an argon atmosphere:

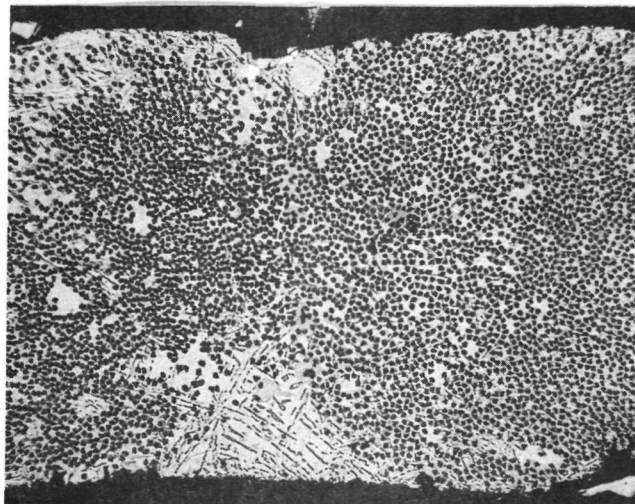
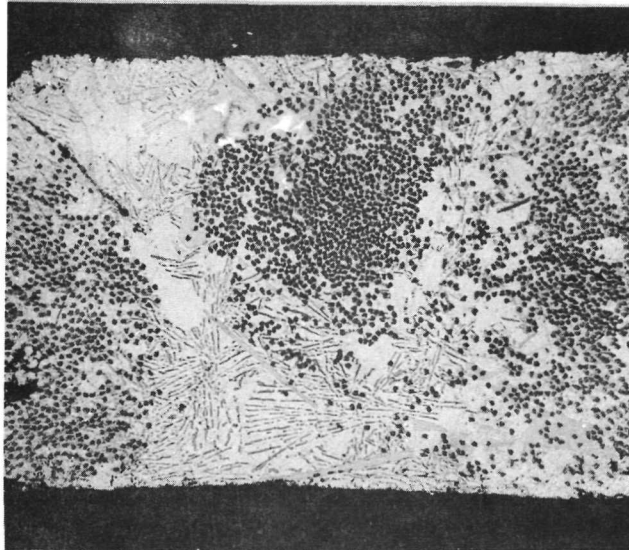
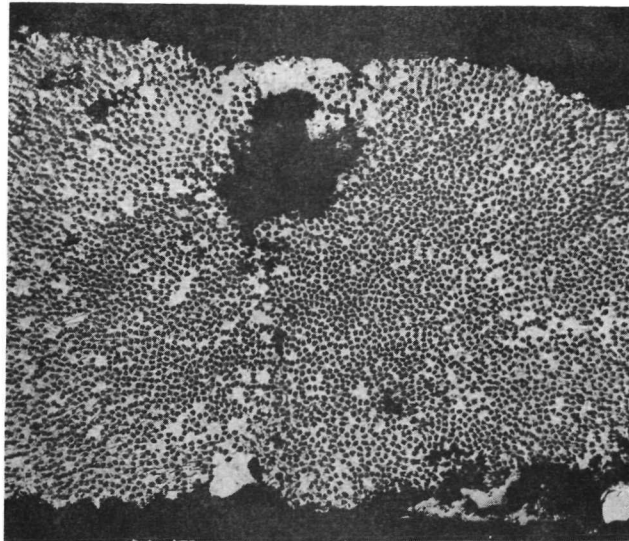
Pressure		Temperature	Time
<u>MN/m²</u>	<u>(psi)</u>	<u>(°C)</u>	<u>(min)</u>
.52	75	640	10
.34	50	640	10
.34	50	600	10

All composites were well consolidated although metallographic examination (Fig. 6) revealed large variations in fiber volume fraction within the composite, apparently as a result of uneven infiltration of the yarn by the aluminum alloy, and some voids due to dewetting during hot pressing. Tensile tests of the composites resulted in poor values, 19 GN/m² (27 ksi), however it was felt that the potential of the material had been demonstrated in the literature (Ref. 3) and it was determined to evaluate the material further during Task III. It should be pointed out that due to cost considerations, only a limited amount of material was available for investigation.

3.2.2 Monofilament Composites

Several composites were fabricated from precursor tapes made by each of the three processes described previously. The primary evaluation criterion was composite tensile strength although other factors such as reproducibility uniform fiber distribution, and ease of processing were considered. The aluminum alloy, 2024, was chosen as the matrix material for all composites. Due to the limited availability of NASA-Hough monofilament, initial composites were made with a low filament volume fraction. UARL monofilament was not available at the time Task I studies were conducted.

THORNEL 50/526 ALUMINUM
AEROSPACE LIQUID INFILTRATION



3.2.2.1 Filament Strength Characterization

Several rolls of NASA-Hough monofilament used during Task I were tested for tensile strength. A summary of these results is presented in Table III. In some instances filament was tested from different portions of a given roll, and these results are presented separately. A bundle strength was calculated for each group of filaments following the procedure described in Ref. 4. The bundle strength of a group of filaments is felt to be a more accurate measure of their composite strengthening potential than the average filament strength because it takes into account the fact that scatter in filament strength reduces its reinforcing effectiveness.

The data in Table III reveal a wide variation in filament strength from roll to roll and to a lesser degree within a given roll. Fiber diameter was found to vary from 2.8 to 3.4 mils although most of the fiber was 3.2 mils. Since some of the rolls were relatively short (less than 1000 ft) it was frequently necessary to use more than one roll in making precursor tapes for composite fabrication. This ultimately resulted in composites reinforced with filament having a wide variation in strength which in turn made composite strength analysis difficult. This will be further discussed subsequently.

3.2.2.2 Styrene Bonded Precursor Tape Composites

Two precursor tapes were prepared by the styrene bonding process; the first was for use in fabricating low fiber volume fraction composites and the second was intended for high fiber volume fraction composites. The first tape was drum wound at a spacing of 42.5 filaments per cm (108 per in.) and the second was wound at 75.5 per cm (192 per in.). Table IV presents the fabrication conditions and tensile data for these composites. Numbers 1628 through 1632 were fabricated from the first tape and the final three composites were fabricated from the second tape.

In order to make a more meaningful comparison of the tensile strength data for composites having different fiber volume fractions, a composite bundle strength, σ_b , has been calculated and presented in the table. The σ_b was calculated by multiplying the bundle strength of fibers in the as-received condition, 1.5 GN/m^2 (218 ksi), times the fiber volume fraction in the composite. This procedure does not account for any matrix contribution and thus should generally result in a lower value than the measured composite strength. (UARL has found this to be the case for boron-aluminum composites.) The final column presents the ratio of measured composite strength to bundle strength calculation.

The first five composites did not possess a low fiber volume fraction as intended. Because there is no aluminum between the filaments in each precursor layer in the styrene bonding process, the fibers above and below a given row tend to squeeze into the space during hot pressing resulting in a relatively

Table III

Task I

Tensile Strength of NASA-Hough Carbon Base Monofilament

Gage Length = 2.54 cm (1 in.)

Roll No.	No. of Tests	Average Strength		Coeff. of Variation (%)	Bundle Strength	
		<u>GN/m²</u>	<u>(ksi)</u>		<u>GN/m²</u>	<u>(ksi)</u>
P-2	10	2.22	322	13.1	1.67	242
P-2	10	1.97	285	11.8	1.52	220
P-2	10	2.35	341	21.0	1.58	229
P-2	10	1.62	235	30.2	0.99	143
P-11	10	2.17	315	11.3	1.68	244
P-13	10	1.53	222	22.2	0.99	144
P-13	10	0.93	135	41.9	0.54	78
P-14	10	2.21	320	19.0	1.50	218
P-14	10	1.91	276	16.7	1.37	198
P-16	10	1.84	267	12.4	1.42	205
P-18	10	1.84	267	16.1	1.34	194
P-19	10	1.24	180	28.3	0.77	112
P-23	10	1.50	217	18.2	1.05	152

Table IV
Task I
Hough Monofilament/2024 Aluminum Composites
Styrene Bonding Precursor Process

No.	Fabrication Conditions				Data					
	Temp (°C)	Pressure MN/m ² (ksi)	Time (min)	Fiber Vol. (%)	Modulus GN/m ² (msi)	UTS GN/m ² (ksi)	Failure Strain (%)	Bundle Strength σ_b GN/m ² (ksi)	UTS/ σ_b	
1628	540	34	5	39	94.5	13.7	0.96	.586	85.0	1.02
1629	450	69	10	41	-	-	-	.617	89.4	1.16
				41	-	-	-	.617	89.4	1.13
1630	480	69	10	38	94.5	13.7	0.89	.571	82.8	0.912
				36	93.8	13.6	0.66	.542	78.5	0.752
1631	495	34	5	38	100.0	14.5	0.86	.571	82.8	0.936
				35	94.5	13.7	0.90	.526	76.2	0.946
1632	510	6.9	1	26	89.0	12.9	0.91	.391	56.7	1.02
				23	80.7	11.7	0.83	.346	50.2	1.01
1723	450	69	10	57	106.0	15.3	0.67	.856	124.0	0.504
				56	114.0	16.6	0.73	.842	122.0	0.545
1728	490	69	10	50	114.0	16.6	1.08	.752	109.0	1.065
				47	106.0	15.3	1.03	.707	102.5	0.898
1738	495	34	5	30	Poor consolidation - no test					

uncontrolled fiber distribution. Figure 7 is a photomicrograph of composite 1628 which illustrates this point. The composite consisted of five layers of precursor tape originally.

Scanning electron microscope (SEM) study was made of fracture surfaces of tensile specimen 1728-1, which exhibited the highest strength of the composites made from styrene bonded tape. Figure 8 is a typical view of the specimen. The fiber spacing was rather nonuniform as was shown by earlier optical photomicrographs. Some filament pullout was evident although the longest pullout length was on the order of only two or three filament diameters. There was no evidence of a reaction between the aluminum and the filaments; most of the pulled out filaments were bare.

On the basis of efficiency of fiber strength translation, the best fabrication conditions for the styrene bonded tapes were 450°C, 69 MN/m² (10 ksi) for 30 minutes (composite 1629). Composite 1728 exhibited higher absolute strength but had a higher filament volume fraction.

Fiber was extracted from composite 1628 to determine if the fabrication process had any detrimental effect on fiber strength. In addition, as-received fiber was subjected to the extraction process (2 minute leaching in hydrochloric + nitric acid) to determine if it had any effect. The results of these tests which are summarized below indicate no degradation of fiber strength as a result of filament extraction or composite consolidation. As-received data are included for comparison.

Tensile Strength of Hough Monofilament
Roll P-2

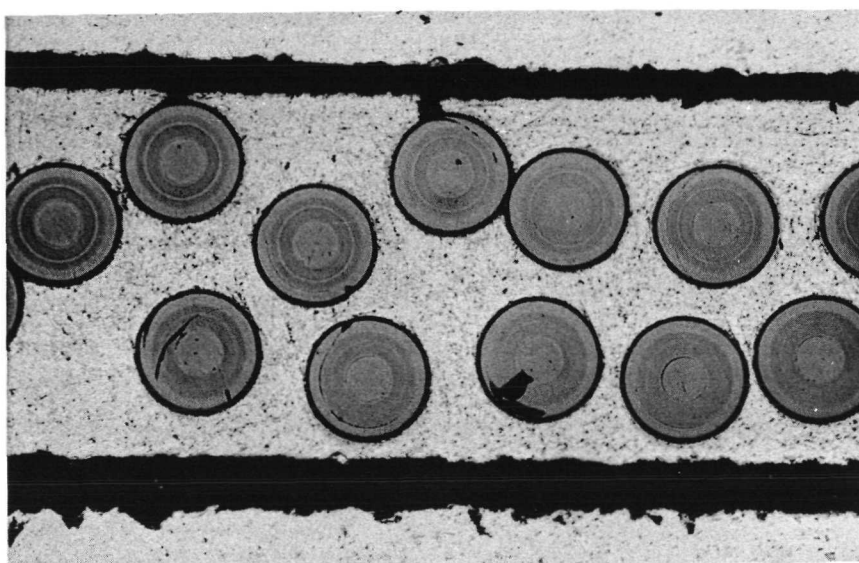
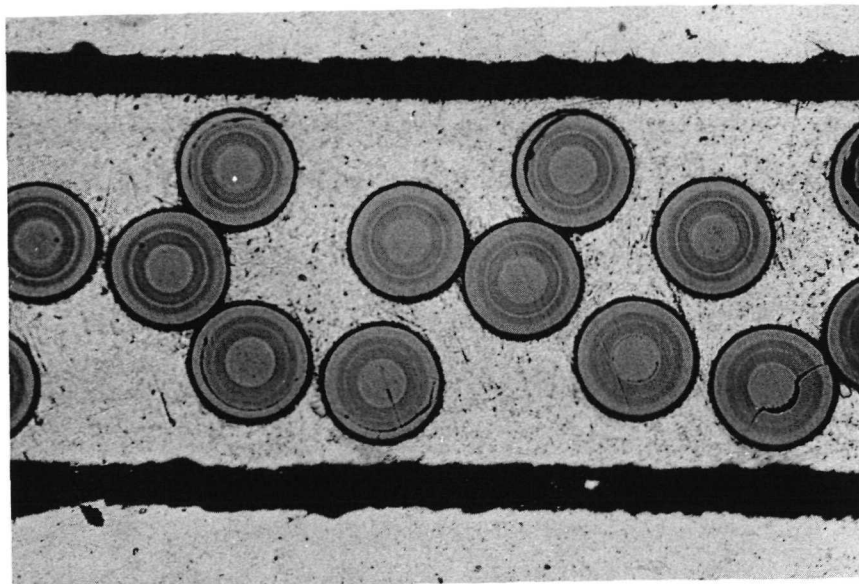
Gage Length = 2.54 cm (1 in.)

<u>Fiber Condition</u>	<u>No. of Tests</u>	<u>Average Strength</u>		<u>Std. Deviation</u>	
		<u>GN/m²</u>	<u>(ksi)</u>	<u>GN/m²</u>	<u>(ksi)</u>
As-received	40	2.12	308	.37	53
2 min. in HCl + HNO ₃	10	2.07	300	.24	35
Extracted from composite 1628	20	2.13	309	.46	66

The composite modulus data in Table IV obey rule of mixtures calculations for a fiber modulus of approximately 138 GN/m² (20 x 10⁶ psi).

The major problem with the styrene bonding technique was the inability to achieve high volume fraction composites (50% fiber) which were well consolidated and had a uniform fiber distribution. In order to achieve a void free composite, it is necessary for the 2024 foil which separates each layer of fibers to deform

HOUGH MONOFILAMENT – 2024 ALUMINUM
STYRENE BONDED PRECURSOR TAPE

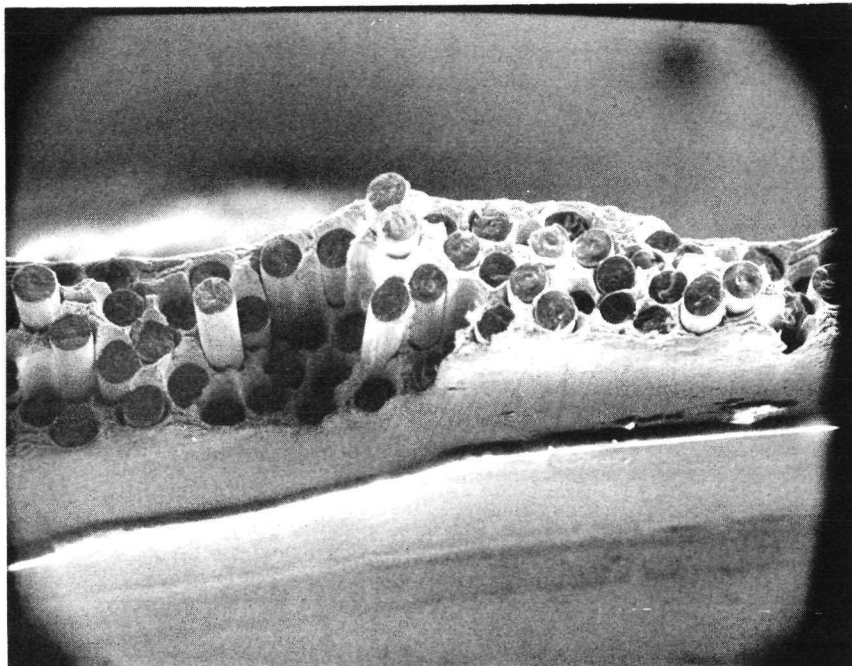


C-1628

200X

FABRICATION: 540°C, 34.5 MN/m² (5 ksi), 30 MIN

NASA-HOUGH MONOFILAMENT/2024 ALUMINUM TENSILE FRACTURE SURFACE



C-1728

PRECURSOR TAPE MADE BY STYRENE BONDING

100 μ

sufficiently to fill the gaps between adjacent fibers. In addition, the foil must form a good bond with the foil in the layer above and below or the composite will have a low interlaminar shear strength. At present the nominal diameter of the NASA-Hough filament is .0081 cm (3.2 mils) which means the fiber must be wound at a spacing of about 79 filaments per cm (200 per in.) over a .00254 cm (1 mil) aluminum foil to obtain a composite with 50 percent reinforcement. This spacing leaves a gap of about .0046 cm (1.8 mils) between the fibers which apparently is sufficiently small to produce inconsistent results during subsequent hot pressing. Composites 1723 and 1738, for example, were not well bonded after hot pressing, and composite 1728, although exhibiting a good tensile strength, did not have a uniform fiber distribution which would be likely to have an adverse effect on transverse tensile strength.

For these reasons the styrene bonding technique was not selected for further study under Task II of the program. The process does have the advantages of simplicity and low cost, however, and should the monofilament become available in a larger diameter which would permit high volume fractions to be obtained at a larger fiber spacing, it would be worthy of reconsideration. It should be noted that the technique has proved successful in making tapes of .0102 and .0142 cm (4 and 5.6 mil) diameter boron-aluminum.

3.2.2.3 Slurry Precursor Tape Composites

A low volume fraction and a high volume fraction precursor tape were prepared by the slurry process. Table V lists the fabrication conditions and tensile data for these composites. Fiber volume fractions were much more controlled than with the styrene bonded tapes as a result of the aluminum powder between each filament in the precursor tape. The three high volume fraction composites (1746, 1748, 1750) had lower volume fractions than desired which reflected the difficulty in controlling the exact amount of aluminum which was brushed on the precursor tape. Nevertheless, control over fiber spacing in the composites was better than with the styrene bonded tapes as evidenced in Fig. 9, although there were regions of fiber-fiber contact and large gaps between fibers.

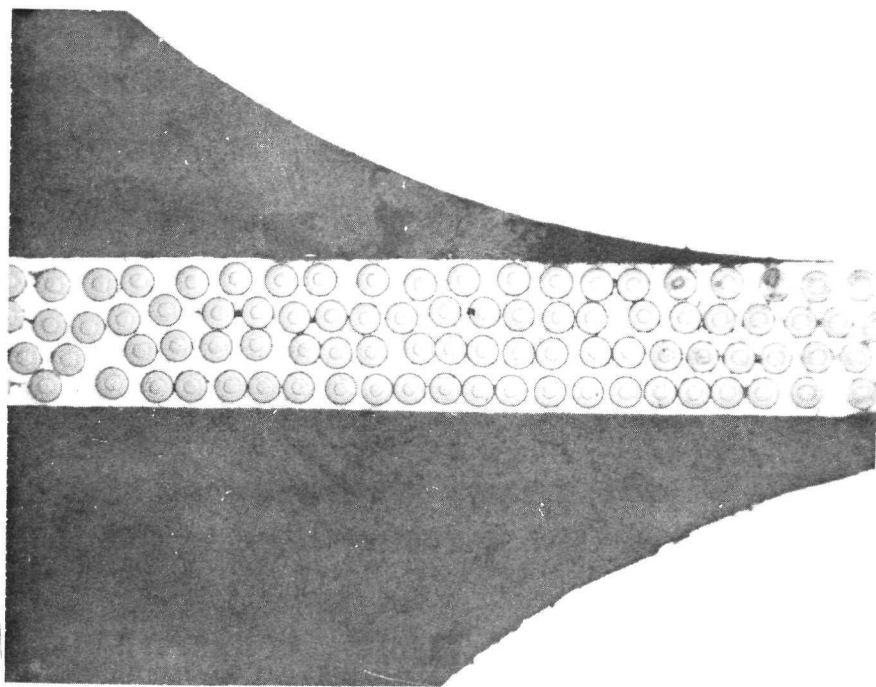
The tensile data as reported in Table V were comparable to those obtained with the styrene bonding process, however fiber strength translation efficiency was generally better, possibly as a result of better fiber distribution. As before, the best fabrication conditions were 450°C, 69 MN/m² (10 ksi), 30 min., this time on the basis of both absolute strength and translation efficiency.

A SEM picture of a tensile fracture surface of composite 1746 is shown in Fig. 10. There is some fiber pullout evident and the matrix appears to be well consolidated. Although it is difficult to see in Fig. 10, previous optical microscope studies showed the fiber spacing to be rather nonuniform and revealed

Table V
Task I
Hough Monofilament/2024 Aluminum Composites
Slurry Precursor Process

No.	Fabrication Conditions				Data				
	Temp (°C)	Pressure MN/m ² (ksi)	Time (min)	Fiber Vol. (%)	Modulus GN/m ² (msi)	UTS GN/m ² (ksi)	Failure Strain (%)	Bundle Strength σ_b GN/m ² (ksi)	UTS/ σ_b
1647	495	34 5	30	17 19	81.4 11.8 75.9 11.0	.301 43.6 .317 45.9	0.95 1.01	.255 37.0 .286 41.4	1.18 1.11
1648	490	69 10	30	23 24	79.4 11.5 89.7 13.0	.304 44.1 .321 46.5	0.67 0.73	.346 50.2 .361 52.3	0.879 0.890
1649	450	69 10	30	25 25	86.2 12.5 86.2 12.5	.424 61.5 .462 66.9	0.88 0.96	.376 54.5 .376 54.5	1.13 1.23
1651	490	69 10	30	24 24	81.4 11.8 84.9 12.3	.343 49.7 .464 67.3	0.72 0.96	.361 52.3 .361 52.3	0.950 1.285
1663	510	23 3.3	30	24 22	86.9 12.6 85.6 12.4	.311 45.1 .321 46.5	0.61 0.72	.361 52.3 .330 47.9	0.863 0.970
1746	450	69 10	30	38 41	101.0 14.6 105.0 15.2	.618 89.6 .729 105.7	0.76 1.00	.409 59.3 .442 64.0	1.51 1.65
1748	490	69 10	30	44 41	111.0 16.1 96.6 14.0	.560 81.2 .586 85.0	0.76 0.86	.474 68.7 .442 64.0	1.18 1.33
1750	495	34 5	30	40 42	78.7 11.4 95.2 13.8	.444 64.3 .478 69.3	0.75 0.73	.430 62.3 .452 65.5	1.03 0.946

HOUGH MONOFILAMENT – 2024 ALUMINUM
SLURRY PRECURSOR TAPE

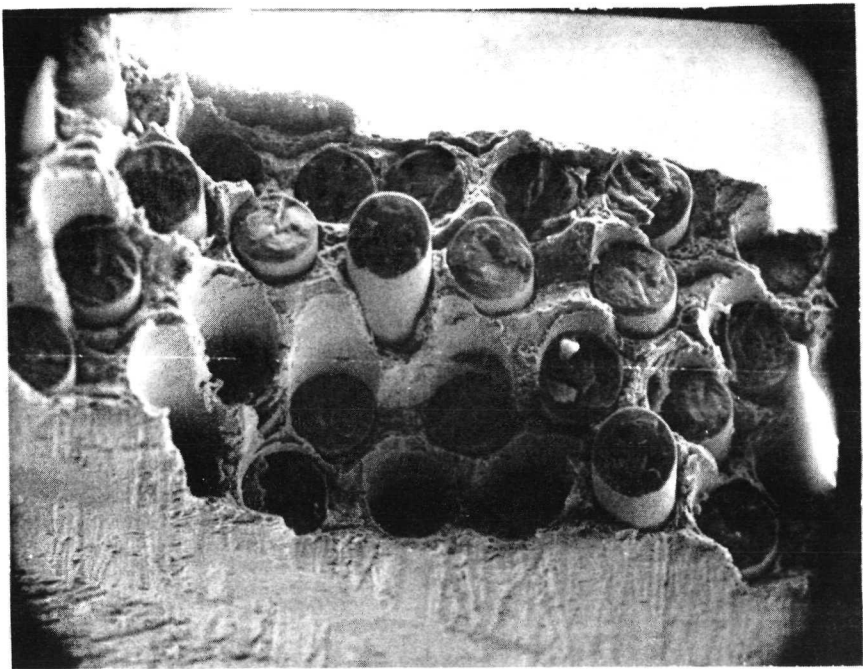


C-1747

200 μ

FABRICATION: 450°C, 69 MN/m² (10 KSI), 30 MIN

NASA-HOUGH MONOFILAMENT/2024 ALUMINUM TENSILE FRACTURE SURFACE



C-1746

100 μ

PRECURSOR TAPE MADE BY SLURRY PROCESS

a relatively high degree of porosity, primarily in the gaps between filaments in a layer. Both these problems resulted from the difficulty involved in uniformly applying the powder slurry by the hand brushing technique. This nonuniformity was felt to be an important disadvantage for this process, especially in view of the requirement for making large 30 cm x 30 cm (12 in. x 12 in.) panels in subsequent portions of the program. In order to obtain an even pressure distribution on such a composite during hot pressing it is necessary that the thickness and matrix distribution of the precursor tape be as uniform as possible. Consequently, this process was not selected for Task II.

3.2.2.4 Plasma Spray Precursor Tape Composites

The final method evaluated for preparing precursor tapes was plasma spraying. Two tapes were prepared as with the other techniques and fiber was extracted from the first to determine if the plasma spray operation had an effect on fiber tensile strength. The results of the tests which are summarized below indicate that some damage may have occurred.

Tensile Strength of Hough Monofilament Roll P-2

Gage Length = 2.54 cm (1 in.)

<u>Fiber Condition</u>	<u>No. of Tests</u>	<u>Average Strength</u>		<u>Standard Deviation</u>	
		<u>GN/m²</u>	<u>(ksi)</u>	<u>GN/m²</u>	<u>(ksi)</u>
As-received	40	2.12	308	.37	53
Extracted from plasma sprayed tape	20	1.92	278	.44	64

It is possible that such a difference simply reflected a variation of fiber strength from one place to another within the roll. However, UARL has observed a similar apparent strength loss in boron filaments extracted from plasma sprayed tapes. Boron-aluminum composites made from such tapes generally do not reflect any loss in filament strength, and it is not clear at present why the fibers seem to show a loss in strength after plasma spraying or how the strength is recovered in the composites if it is truly reduced in the tape.

Table VI lists the results obtained on composites under Task I of the program. Again the tensile strengths are in line with the values achieved in testing composites made from the other two precursor tapes. The strengths of composites 1747, 1749, and 1751 were lower than expected based on the utilization of bundle strength found with the previous composites. In order to investigate

Table VI

Task I

Hough Monofilament/2024 Aluminum Composites
Plasma Spray Precursor Process

No.	Fabrication Conditions			Data						
	Temp (°C)	Pressure MN/m ² (ksi)	Time (min)	Fiber Vol. (%)	Modulus GN/m ² (msi)	UTS GN/m ² (ksi)	Failure Strain (%)	Bundle Strength σ_b GN/m ²	Strength (ksi)	UTS/ σ_b
1694	450	69	30	21	88.3	12.8	.495	71.7	1.26	45.8
				20	98.7	14.3	.461	66.8	1.08	43.6
1699	495	34	5	18	89.0	12.9	.297	43.0	0.85	39.2
				16	62.1	9.0	.259	37.5	0.83	34.8
1700	490	69	30	20	80.0	11.6	.369	53.5	0.98	43.6
				20	69.0	10.0	.435	63.0	1.12	43.6
1706	510	23	3.3	23	89.0	12.9	.322	46.7	0.70	50.2
				22	69.7	10.1	.317	45.9	0.78	47.9
1747	450	69	30	35	96.6	14.0	.603	87.4	1.04	79.4
				38	94.5	13.7	.545	79.0	0.87	84.0
1749	490	69	30	40	105.0	15.2	.549	79.6	0.73	90.3
				36	101.0	14.7	.513	74.3	0.67	81.7
1751	495	34	5	41	92.5	13.4	.450	65.2	0.67	93.0
				44	93.2	13.5	.531	76.9	0.72	99.8
1789	450	69	30	48	91.8	13.3	.662	96.0	1.00	-
				48	102.0	14.8	.728	105.5	1.04	-
1798	490	69	30	47	102.0	14.8	.524	76.0	0.68	-
				48	93.4	14.4	.570	82.6	0.78	-

this and to further explore the question of fiber degradation as a result of plasma spraying, fiber was extracted from composite 1747 and tested in tension along with fresh fiber from the roll (P-11) to determine if any fabrication induced damage had occurred. The average strengths were 2.18 GN/m^2 (315 ksi) for the fresh fiber and 2.41 GN/m^2 (349 ksi) for the extracted fiber. This indicated that the roll strength was good and that no damage had occurred to the filaments as a result of fabrication.

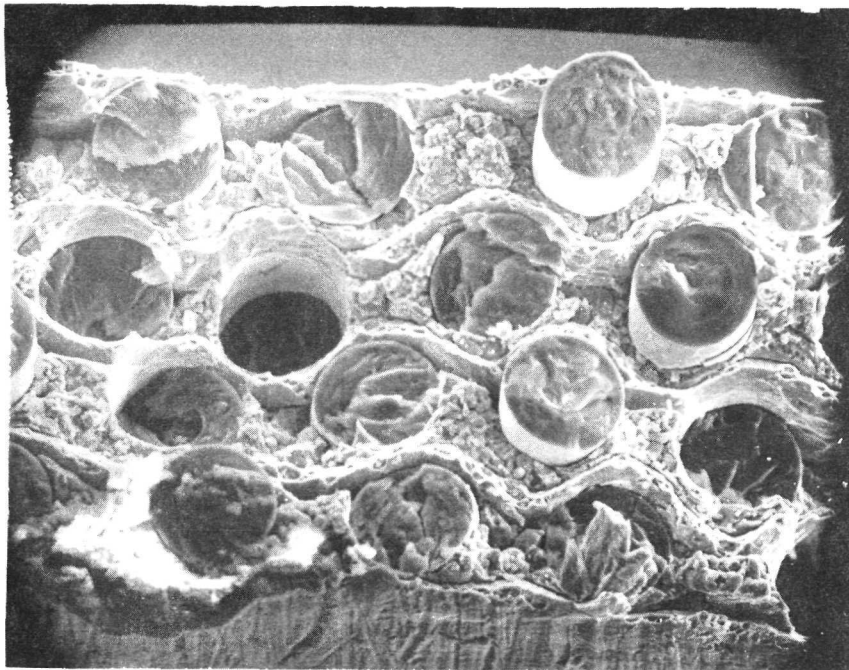
Figure 11 is a SEM picture of a fractured tensile specimen from 1747 and reveals what may have been the cause of the poor strengths. The plasma-sprayed aluminum matrix was not well consolidated. Individual particles can be easily identified over most of the specimen cross section. This may have been caused by an insufficient quantity of powder being deposited in the plasma spray operation. This was due to the fact that the diameter of the extracted filaments was found to be .0081 cm (3.2 mils) compared to .0086 cm (3.4 mils) measured at the beginning of the roll. Since the fiber was smaller than assumed, the gaps between the fibers in the precursor tape were larger than calculated and the amount of aluminum deposited during plasma spray may not have adequately filled these gaps. This may explain the relatively low strengths of composites 1747, 1749, and 1751 which were all made from the same precursor tape.

In general the composite tensile data presented in Table VI do not indicate any damage to the fibers. In fact the tensile strength/bundle strength ratios were the best of the three precursor tape techniques. The fiber spacing in the composites was very good as shown in Fig. 12 which no doubt contributed to good composite strengths. As with the other techniques, the fabrication conditions of 450°C , 69 MN/m^2 (10 ksi), 30 minutes resulted in the best composite strengths. Composite 1694 was much better, on the basis of bundle strength, than any other monofilament composite tested during Task I.

In an effort to achieve higher absolute values of composite strength, a plasma-sprayed tape was fabricated at a filament spacing of 99 per cm (250 per in.) compared to 88 (224) with the previous tape. Two composites, 1789 and 1798, were fabricated as shown in Table VI. Composite 1789 exhibited the highest strength of any made from the plasma sprayed tapes, but the absolute values were still somewhat lower than expected. This was probably a result of the filament which went into the precursor tape. Rolls P-13 and P-14 were used in the preparation of the tape, and as indicated in Table III the strength of the P-13 filament was very poor. Since two rolls of filament having different strength distributions were used in these tapes, bundle strength calculations were not made for the composites.

Plasma spraying was selected as the precursor tape technique to be used in the remainder of the program primarily as a result of the uniformity of the tapes and fiber distributions in the hot pressed composites. The strengths of

NASA-HOUGH MONOFILAMENT/2024 ALUMINUM TENSILE FRACTURE SURFACE

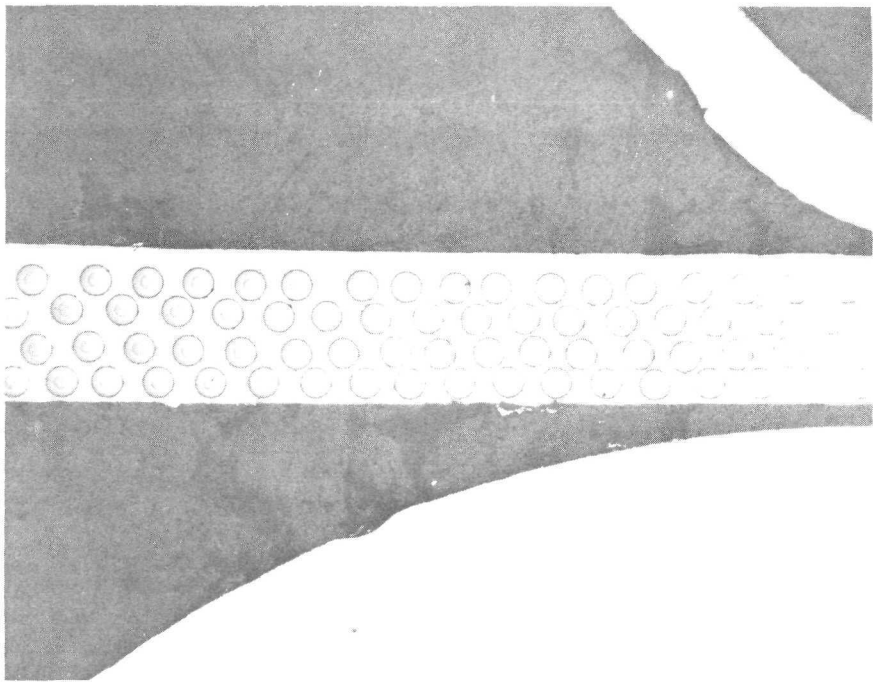


C-1747

50 μ

PRECURSOR TAPE MADE BY PLASMA SPRAY PROCESS

HOUGH MONOFILAMENT – 2024 ALUMINUM
PLASMA SPRAY PRECURSOR TAPE



C-1746

200 μ

FABRICATION: 450°C, 69 MN/m² (10 KSI), 30 MIN

the high volume fraction composites were difficult to analyze due to the problems cited above, however 1789 exhibited a strength of $.72 \text{ GN/m}^2$ (105 ksi) which was as high as any measured in Task I, and the initial composites (1694, 1699, 1700) showed very good ratios of measured strength to bundle strength.

The fabrication conditions which generally resulted in the best composite properties were 450°C , 69 MN/m^2 (10 ksi), 30 minutes. All hot pressing was carried out under an argon atmosphere. The superiority of these conditions is demonstrated in Table VI. Three precursor tapes were used to prepare the composites listed. Composites 1694, 1699, 1700, and 1706 were made from the first, 1747, 1749, and 1751 from the second, and 1789 and 1798 from the third. Within each group the selected conditions resulted in the highest composite strength.

IV. TASK II - COMPOSITE OPTIMIZATION AND SCALE-UP

4.1 Experimental Procedure

As a result of Task I screening only NASA-Hough monofilament 2024 aluminum composites were included in Task II. The experimental procedures were generally the same as those in Task I with most of the optimization studies having to do with refinement of the hot pressing parameters in order to achieve the highest composite tensile strength. Tensile testing procedures were identical to those utilized in Task I.

The scale-up portion of Task II was conducted under subcontract to Pratt and Whitney Division of United Aircraft who purchased and machined a mold suitable for hot pressing composites of 30 cm x 30 cm (12 in. x 12 in.) lateral dimensions. The bonding tool consists of two flat plates, 8.9 cm (3 1/2 in.) thick, with recessed grooves for an induction coil in both plates. Thermo-couples are located in two positions in each plate on the face in contact with panels being bonded. Extra turns of induction coil were added near the carbon-aluminum panel area to prevent heat loss and insulation was packed around both plates to improve the temperature profile. The final temperature of the carbon-aluminum panel varied $\pm 8^{\circ}\text{C}$. Material used to make this tool was PES 220 (also known as AMS 5382 or Stellite 31).

4.2 Results and Discussion

4.2.1 Filament Strength Characterization

Two of the filament lots which were utilized in Task II were sampled for tensile strength. The results of these tests are summarized in Table VII.

By comparing these data with those presented in Table III, it can be seen that the strength of the filament used in Task II was generally lower than that used in Task I. This made it difficult to compare composite tensile data with Task I results to determine the degree of fabrication optimization in Task II.

4.2.2 Composite Optimization

A series of composites was fabricated under the conditions outlined in Table VIII to determine if composite strength could be improved by modification of the best hot pressing conditions as determined in Task I. Variables investigated were time and pressure since it was felt that the effects of hot pressing temperature were adequately covered during Task I studies.

Table VII

Task II

Tensile Strength of NASA-Hough Carbon Base Monofilament

Gage Length = 2.54 cm (1 in.)

<u>Lot No.</u>	<u>No. of Tests</u>	<u>Average Strength</u>		<u>Coefficient of Variation</u>
		<u>(GN/m²)</u>	<u>(ksi)</u>	<u>(%)</u>
P-19	10	1.24	180	28.3
P-23	10	1.50	218	18.1
1080	10	1.32	192	37.3
1080	10	1.87	271	25.3
1080	10	1.33	194	39.1
1090	8	1.55	226	25.1
1090	10	1.63	237	23.9
1090	10	1.78	258	15.5
1090	10	1.23	179	36.9
1100	10	1.32	202	16.4
1100	10	1.69	245	18.1
1100	10	1.45	211	34.2

Table VIII

Task II
NASA-Hough Monofilament/2024 Aluminum Composites
Plasma Spray Precursor Process
Fabrication Optimization

No.	Fabrication Conditions				Fiber Vol. (%)	Test Temp	Data		UTS GN/m ²	UTS (ksi)	Failure Strain (%)
	Temp (°C)	Pressure MN/m ²	Time (min)	Modulus GN/m ²			Modulus (msi)				
1803	450	69	10	30	48	R.T.	98.7	14.3	.597	86.5	0.88
					48	R.T.	103.0	14.9	.626	90.7	0.88
					48 ^a	R.T.	97.3	14.1	.658	95.4	0.93
1854	450	69	10	30	52	R.T.	88.3	12.8	.415	60.2	0.72
					48	R.T.	101.0	14.6	.368	53.4	0.56
1861	450	69	10	60	52	R.T.	85.6	12.4	.566	82.1	1.00
					50	R.T.	92.5	13.4	.535	77.5	0.98
1874	450	69	10	15	45	R.T.	122.0	17.7	.421	61.0	0.69
1875	450	104	15	30	48	R.T.	-	-	.435	63.0	-
1891	450	69	10	30	48	R.T.	115.0	16.7	.731	106.0	0.84
					52	R.T.	126.0	18.2	.973	141.0	1.00
1893	450	69	10	60	48	R.T.	124.0	18.0	.745	108.0	0.80
					49	R.T.	123.0	17.8	.821	119.0	0.86

Table VIII (Cont'd)

No.	Fabrication Conditions			Fiber Vol. (%)	Data				Failure Strain (%)		
	Temp (°C)	Pressure MN/m ² (ksi)	Time (min)		Test Temp	Modulus GN/m ² (msi)	UTS GN/m ² (ksi)				
1854	450	69	10	30	49	427°C	86.2	12.5	.246	35.7	0.41
					48	427°C	-	-	.348	50.5	-
1853 ^b	450	69	10	30	51	R.T.	96.6	14.0	.064	9.4	0.095
					51	R.T.	74.5	10.8	.045	6.6	0.075

^aSpecimen in T-6 condition^bFor transverse tensile tests

Composite 1803 was 2.54 cm x 12.8 cm (1 in. x 5 in.), or 5.1 cm (2 in.) longer than the composites fabricated in Task I. The tensile specimens from this composite were also 12.8 cm (5 in.) long and had a 5.1 cm (2 in.) gage length, twice that normally used. The longer specimen gage length may have resulted in the slightly lower strengths for this composite in comparison with 1789 (see Table VI) which was made from the same precursor tape. A third specimen was cut from this composite and given a T-6 heat treatment (490°C for 40 min, water quench, aged for 16 hrs at 195°C). The treatment did not have a dramatic effect on the tensile behavior although the UTS was increased slightly.

Composites 1853 through 1875 in Table VI were made from a precursor tape which was reinforced with filament from Rolls P-19 and P-23 which were not very strong (see Table VII). As a result fairly low composite strengths were expected, however 1854 was made at the standard conditions so the relative effects of the variations in pressure and time with the other composites could be determined. Composites 1891 and 1893 were fabricated from lot 1080 which also was not as strong as some of the previous lots. Lot 1080 and all higher lot numbers were received in a second shipment and had a higher tensile modulus than the earlier filament. This will be further discussed in a later section of the report.

The room temperature tensile strengths of composite 1854 which was fabricated under the best conditions found in Task I were .415 and .358 GN/m² (60.2 and 53.4 ksi). Composites 1874 and 1875 which were fabricated for shorter time and higher pressure, respectively, exhibited essentially the same strength. However, composite 1861 was hot pressed for a longer time (60 min) and the same temperature (450°C) and pressure, 69 MN/m² (10 ksi), and showed higher strengths than those obtained with 1854 under the standard conditions.

Composites 1891 and 1894 were fabricated to determine if the longer hot press time had a similar effect with the second batch of filament. Based on the data in Table VIII, this was not the case, in fact the reverse was true. Composite 1891, hot pressed for 30 minutes, exhibited tensile strengths of .731 and .973 GN/m² (106 and 141 ksi) with the latter value being the highest measured in Task II. Composite 1893, pressed for 60 minutes, had strengths of .745 and .821 GN/m² (108 and 119 ksi). Based on these results it did not appear that there was a significant difference in the strengths of the composites as a result of being pressed for different time periods. The differences which were observed between 1854 and 1861 and 1891 and 1893 were probably due to other variables such as variations in the fiber strength, fiber alignment, etc. Consequently, it was concluded that at 450°C and 69 MN/m² (10 ksi), hot pressing time could range from 30 to 60 minutes without significantly affecting the composite longitudinal tensile strength.

A limited number of longitudinal tensile tests were conducted at 427°C in order to obtain a preliminary measure of elevated temperature behavior. There

was a good bit of variation in the two tensile strengths of composite 1854. The first specimen was instrumented with a strain gage and had the lower strength $.246 \text{ GN/m}^2$ (35.7 ksi). The second specimen was uninstrumented and its strength of $.348 \text{ GN/m}^2$ (50.5 ksi) compares well with the room temperature values obtained with composite 1854.

Composite 1853 which was tested in transverse tension exhibited strengths of $.064$ and $.045 \text{ GN/m}^2$ (9.4 and 6.6 ksi), both of which were quite low. Fracture surfaces were examined in the scanning electron microscope to determine the nature of the failures. Figure 13 shows that interfacial debonding was the primary mode of failure in the composites. This behavior is quite different from boron- or BORSIC[®]-aluminum which tend to fail due to fiber splitting with .01 cm (4 mil) fiber as the reinforcement, and by matrix failure with .014 cm (5.6 mil) fiber as the reinforcement (Ref. 5). As a result of the good interfacial bond, transverse tensile strength of boron-aluminum is much better than the measured values of carbon-aluminum. Typical values are $.138 \text{ GN/m}^2$ (20 ksi) for .01 cm (4 mil) composites, and $.276 \text{ GN/m}^2$ (40 ksi) for .014 cm (5.6 mil) composites using 6061 in the T-6 condition as the matrix (Ref. 5).

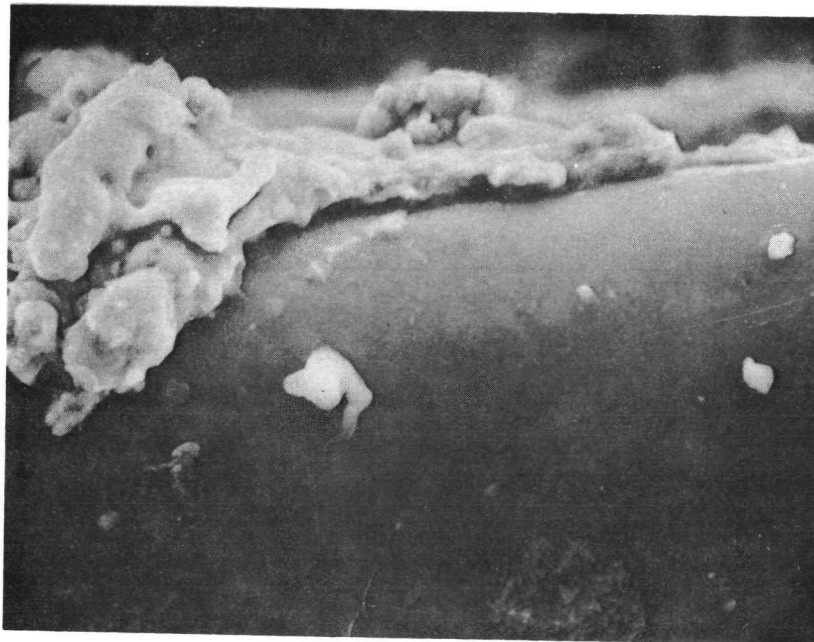
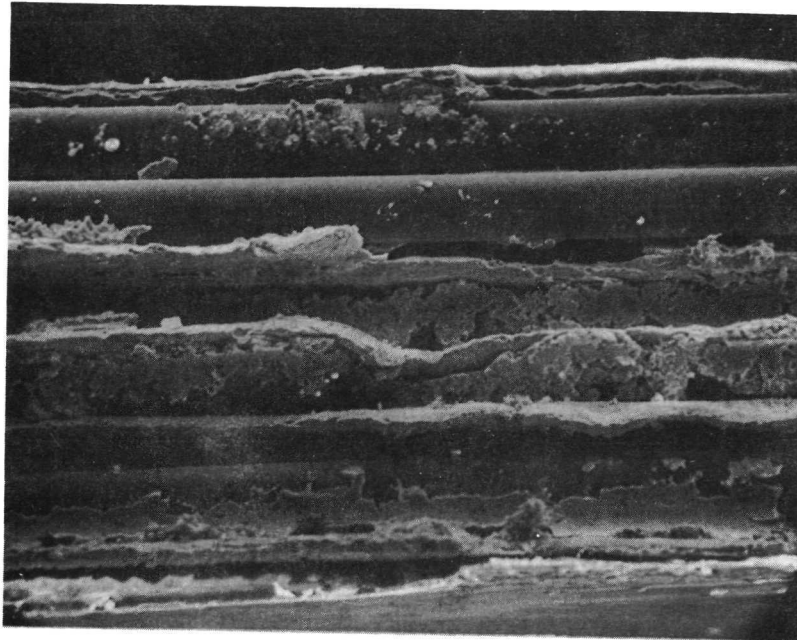
The conclusion drawn from Task II optimization work was that the fabrication conditions arrived at in Task I could not be improved upon in terms of increasing composite longitudinal tensile strength. The testing at 427°C indicated that a large fraction of the room temperature tensile strength could be retained at elevated temperature. The transverse tensile strengths were quite low as a result of a weak interfacial bond between the filament and the matrix.

4.2.3 Composite Scale-Up

An initial trial run in the 30 cm x 30 cm (12 in. x 12 in.) mold was made using BORSIC-aluminum tape in order to work out any molding difficulties without risking carbon monofilament. Thermocouple readouts from the mold indicated a temperature gradient of 40°C from the center to the outside edge. Nevertheless, the composite appeared to be well consolidated on visual inspection although there was evidence that a region about 2.54 cm (1 in.) wide and around the circumference was not as well bonded as the remainder of the panel. It was believed that the temperature gradient could be largely eliminated through the use of additional insulation around the edges. Previous experience at P&WA indicated that good quality parts could be fabricated from BORSIC-aluminum with a temperature differential of about 15°C .

Two plasma sprayed tapes 15 cm x 150 cm (6 in. x 60 in.) were fabricated from NASA-Hough lots 1080, 1090, and 1100 for incorporation into a large composite panel. There were no serious problems encountered in winding the tapes although there were several instances of fiber breakage which disrupted uniformity of the fiber spacing. The tape was wound at a spacing of 88 per cm (224 per inch).

TRANSVERSE TENSILE FRACTURE SURFACE
NASA-HOUGH MONOFILAMENT/2024



During hot pressing of the panel, NAS-1, it was found that the center to edge temperature gradient was retained in spite of the additional insulation around the edge of the mold. The panel was held under pressure for 1 1/2 hrs in the hope that the gradient would even out but it did not. The visual appearance of the panel was good and the thickness was fairly uniform at .051 cm (.020 in.). The molding tool was modified following this run by placing an additional heating coil around the outer perimeter. A second panel, NAS-2, was fabricated and the temperature gradient was reduced to a maximum of 15°C. Hot press time was 30 minutes as planned.

Panel NAS-1 was machined into test specimens. The results of longitudinal and transverse tensile tests of the specimens are presented in Table IX. The average longitudinal tensile strength of the panel was as good as those obtained with the small panels in the optimization phase (Table VIII), although none of the individual values was as high as the best strength measured for 1891. In general, however, there was no loss in longitudinal tensile strength as a result of the scale-up process. The transverse tensile strengths were also in good agreement with the data obtained on small specimens (1853) although again the small specimens produced a higher individual value.

Elevated temperature tensile tests of specimens cut from the scaled-up panel were also carried out. Some difficulty was encountered in the tests of specimens NAS-1A-3 and 4 in that failure occurred in the grips. An additional specimen (NAS-1B-14) was tested using thicker aluminum doublers and failure occurred just outside the grips at a much higher stress level.

As a result of these tests the scaled-up process was used to fabricate panels for Tasks III and IV.

Table IX

Task II
 NASA-Hough Monofilament/2024 Aluminum Composites
 Composite Scale-Up

<u>No.</u>	<u>Orientation</u>	<u>Test Temp (°C)</u>	<u>Fiber Vol. (%)</u>	<u>Tensile Modulus</u>		<u>UTS</u>		<u>Failure Strain (%)</u>
				<u>GN/m²</u>	<u>(msi)</u>	<u>MN/m²</u>	<u>(ksi)</u>	
NAS-1A-1	0	R.T.	49	113	16.4	780	113	0.83
NAS-1A-2	0	R.T.	49	116	16.8	820	119	0.84
NAS-1A-3	0	427	49	114	16.5	366	53 ^a	-
NAS-1A-4	0	427	49	91	13.2	248	36 ^a	0.28
NAS-1B-14	0	427	49	-	-	573	83	-
NAS-1A-21	90	R.T.	49	52	7.5	46	6.7	0.09
NAS-1A-22	90	R.T.	49	70	10.2	45	6.5	0.06
NAS-1A-23	90	427	49	29	4.2	17	2.4	0.22
NAS-1A-24	90	427	49	-	-	12	1.8	0.05

^aSpecimen failed in the grips

V. TASK III - FABRICATION AND CHARACTERIZATION OF COMPOSITES

The primary objective of this task was to characterize the mechanical behavior of the previously screened and optimized materials. The material most widely studied in Task III was NASA-Hough monofilament/2024 aluminum at a nominal filament volume fraction of 0.50. More limited evaluations were also to be conducted on the same material at high and low filament volume fractions (0.35 and 0.65), UARL monofilament/2024 aluminum, and Thornel 50/526 aluminum supplied by Aerospace Corp. in the form of infiltrated rods.

Filament volume fraction of the NASA-Hough composites was varied by changing the filament spacing and/or the number of plasma spray passes in the preparation of the precursor tapes. To produce 50 v/o composites, the tape was wound at a spacing of 88 filaments per cm (224 per inch) and given two plasma spray passes. The 35 v/o composite tapes were wound at 57 filaments per cm (144 per in.) with three plasma spray passes, while the 65 v/o composites were wound at an intended spacing of 99 per cm (250 per in.) and given two plasma spray passes. As will be discussed subsequently, microscopic examination of some of the composites indicated that this spacing was not actually achieved. All UARL monofilament composites were wound at 88 per cm (224 per in.) and given two plasma spray passes.

The following sections describe the apparatus and procedures used in each of the test areas, and present the results and discuss their significance.

5.1 Filament Strength Characterization

Table X presents tensile strength and modulus data on the rolls of NASA-Hough monofilament and UARL monofilament which were utilized in Task III. In addition to these, lots 1080, 1090, and 1100 were used, the data being previously reported in Table VII. The NASA-Hough monofilament exhibited a good deal of strength variability with portions of some of the lots having very high strength (greater than 2.07 GN/m² (300 ksi)) while other portions of the same lot had low strength. This type of scatter in filament strength would be expected to produce scatter in composite tensile strength. The UARL monofilament appeared to have less scatter in the strength distribution and a higher overall average.

5.2 Tension Testing

All composite materials were tested in tension at room temperature. In addition the 50 v/o and 65 v/o NASA-Hough composites were tested at elevated temperatures. The test specimen for the NASA-Hough composites was .64 cm x .41 cm x .014 cm (1/4 in. x 6 in. x .020 in.). The test specimen for the other materials was .64 cm x 21 cm x .014 cm (1/4 in. x 3 in. x .020 in.).

Table X

Task III
Tensile Strength of Carbon Base Monofilaments

<u>Type</u>	<u>Lot</u>	<u>No. of Tests</u>	<u>Average Strength</u>		<u>Coeff. of Variation (%)</u>	<u>Average Modulus</u>	
			<u>GN/m²</u>	<u>(ksi)</u>		<u>GN/m²</u>	<u>(msi)</u>
NASA-Hough	1030	10	1.35	196	27.5	198	28.7
	1030	10	1.96	284	19.5		
	1050	10	1.82	265	16.2	199	28.9
	1050	10	2.11	306	23.3		
	1120	10	2.01	292	20.9		
	1120	10	2.44	355	22.5		
	1060	10	1.38	201	24.0		
	1050	10	2.30	334	20.9		
UARL	N371	10	2.10	305	22.6		
	N373	10	2.33	338	13.8		
	N376	10	2.38	345	14.1		
	N378	10	1.96	285	37.5		
	N380	10	2.24	321	16.3		

The results of the longitudinal tensile tests at room temperature are presented in Table XI. The data for the 50 v/o NASA-Hough composites were in agreement with the results obtained previously in the program for specimens having a similar volume fraction of filament. Specimen NAS-2B-1 had the highest strength measured, 1.03 GN/m^2 (149 ksi).

The composite tensile tests were performed on specimens reinforced with filament from lots 1070, 1110, 1080, and 1090. The average strength of those lots was 1.5 GN/m^2 (217 ksi) with a coefficient of variation of 28.9 percent. Using those figures the bundle strength of the filament was calculated to be $.93 \text{ GN/m}^2$ (135 ksi) which would lead to a composite strength of $.5 \text{ GN/m}^2$ (72 ksi) assuming no contribution from the matrix. Since the average strength of the composites was $.8 \text{ GN/m}^2$ (116 ksi) the ratio of measured composite strength to calculated strength was 1.6 which is much higher than calculated during Task I testing. This means that either the Task III specimens were of better quality than those of Task I or that the measured filament strengths did not accurately reflect the true strength distribution.

It is quite likely that the composites were of better quality simply due to the fabrication experience gained during the program. However, it is also possible that the measured filament strengths were biased. Approximately $1/4$ of the strength measurements were made on filament taken just after a break had occurred during the tape winding process. Such breaks obviously occurred at weak spots in the filament. If such weak spots were caused by problems in the filament manufacturing process such as temperature fluctuations or improper gas ratios, then it is possible that all filament in the vicinity of the break would be affected to a degree. More testing would be required to clarify this situation.

SEM study of the fracture surfaces of composite tensile specimens indicated a relatively high degree of filament pullout and a fairly poor bond between the filament and the matrix, much as was found during Task II. Figure 14 presents typical views of longitudinal tensile fracture surfaces.

Composites 1918 and 1928 were intended to have low and high filament volume fractions, respectively. The filament volume fraction of 1918 was in the expected range and the composite tensile properties were also in agreement with what would be expected. The tensile strengths measured for 1928 were much lower than anticipated for high volume fraction composites, and microscopic examination of the composite revealed that an error had been made in the filament spacing during the winding of the precursor tape. The tape was to have been wound at a filament spacing of 99 per cm (250 per in.). However, the actual spacing was apparently much less than that although the filaments were so misarranged after hot pressing that it was difficult to determine. Figure 15 shows the fiber distribution of the two composites. Aerial analysis of the composites was made

Table XI

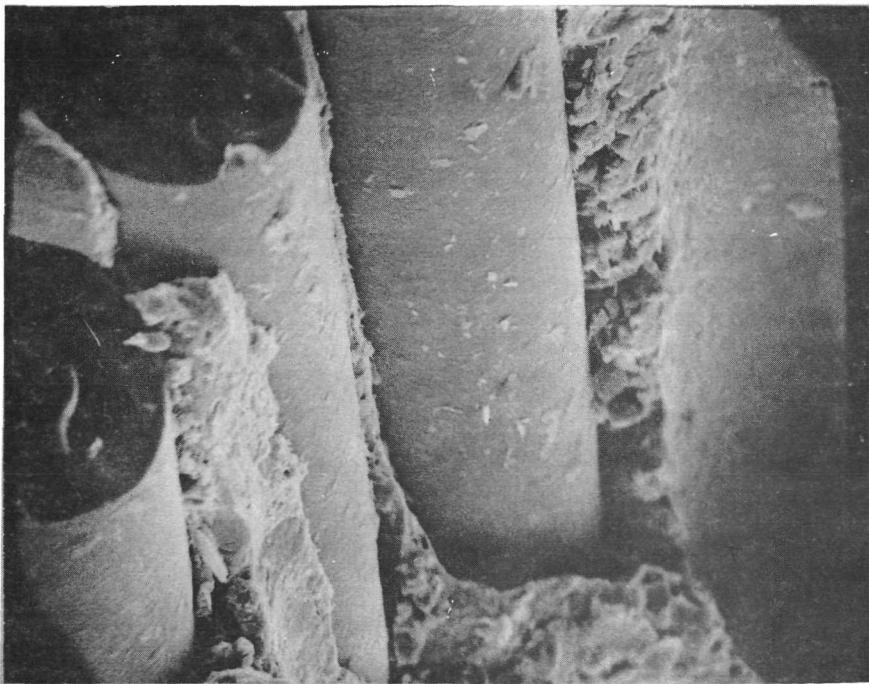
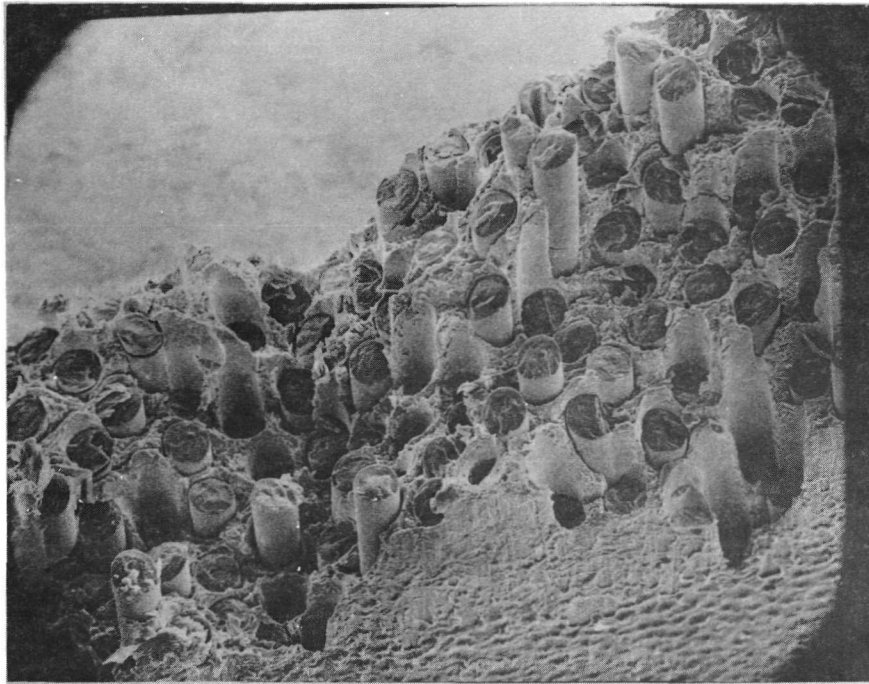
Task III
Longitudinal Tensile Properties
Room Temperature

Description	No.	UTS		Modulus		Failure Strain		Ave. UTS		Ave. Modulus		Ave. Failure Strain %
		GN/m ²	(ksi)	GN/m ²	(msi)	(%)	(%)	GN/m ²	(ksi)	GN/m ²	(msi)	
NASA-Hough 50 v/o	NAS-1B-1	0.742	107.0	114	16.5	0.85						
	-8	0.728	105.5	123	17.8	0.79						
	NAS-1A-1	0.685	99.3	99	14.4	0.82						
	-2	0.768	111.4	108	15.7	0.84		0.800	115.90	109.3	15.84	0.89
	NAS-2B-1	1.03	149.0	117	16.9	1.12						
	-2	0.738	107.0	93	13.5	0.86						
NASA-Hough 35 v/o	NAS-2A-1	0.821	119.0	116	16.8	0.84						
	-2	0.880	129.0	104	15.1	1.00						
	1928-1	0.535	77.5	96	13.9	0.82		0.546	79.15	92.5	13.40	0.84
NASA-Hough 35 v/o	-2	0.557	80.8	89	12.9	0.86						
	1928-1	0.695	100.7	105	15.2	0.89		0.625	90.60	98.3	14.25	0.91
UARL 48 v/o	-2	0.555	80.5	92	13.3	0.93						
	1963-1	0.508	73.7	188	27.2	0.39						
	-2	0.503	73.0	140	20.3	0.46						
	1964-1	0.600	87.0	142	20.6	0.49						
	-2	0.690	100.2	171	24.8	0.53		0.660	95.69	170.7	24.74	0.4313
	1950-1	0.742	107.5	195	28.2	0.45						
UARL 48 v/o	-2	0.674	97.6	164	23.8	0.48						
	1951-1-1	0.689	99.9	171	24.8	0.48						
	-1-2	0.874	126.6	195	28.2	0.56						

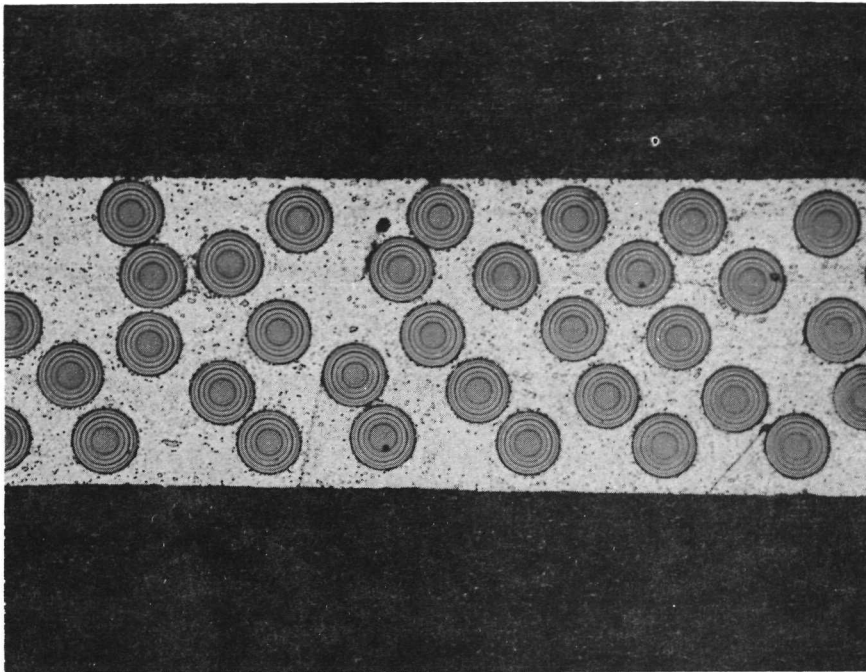
Table XI (Cont'd)

Description	No.	UTS		Modulus		Failure Strain		Ave. UTS		Ave. Modulus		Ave. Failure Strain %
		GN/m ²	(ksi)	GN/m ²	(msi)	(%)		GN/m ²	(ksi)	GN/m ²	(msi)	
Aerospace	1960-1	0.314	45.5	186	27.0	0.18						
	-2	0.217	31.4	162	23.4	0.13						
	1961-1	0.296	42.9	180	26.0	0.19						
	-2	0.359	52.0	186	26.9	0.22						
	1962-1	0.538	77.8	152	22.0	0.46						
	-2	0.532	77.0	143	20.8	0.46						
								0.376	54.43	168.0	24.35	0.273

LONGITUDINAL TENSILE FRACTURE SURFACE
NASA-HOUGH MONOFILAMENT/2024

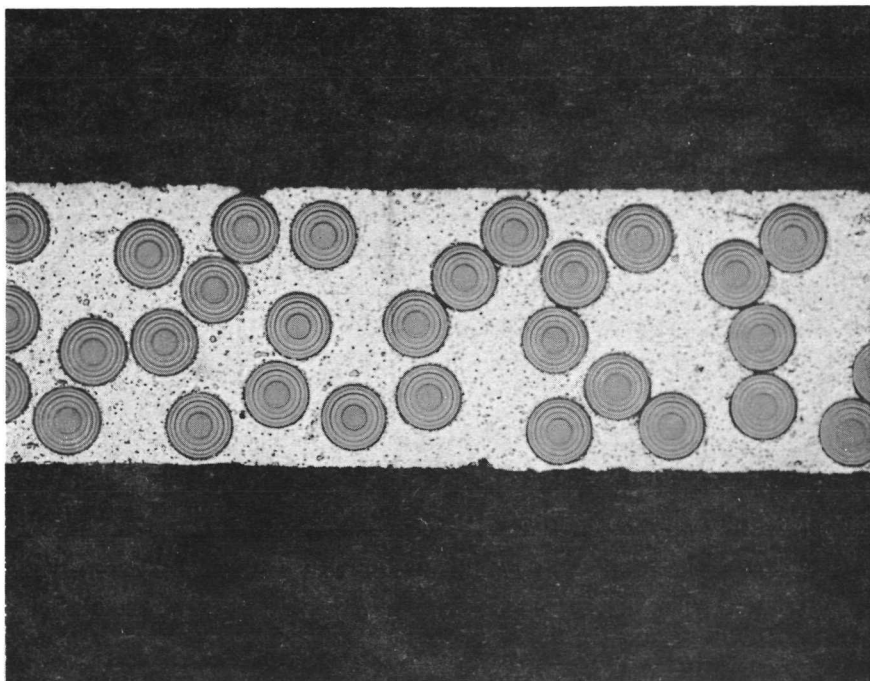


FILAMENT VOLUME FRACTION VARIATION STUDY
NASA-HOUGH/2024



$V_f = 0.35$

COMPOSITE 1918



$V_f = 0.35$

COMPOSITE 1928

at a magnification of 100X and it was found that both had filament volume fractions of about 35 percent. Unfortunately the problem was detected late in the program and there was no time to make additional composites at the proper volume fraction.

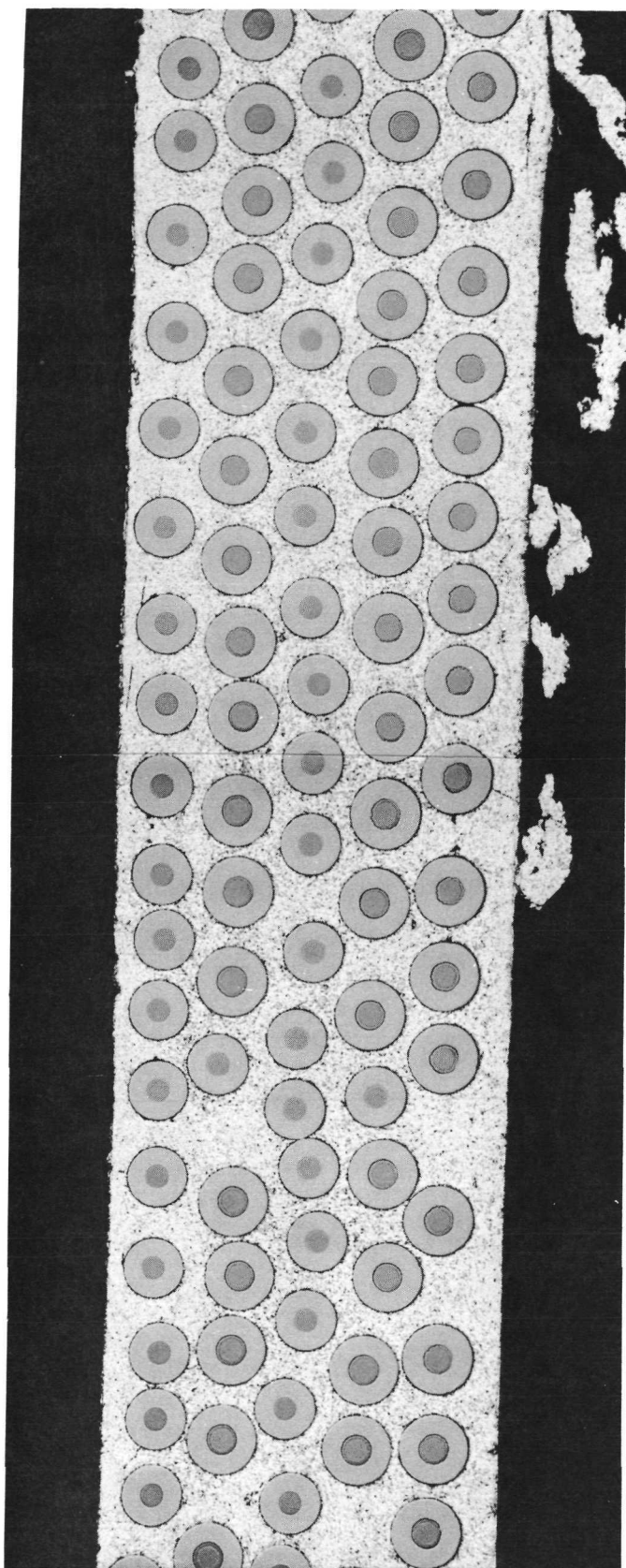
The tensile strengths of the UARL/2024 composites were not as high as anticipated based on the strength of the filament. The composites exhibited a uniform fiber distribution and appeared to be well consolidated as shown in Fig. 16. The photomicrograph does indicate that the particular composite (No. 1963) was reinforced with filament which varied in diameter. Closer examination of the filaments revealed that the larger ones had zones of different composition as shown in Fig. 17. These zones are believed to result from an excessive hot spot ($>1250^{\circ}\text{C}$) in the DC reactor temperature profile. This undoubtedly had an adverse effect on the filament strength and may explain the low tensile strengths of composite 1963. Other UARL composites were examined microscopically (1951-1, 1964) and the fiber diameter was more uniform with no evidence of a reaction zone.

The tensile fracture surface of the UARL composites exhibited much less filament pullout and a better interfacial bond than the NASA-Hough composites. The fracture surfaces were similar in appearance to those of boron-aluminum composites. Figure 18 presents typical views of UARL/2024 after tensile testing. The maximum pullout length was less than one fiber diameter and the filament which was exposed was generally coated with matrix in definite contrast to the appearance of the NASA-Hough composites in Fig. 14. The increased adhesion between the UARL filaments and the aluminum compared with that between the NASA-Hough and aluminum is tentatively attributed to the higher boron content of the former. The boron apparently reacts with the aluminum to a greater degree than does carbon under the hot pressing conditions used in fabricating the composites, thus forming a better bond.

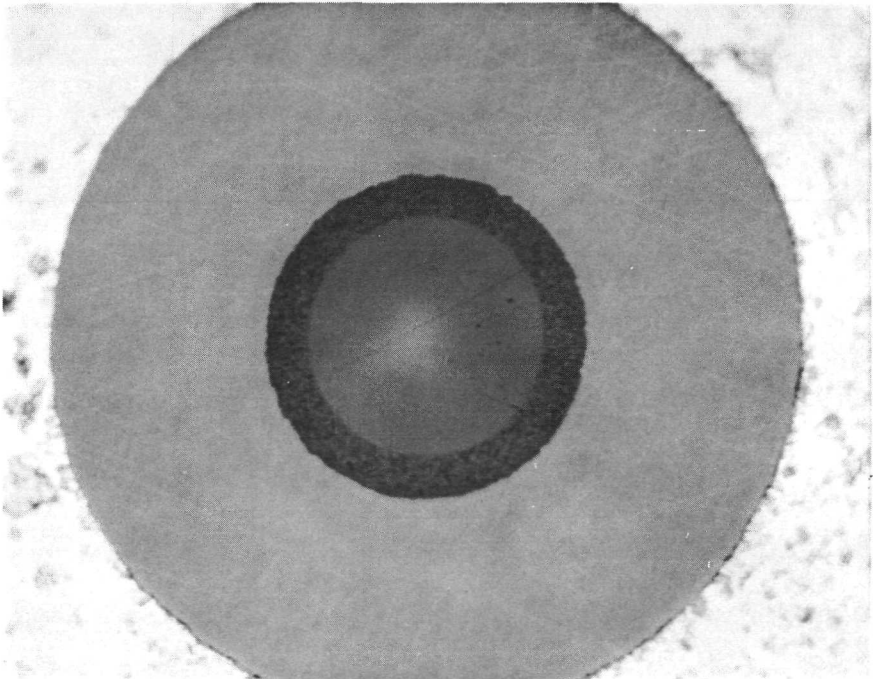
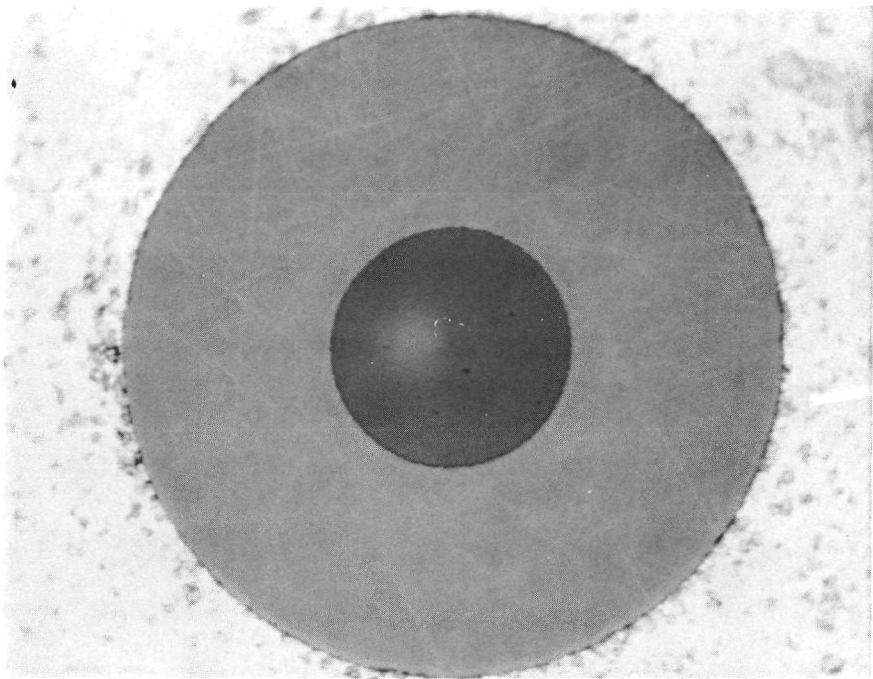
The final material tested in tension during Task III was the Aerospace prepared Thornel 50/526 aluminum. The strengths were generally lower than expected based on published information on the material (Ref. 3). As in Task I, it was found difficult to fabricate void free composites because the aluminum tended to dewet during melt bonding in the hot press. The three composites listed in Table XI were fabricated at different temperature/pressure conditions; 1960 was pressed at 640°C under 345 KN/m^2 (50 psi), 1961 was 640°C and 69 KN/m^2 (10 psi), and 1962 was 600°C and 69 KN/m^2 (10 psi). Obviously the conditions for 1962 were the best of those investigated based on the tensile strength of the composites. The pressure of 69 KN/m^2 (10 psi) was the minimum possible, representing the weight of the upper ram of the hot press.

Elevated temperature longitudinal tensile tests were conducted on NASA-Hough composites at 260°C and 427°C . All specimens were held at temperature for 30 minutes prior to testing. Tests were carried out in an air environment and

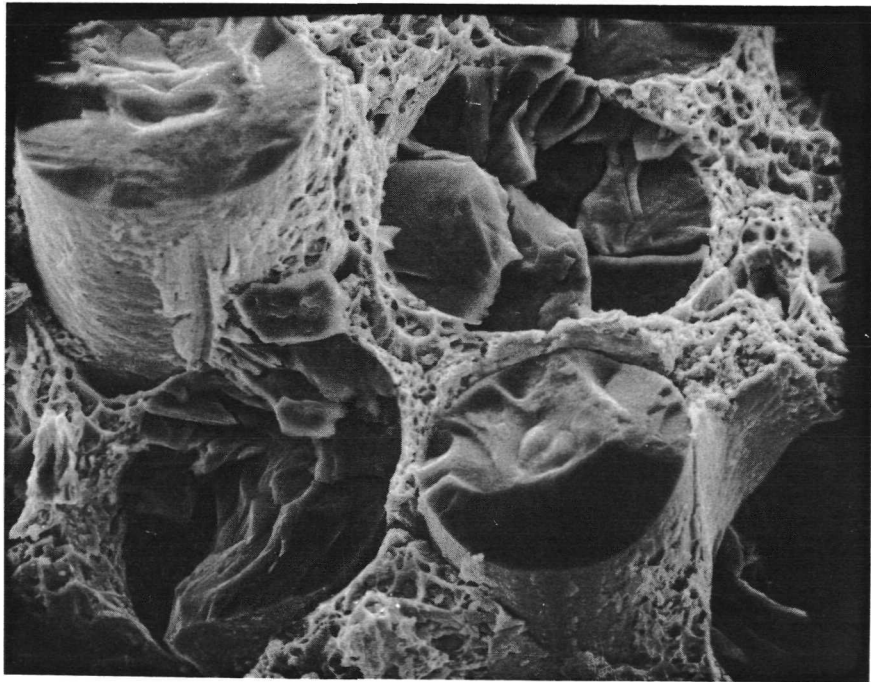
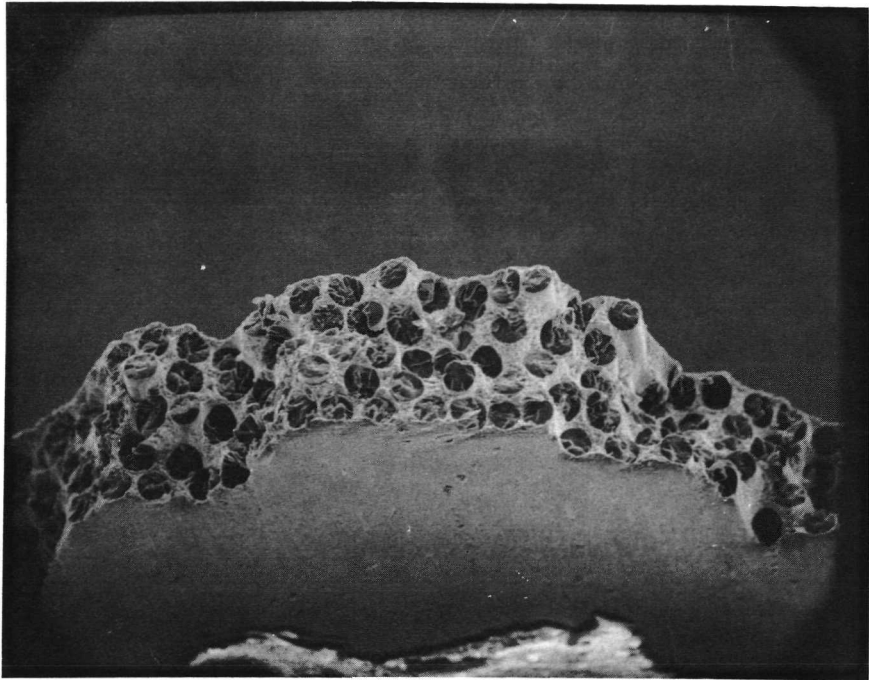
UARL MONOFILAMENT/2024



UARL MONOFILAMENT
COMPOSITE NO. 1963



LONGITUDINAL TENSILE FRACTURE SURFACE
UARL MONOFILAMENT/2024



strain was measured with strain gages. The results of the tests are tabulated in Table XII. The average strength at 260°C was 80.5 percent of the room temperature strength while the 427°C value was 75.8 percent for 50 v/o composites. These retention percentages are comparable to those reported for boron-aluminum (Ref. 5). The strength retention of the 35 v/o composite at 427°C was even better, being 82 percent of the room temperature average.

Figure 19 shows the fracture surface of a specimen tested at 427°C. The filament pullout lengths were even longer than those which were observed in specimens tested at room temperature, and the filaments were again essentially bare. The lack of evidence of shear failure in the matrix suggests that the major interfacial forces were mechanical ones resulting from differential thermal contraction between the filaments and matrix during the cool down from the fabrication temperature. The magnitude of the interfacial stress would be directly proportional to the temperature differential between the fabrication temperature and the temperature at which the tensile specimens were tested. At room temperature the ΔT would be approximately 430°C, while at 427°C the ΔT would be only 20°C resulting in a very low residual stress at the interface.

The results of the room temperature transverse tensile tests on NASA-Hough composites are presented in Table XIII. The results were generally similar to those obtained in previous portions of the program. The strengths were very low, 57 MN/m² (8.3 ksi) on the average. The failure strains and moduli were also quite low. The low strain to failure is not surprising in view of the poor interfacial bond, but the modulus values indicate the possibility of anisotropic behavior of the filament. Assuming a transverse composite modulus of 83 GN/m² (12 msi) which was the highest measured, the analysis of Adams, Doner, and Thomas (Ref. 6) was used to determine the fiber modulus which would produce that value for a 50 v/o composite having a matrix modulus of 69 GN/m² (10 msi). The calculated value was 103 GN/m² (15 msi) compared to 193 GN/m² (28 msi) measured in the longitudinal direction. This result is somewhat complicated by the poor interfacial condition in the composites in that large strains may have occurred locally at the interface which produced a low overall composite modulus. This seems unlikely, however, at the very low strain levels at which the composite transverse tensile moduli were measured. Thus, the most logical conclusion is that the NASA-Hough filament is anisotropic.

The poor transverse tensile strength is considered to be a problem which must be overcome if the composites are to be useful. The low transverse strain capability means that off-axis behavior will severely limit the load carrying ability of multidirectional composites.

The elevated temperature transverse tensile data are listed in Table XIV. The results reflect the poor properties at room temperature.

Table XII

Task III
 Longitudinal Tensile Properties
 Elevated Temperature
 NASA-Hough Monofilament/2024

<u>No.</u>	<u>Temp.</u> <u>(°C)</u>	<u>V_f</u> <u>(%)</u>	<u>UTS</u>		<u>Modulus</u>		<u>Failure</u> <u>Strain</u> <u>(%)</u>
			<u>GN/m²</u>	<u>(ksi)</u>	<u>GN/m²</u>	<u>(msi)</u>	
NAS-1A-17	260	50	.695	99.3	126	18.2	0.63
NAS-1B-17	260	50	.550	79.6	114	16.6	0.56
NAS-1B-19	260	50	<u>.702</u>	<u>102.0</u>	112	16.3	0.75
Ave.			.645	93.5			
NAS-1B-18	427	50	.697	101.0	102	14.8	0.76
NAS-1B-20	427	50	.558	80.9	121	17.5	0.50
NAS-2A-20	427	50	.571	82.8	113	16.4	0.63
NAS-2A-21	427	50	<u>.605</u>	<u>87.6</u>	90	13.0	-
Ave.			.608	88.0			
1930-1	427	35	.504	73.1	-	-	-
1930-2	427	35	.478	69.3	-	-	-

LONGITUDINAL TENSION FRACTURE SURFACE

TEST TEMP: 427°C

NASA-HOUGH MONOFILAMENT/2024

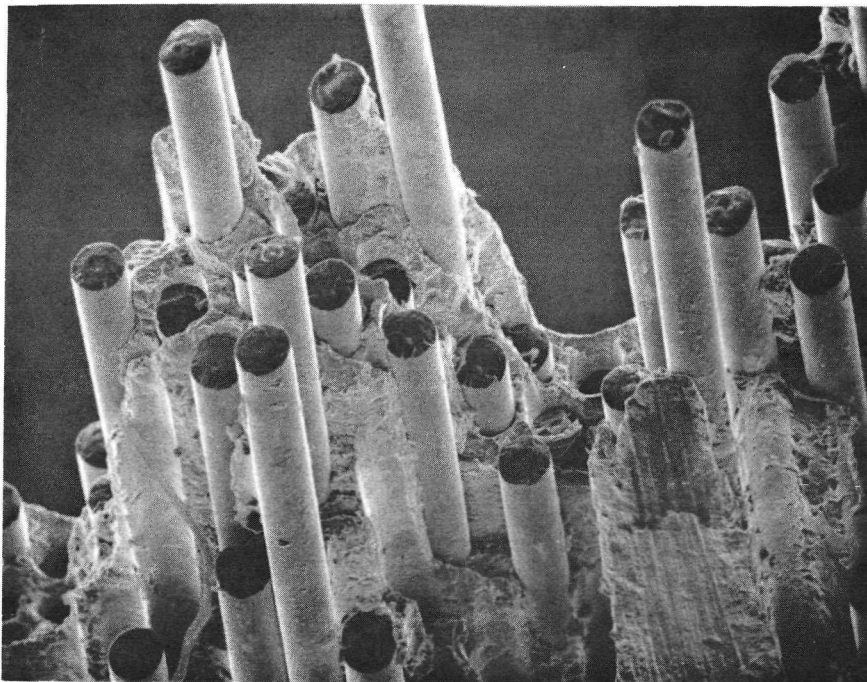


Table XIII

Task III
 Transverse Tensile Properties
 Room Temperature

<u>No.</u>	<u>UTS</u>		<u>Modulus</u>		<u>Failure</u>
	<u>GN/m²</u>	<u>(ksi)</u>	<u>GN/m²</u>	<u>(msi)</u>	<u>Strain</u>
					<u>%</u>
NAS-1B-21a	.069	10.0	79	11.5	.105
NAS-1B-21b	.068	9.9	83	12.0	.093
NAS-1A-21	.046	6.7	52	7.5	.09
NAS-1A-22	.045	6.5	70	10.2	.06
NAS-2A-3	.053	7.7	58	8.4	.13
NAS-2A-4	.061	8.9	78	11.3	.093

Table XIV

Task III
 Transverse Tensile Properties
 Elevated Temperature

<u>No.</u>	<u>Temp.</u> <u>(°C)</u>	<u>UTS</u>		<u>Modulus</u>		<u>Failure</u> <u>Strain</u> <u>(%)</u>
		<u>MN/m²</u>	<u>(ksi)</u>	<u>GN/m²</u>	<u>(msi)</u>	
NAS-1B-26a	260	30	4.3	48	7.0	.093
NAS-1B-26b	260	27	3.9	64	9.3	.050
NAS-2A-27a	260	42	6.1	51	7.4	.163
NAS-2A-27b	260	39	5.6	59	8.4	.105
NAS-1B-27a	427	10	1.5	33	4.8	.29
NAS-1B-27b	427	11	1.6	43	6.2	.07
NAS-1A-29a	427	7.6	1.1	31	4.5	.14
NAS-1A-29b	427	19	2.7	52	7.5	.26

5.3 Stress-Rupture and Creep

5.3.1 Experimental Procedure

Stress-rupture tests were carried out at 260°C and 427°C in constant load machines, the temperature being monitored with chromel-alumel thermocouples positioned adjacent to the specimen. Friction type grips were used with copper doublers to protect the specimen surface. The machines shut off automatically upon fracture of the sample and the time to rupture was recorded to the nearest 0.1 hr. The intent of the tests was to measure the stress to rupture at 100 hrs for each temperature.

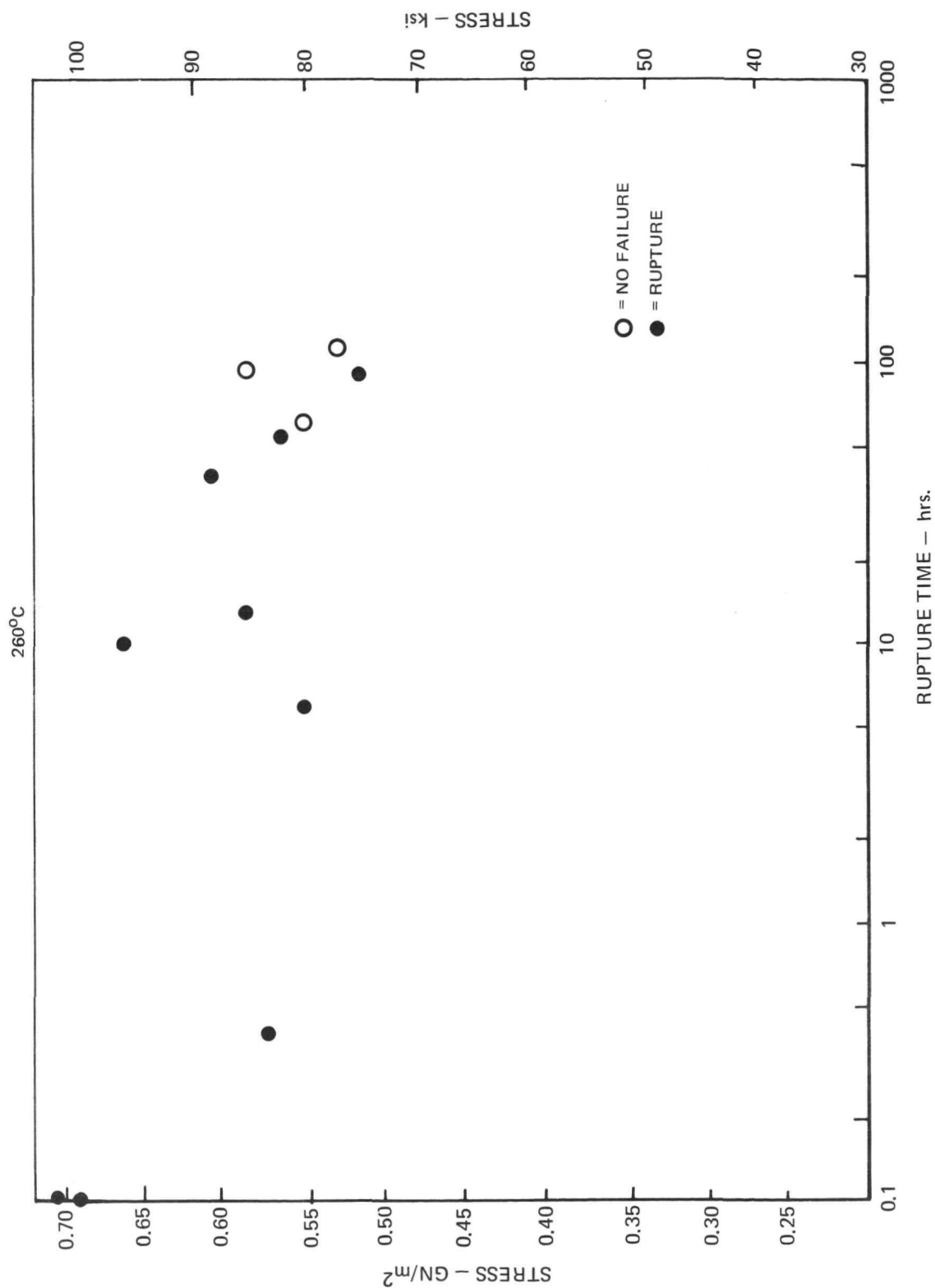
Creep tests were conducted at 427°C only. The test machine was similar to those used for stress rupture except that elongation was continuously recorded during the test by means of an extensometer activated LVDT. The extensometer was attached to the grips holding the specimen.

5.3.2 Results and Discussion

The results of the stress-rupture tests at 260°C and 427°C are summarized in Figs. 20 and 21, respectively. The data at 260°C indicated very little difference between the stress to rupture in 100 hrs versus that which produced failure in a static tension test. The average static tensile strength was .635 GN/m² (92 ksi), while the stress to rupture in 100 hrs was approximately .55 GN/m² (80 ksi).

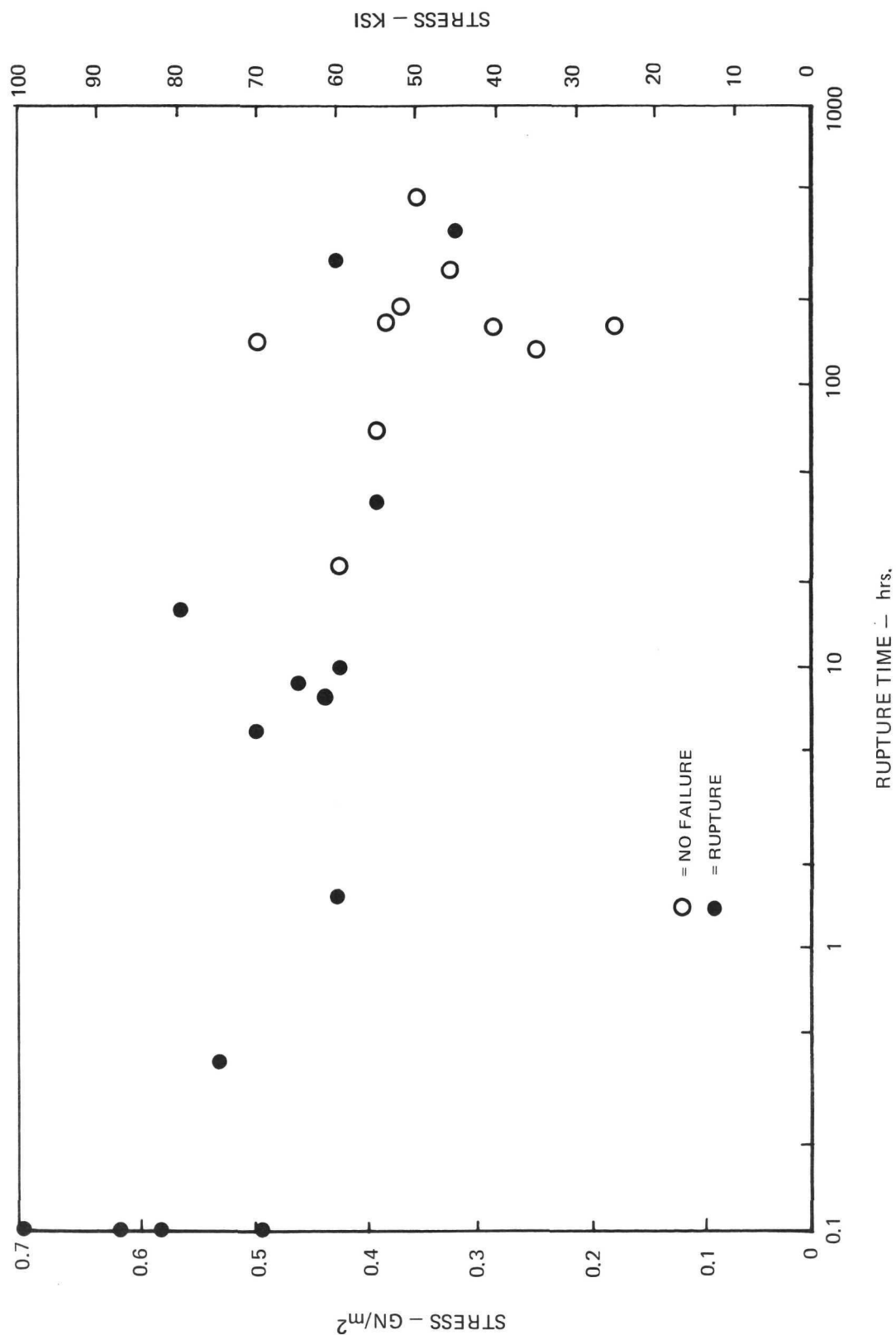
The tests at 427°C showed a somewhat greater effect. The average static strength was .59 GN/m² (86 ksi) while the stress to rupture in 100 hrs was approximately .41 GN/m² (60 ksi) although one specimen ran for 145 hrs at .48 GN/m² (70 ksi).

The behavior of the NASA-Hough composites compares very favorably with published information on the stress-rupture performance of BORSIC-6061 aluminum. Breinan and Kreider (Ref. 7) conducted tests at 300°C, 400°C, and 500°C and found 100 hr rupture stresses of approximately .69 GN/m² (100 ksi), .62 GN/m² (90 ksi) and .48 GN/m² (70 ksi) respectively. At 400°C, the 100 hr stress to rupture 37 v/o boron-6061 was found to be only about .28 GN/m² (40 ksi) or .35 GN/m² (50 ksi) when normalized to 50 v/o composites. The relatively poor behavior of boron-aluminum was attributed to chemical reaction between the boron filament and the aluminum which resulted in degradation of the filaments. Although there is no direct comparison because of the different test temperatures involved, it appears that NASA-Hough composites are very similar to BORSIC-aluminum in terms of absolute stress required to rupture in 100 hrs and better than boron-aluminum.

STRESS-RUPTURE
NASA-HOUGH CARBON/2024 ALUMINUM



427°C



A fracture surface of a specimen tested at 427°C was examined in the scanning electron microscope. Figure 22 shows typical views of the specimen. There was much more matrix shear failure than in the specimen which was tested in static tension at 427°C (see Fig. 19). This trend is in agreement with the observations of Ref. 7.

The creep data obtained at 427°C are presented in Table XV, and a typical creep curve is shown in Fig. 23. The creep rates were very low as would be expected since the elastic filaments were carrying the tensile loads. The data do indicate some dependence on stress level in that somewhat higher creep rates were associated with higher stress levels. Creep would be expected to be a more significant problem in structural configurations (multidirectional) in which tensile loads were applied in directions other than along the filament axis. Creep of unidirectional BORSIC-aluminum was also found to be very low in Ref. 7.

5.4 Mechanical Fatigue

5.4.1 Experimental Procedure

Cantilever bending tests were performed on unidirectional NASA-Hough composites at a testing speed of 3600 cpm. Bending loading was selected rather than axial loading because unidirectional composites have generally been found to be fairly insensitive to axial fatigue due to the elastic nature of the filaments. Under bending fatigue, both the filaments and the matrix can be highly stressed. Furthermore, bending fatigue response is an important design consideration for structures such as gas turbine engine blades which represents an important potential application for carbon-aluminum.

The test specimen was .64 cm x 21 cm x .014 cm (1/4 in. x 3 in. x .020 in.) with a 2.54 cm (1 in.) cantilever length. Small aluminum doublers were bonded to the specimen at the point of load introduction to minimize stress concentrations and wear. One method used to measure damage to the specimens as a result of fatigue was to determine the bending stiffness of the specimen before and after the test. This was accomplished by incremental dead weight loading the specimen. A lightweight 25.4 cm (10 in.) pointer was attached to the end to measure the deflection. This technique has been used successfully by UARL in determining the modulus reduction of resin matrix composites due to fatigue (Ref. 8). It was found that internal damage in the form of cracks and delaminations occurred before any gross damage was visible. The internal damage resulted in stiffness losses which could be used as a failure criterion in structures. The other specimen failure criterion was visible bending or delamination fracture.

NASA-HOUGH/2024 STRESS-RUPTURE

427°C, 0.39GN/m² (55ksi), 39 HOURS

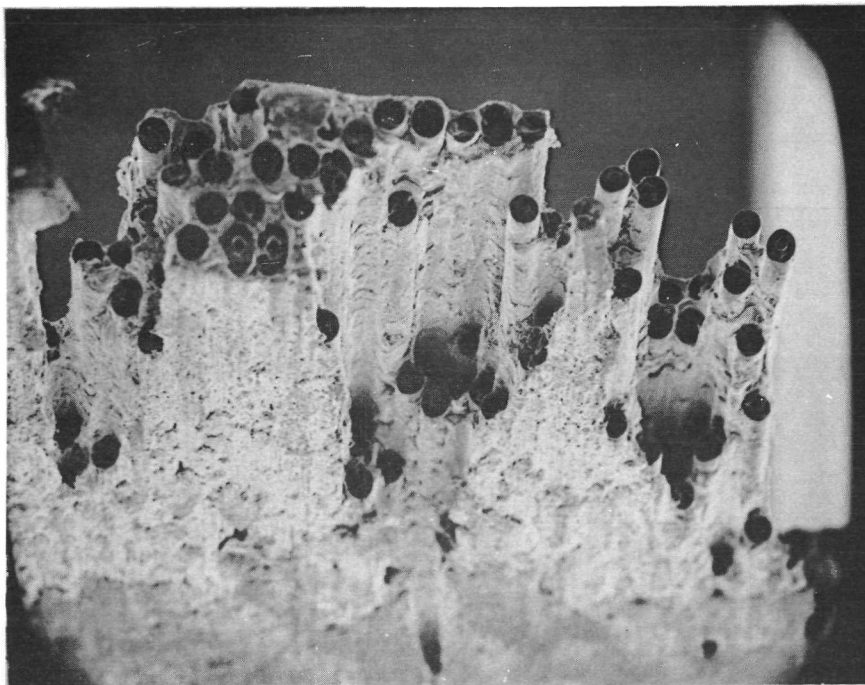
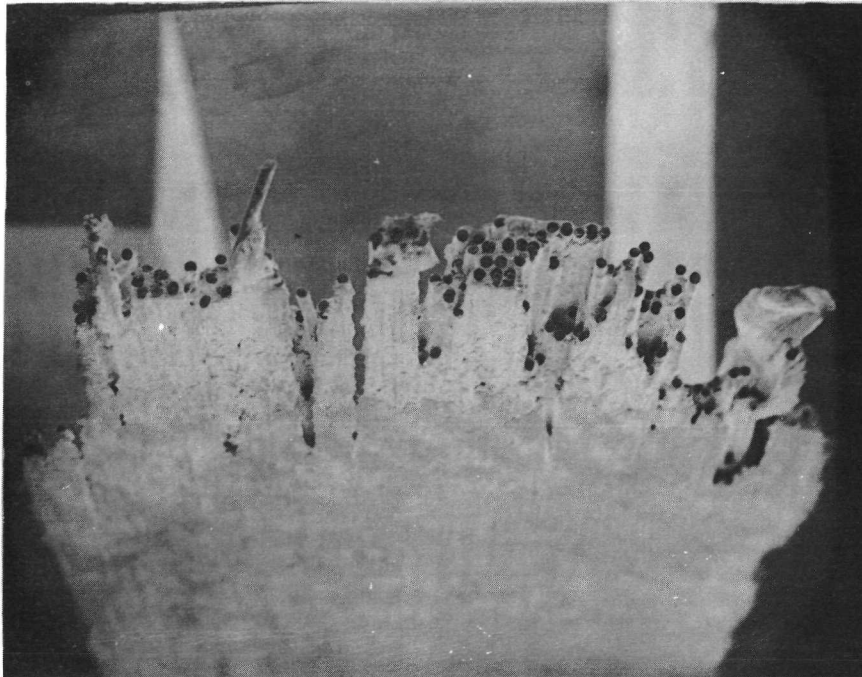


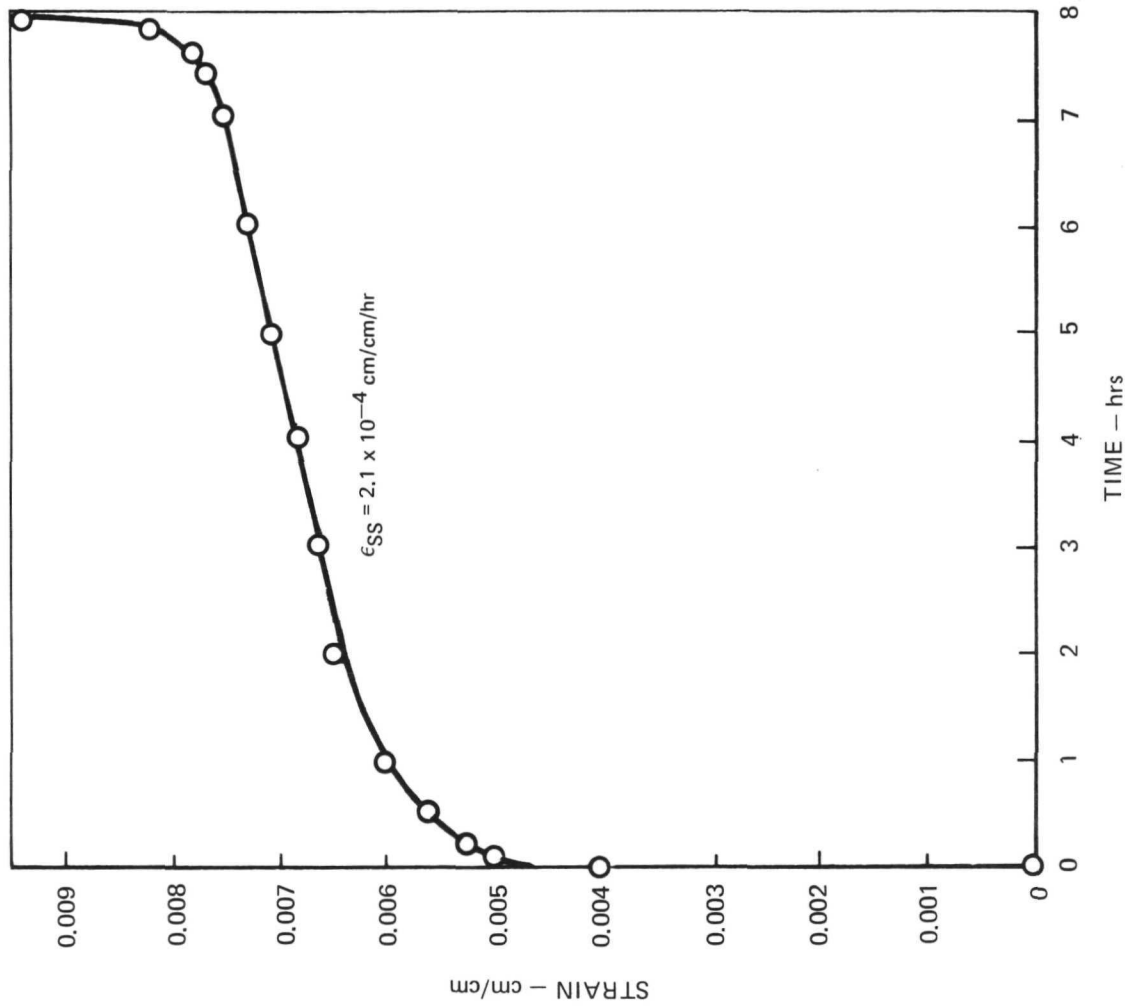
Table XV

Creep Test Data
NASA-Hough Monofilament/2024 Aluminum
Test Temperature: 427°C

<u>No.</u>	Stress		Time (hrs)	Steady State
	<u>GN/m</u>	<u>(ksi)</u>		Creep Rate <u>(cm/cm/hr)</u>
NAS-2A-19	.38	55	70	6.6×10^{-6}
NAS-2B-13	.43	62	7	2.1×10^{-4}
NAS-2B-12	.45	65	8	2.5×10^{-4}
NAS-2B-11	.48	70	6	4.8×10^{-4}

CREEP
NASA-HOUGH CARBON/2024 ALUMINUM

427°C
0.428 GN/m² (62 ksi)



5.4.2 Results and Discussion

The S-N data for specimens which actually failed either by bending fracture or severe delamination are presented graphically in Fig. 24. The results show a flat S-N behavior, much as would be expected under axial fatigue loading. It is possible that some of the failures were associated with problems in testing. The specimens were quite thin and dynamic effects may have produced higher stresses than were calculated from simple cantilever bending theory due to excitation of higher frequency modes. Similar problems were encountered previously in testing resin matrix composites and it was found that increasing the specimen stiffness by making it thicker alleviated the problem. The specimens used in this study were cut from large panels, the thickness of which was determined by material availability and optimum dimensions for tensile testing, the test most widely used in the program.

Several specimens were runouts at 10^6 cycles. The residual modulus measurements on these specimens indicated that damage did occur, however. Figure 25 shows the bending modulus retention of all specimens run for 10^6 cycles versus the alternating bending stress level. The two specimens with approximately 60 percent modulus retention were plotted as failures in Fig. 24 because they both contained visible delaminations. From Fig. 25 it is clear that if modulus retention is an important design parameter, then it is not sufficient to use visible fracture of the specimen as a failure criterion. Although a failure analysis of the specimens was not conducted, it is likely that the modulus reduction was caused by localized fiber-matrix debonding which led to larger cracks, similar to what has been observed in resin matrix composites. This type of failure would be minimized by improving the bond strength between the fiber and the matrix.

5.5 Thermal Fatigue

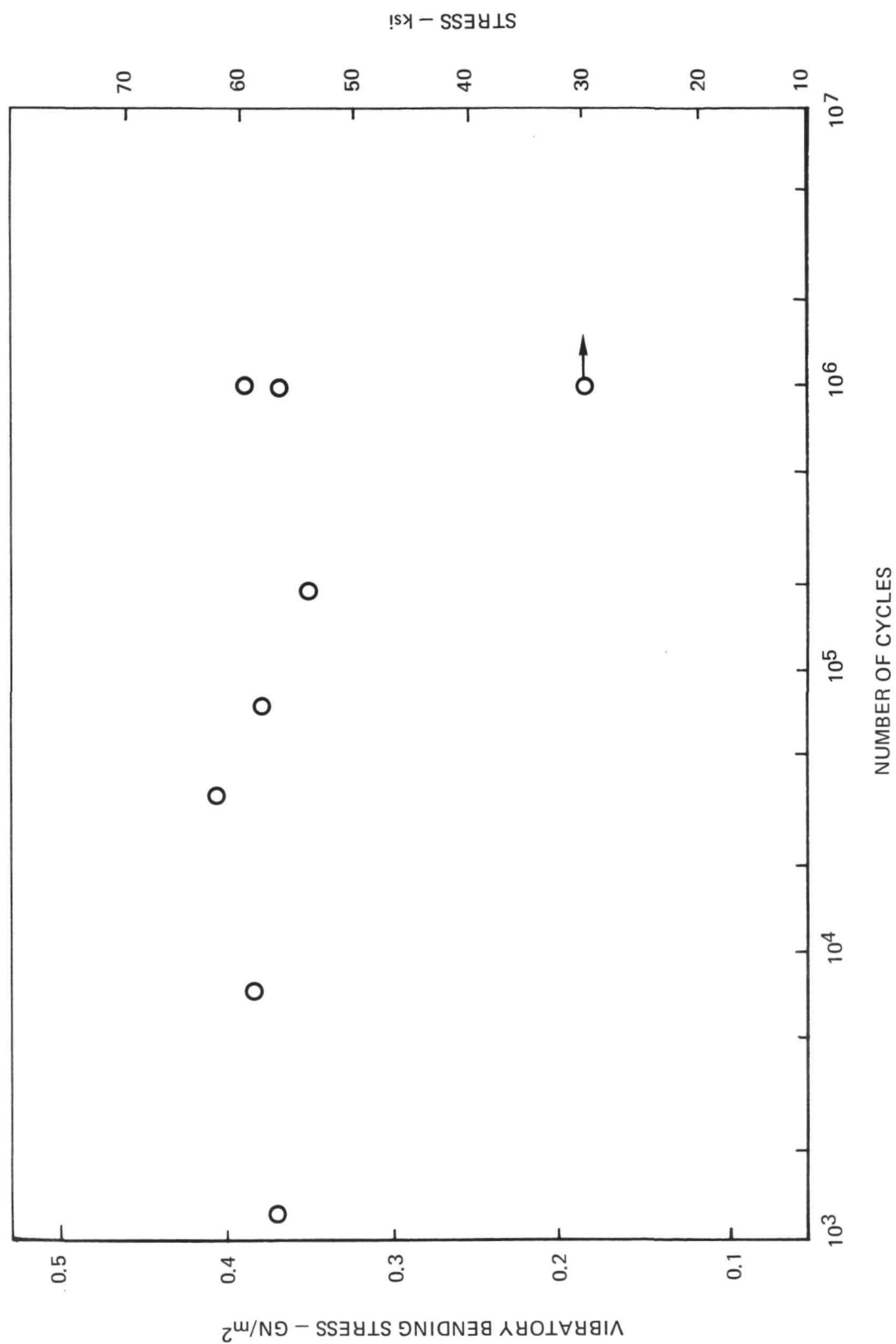
5.5.1 Experimental Procedure

Composite thermal fatigue tests were conducted over a series of temperature ranges for various numbers of cycles as outlined below:

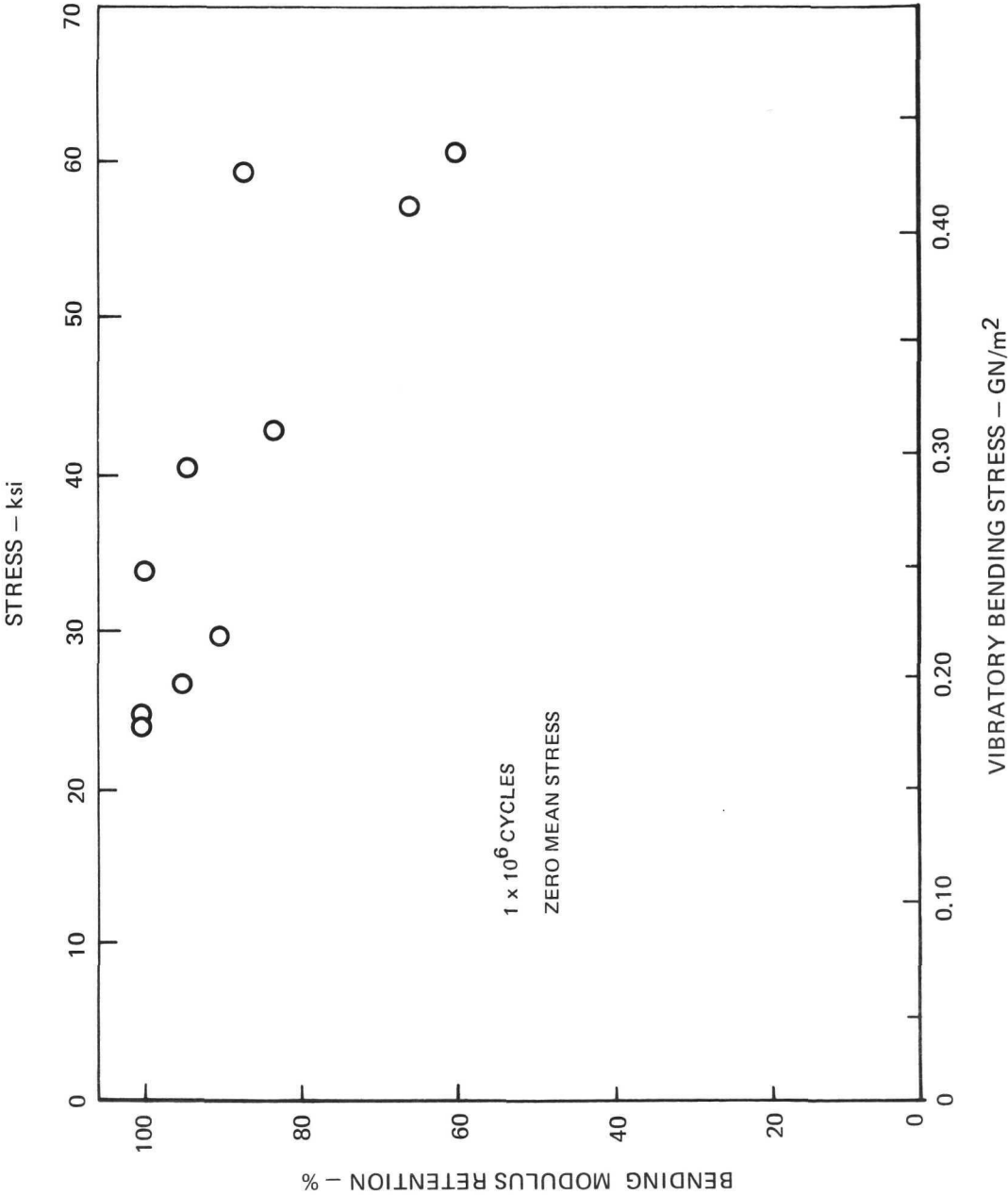
<u>Temp. Range</u> <u>(°C)</u>	<u>No. of Cycles</u>
RT → 260	250, 500, 750, 1000
RT → 427	250, 500, 750, 1000
-160 → 260	500, 1000
-160 → 427	500, 1000

Materials tested included NASA-Hough and UARL monofilament/2024 aluminum and Thornel-50/526 aluminum infiltrated by Aerospace.

BENDING FATIGUE
NASA-HOUGH CARBON/2024 ALUMINUM
ZERO MEAN STRESS



BENDING FATIGUE
NASA-HOUGH CARBON/2024 ALUMINUM



The thermal cycling apparatus consisted of a vertical tube furnace and a motor driven screw which was used to raise the specimens into the furnace for heating, then lower the specimens out of the furnace for cooling. When the desired lower temperature was room temperature, fans were used to cool the specimens as they were lowered out of the furnace. The lower temperature limit of -160°C was achieved by lowering the specimens into a thin walled copper tube which was placed in a dewar flask filled with liquid nitrogen. The number of cycles was monitored with an automatic counter. Each heating and cooling cycle took approximately five minutes.

Following the thermal cycling the specimens were tested in tension at room temperature and the results were compared to base line room temperature tensile data reported previously. For the 50 v/o NASA-Hough composites only one specimen was tested per condition so typical scatter in the data might have a large effect on the result of a given test. Consequently, it is necessary to consider all the data for a set of conditions to determine trends. The other composites involved two test specimens per condition.

5.5.2 Results and Discussion

The results of cycling NASA-Hough composites between room temperature and 260°C are presented in Fig. 26 which compares the base line room temperature tensile strength with that of the thermally-cycled specimens after various numbers of cycles. The longitudinal specimens showed very little, if any, effect even after 1000 cycles. The residual strength of the 1000 cycle specimen was $.687 \text{ GN/m}^2$ (99.5 ksi) which is within the scatter of the base line measurements. There was also no distortion of the specimens after exposure.

The transverse tensile specimens also showed no effect in terms of strength reduction, although some of the specimens were slightly distorted. The low strength after 750 cycles is felt to be the result of scatter since the specimen cycled for 1000 cycles retained the base line strength.

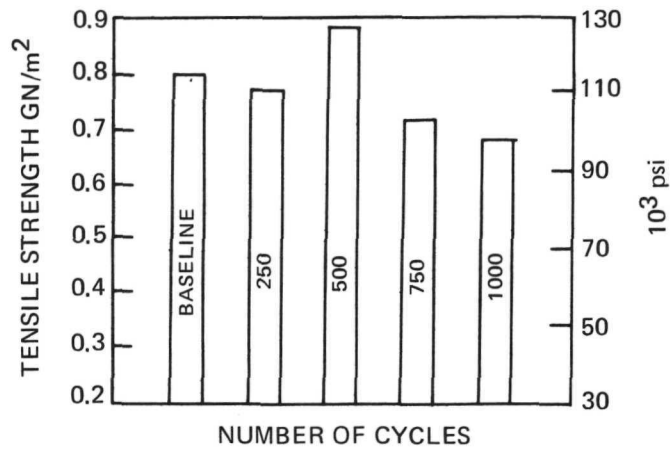
Thermal cycling between room temperature and 427°C had a more pronounced effect as indicated in Fig. 27. The transverse tensile specimens were so badly distorted that they were not tested; in fact some broke during removal from the thermal fatigue fixture. The specimen pictured on edge in Fig. 27 was cycled only 250 times. Those cycled 500 and 750 times suffered even more distortion. The implication of this behavior is that off-axis plies in multidirectional composites may suffer damage during thermal cycling. Plastic deformation of the type shown in Fig. 27 could not occur in multidirectional composites due to the restraint of adjacent plies and cracking might result.

**THERMAL FATIGUE
NASA-HOUGH/2024 COMPOSITES**

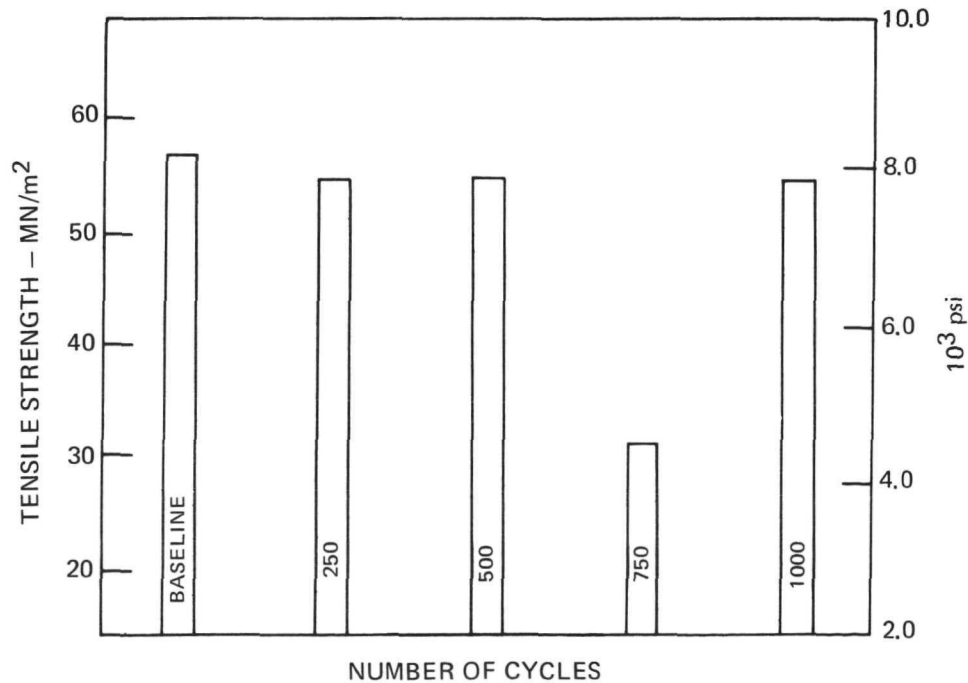
R.T. \rightarrow 260°C

$V_f = 0.5$

LONGITUDINAL SPECIMENS



TRANSVERSE SPECIMENS



**THERMAL FATIGUE
NASA-HOUGH/2024
TRANSVERSE REINFORCEMENT**

250 CYCLES: R.T. → 427°C

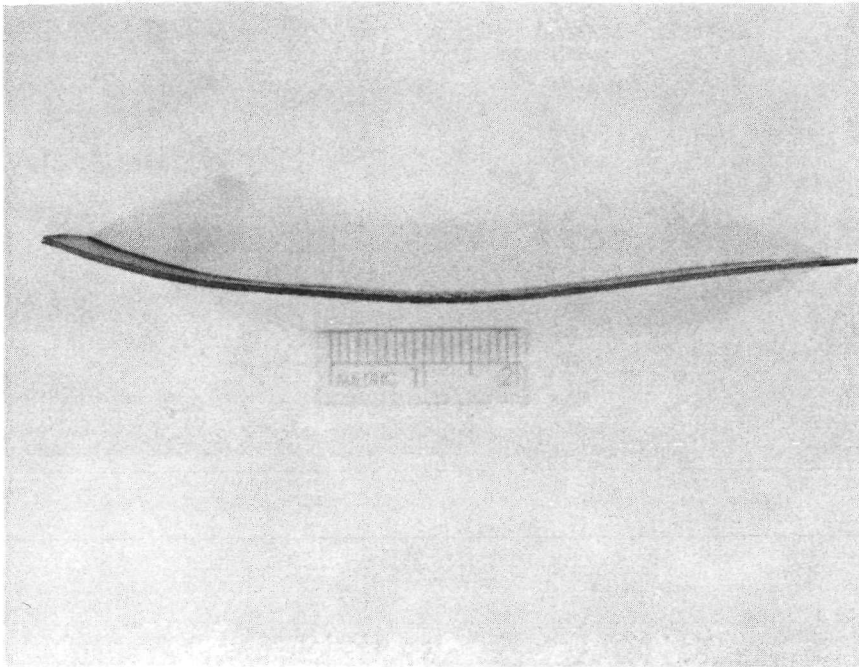


Figure 28 presents the R.T. \rightarrow 427°C thermal cycling data for several materials reinforced in the longitudinal direction. The results were somewhat unclear for the 50 percent NASA-Hough material. The good strength retention after 750 cycles cast some suspicion on the low value after 500 cycles, but the specimen cycled for 1000 cycles was also low in strength. Both the 500 and 1000 cycle specimens were taken from panel NAS-2, while the 250 and 750 cycle specimens were taken from NAS-1. The two NAS-2 specimens were examined microscopically and, as shown in Fig. 29, were found to contain a high degree of poorly consolidated matrix. Most of the porosity visible in the composites was the result of unconsolidated plasma-sprayed matrix being pulled out of the specimen during polishing. At first it was felt that the thermal cycling might have contributed to the matrix failure, but microscopic examination of other untested portions of the panel revealed that the porosity was the result of fabrication.

Examination of Fig. 29 shows that the poor consolidation most likely had to do with the nature of the plasma sprayed tape. Whenever filaments were missing in the tape due to breakage during winding the local pressure during hot pressing was lower and consolidation was poor.

The static tensile properties of uncycled specimens from NAS-2 were the same as those of NAS-1 (Table XI) so the thermal cycling apparently did have an effect on those specimens which were not well consolidated. Micros of specimens from NAS-1 revealed a very good microstructure and the 250 and 750 cycles to 427°C did not have much effect on specimens from that panel. This work points out the importance of uniformity in the precursor tape, especially in making large, thin parts.

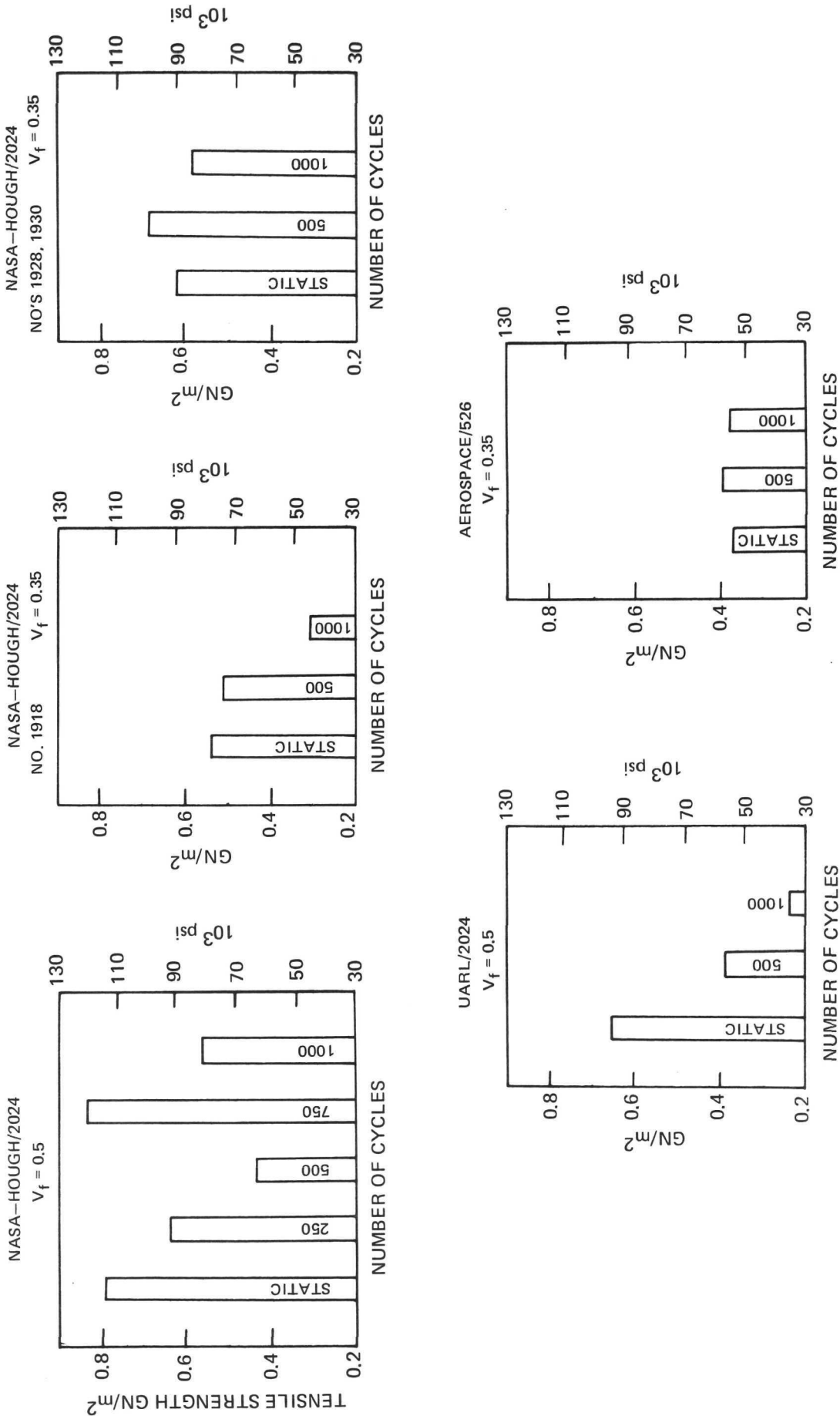
The thermal fatigue data for composite 1918 having a volume fraction of 0.35 indicate a greater susceptibility for low volume fraction composites. Two specimens were run at each condition and the individual specimens tested for 1000 cycles had strengths of .43 and .20 GN/m² (63 and 29 ksi). The composite was well consolidated (Fig. 15) and there is no explanation for the very low value.

Composites 1928 and 1930 were intended to be high volume fraction materials but as discussed previously were the same as 1918. The thermal fatigue data for those composites indicated no tendency toward strength loss. Thus considering all the low volume fraction data (composites 1918, 1928, and 1930) it was concluded that the composites were not adversely affected by the RT \rightarrow 427°C thermal cycle for up to 1000 cycles.

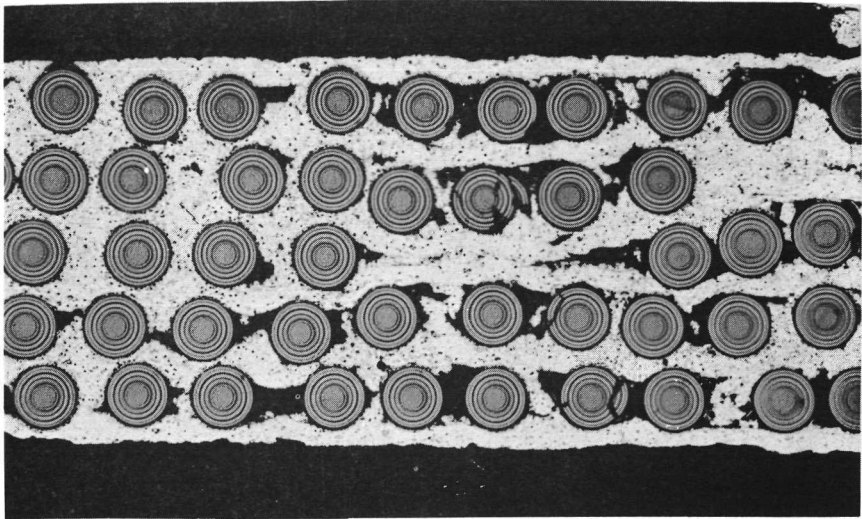
The data for the UARL composites indicated a large degradation of composite strength, however, the quality of the composites may again have been a factor in the results. Figure 30 shows a typical cross section of an untested portion of composite 1951, the one used for the thermal cycling. Due to the variation in

THERMAL FATIGUE

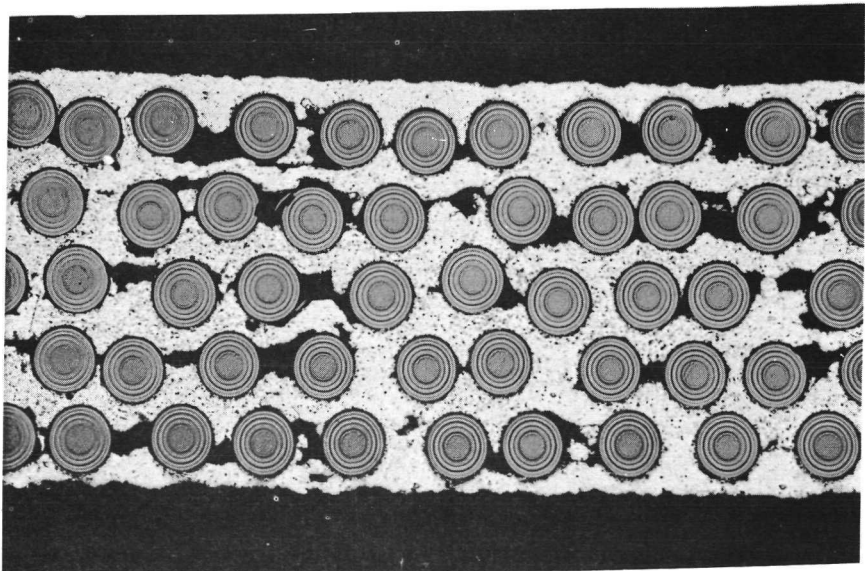
R.T. → 427°C



THERMAL FATIGUE SPECIMENS
50 V/O NASA-HOUGH/2024

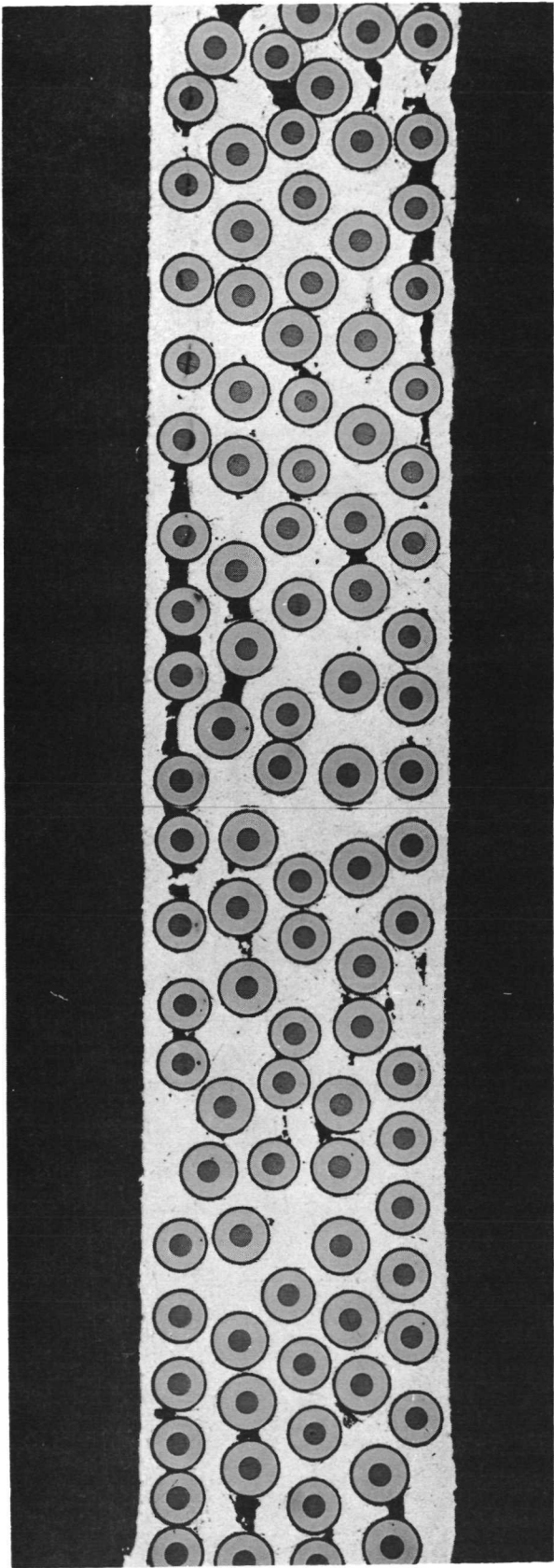


500 CYCLES R.T. → 427°C
SPECIMEN NAS-2A-13



1000 CYCLES R.T. → 427°C
SPECIMEN NAS-2A-14

UARL/2024
UNTESTED COMPOSITE
NO. 1951



fiber diameter and the fact that several breaks occurred during the winding and plasma spraying of the tape, the composite was not well consolidated. Figure 31, which is a photomicrograph of a UARL/2024 specimen after 1000 cycles between RT and 427°C, appears worse than the uncycled specimen in terms of void content (unconsolidated matrix). This may have been due to variation in the quality of the original composite from place to place, or the thermal cycling may have caused interfacial failure. In any event it is clear that poorly consolidated UARL composites are very susceptible to thermal fatigue up to 427°C. This is not too surprising since the fibers contain a large amount of boron which is susceptible to degradation at that temperature. Additional tests carried out between -160 and +427°C indicated that the composite quality played a role in the particularly poor response indicated in Fig. 28. These tests will be discussed subsequently.

The Aerospace T-50/526 composites showed no apparent effect of either 500 or 1000 cycles between RT and 427°C. Metallographic examination of cycled and uncycled specimens revealed no change in microstructure.

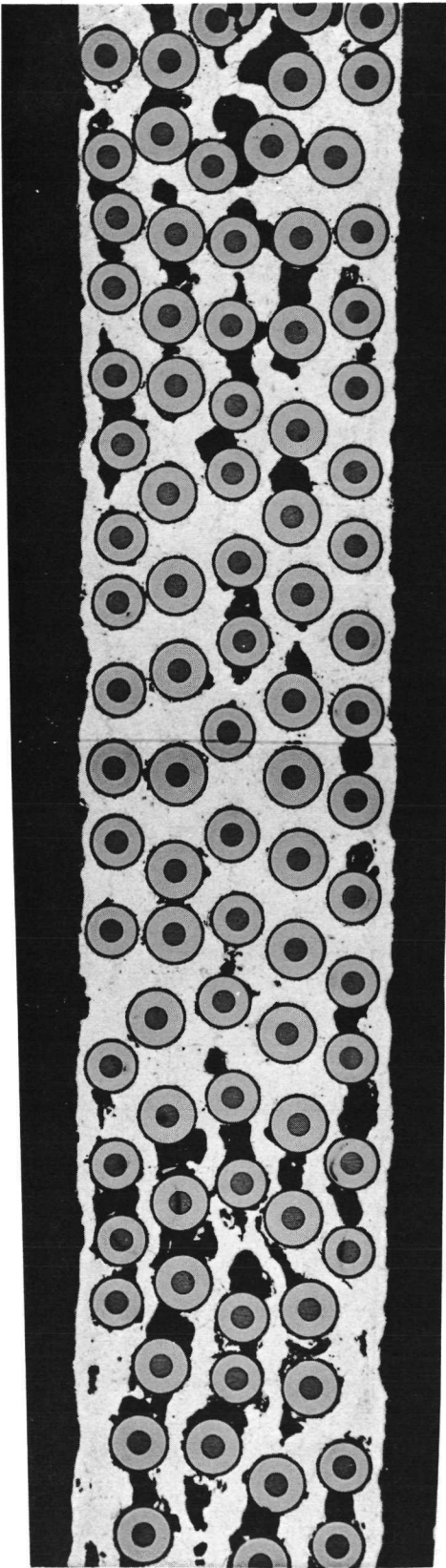
The NASA-Hough and UARL composites were also cycled between cryogenic (-160°C) and elevated temperatures. NASA-Hough composites were cycled between -160°C and +260 and +427°C, while the UARL composites were cycled between -160°C and +427°C only. The results of the tests shown in Fig. 32 imply that the larger ΔT , especially that associated with the higher upper temperature, is sufficient to cause damage to the specimens. Cycling the NASA-Hough composites between -160°C and +260°C did not seem to have an effect. It should be noted that the ΔT in this test (420°C) was not much different than in the RT \rightarrow 427°C test discussed previously. Thus, any degradation caused by thermal stress rather than high temperature exposure should not differ greatly in the two thermal cycles. This was the case in these tests.

The specimens cycled between -160°C and +427°C resulted in definite damage to both NASA-Hough and UARL materials, especially after 1000 cycles. It is interesting to note that the UARL specimens for this series of tests were taken from a different composite than was used for the previous tests where room temperature was the lower limit. A photomicrograph from an untested portion of the composite shown in Fig. 33 indicates the excellent quality of the material. This was perhaps reflected in the good performance after 500 thermal fatigue cycles compared with that of the NASA-Hough composites. An additional 500 cycles, however, had a drastic effect on the residual strength of the UARL composites. The NASA-Hough composites were also severely degraded after 1000 cycles between -160°C and +427°C.

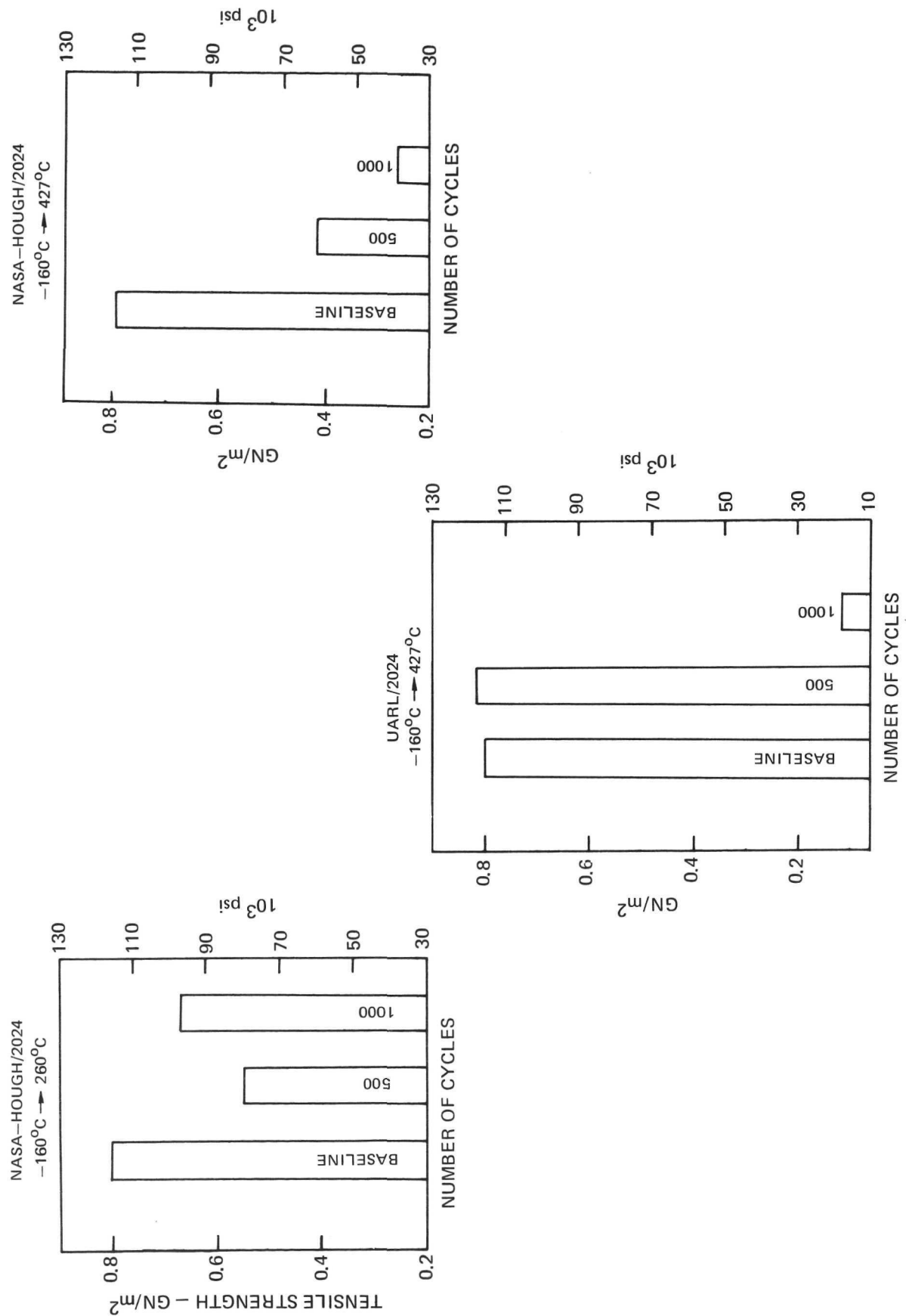
Summarizing the results of the tests it is clear that thermal fatigue is an area of concern especially between -160°C and +427°C for 1000 cycles. Under less severe temperature differentials most of the materials performed adequately

THERMAL FATIGUE
UARL/2024

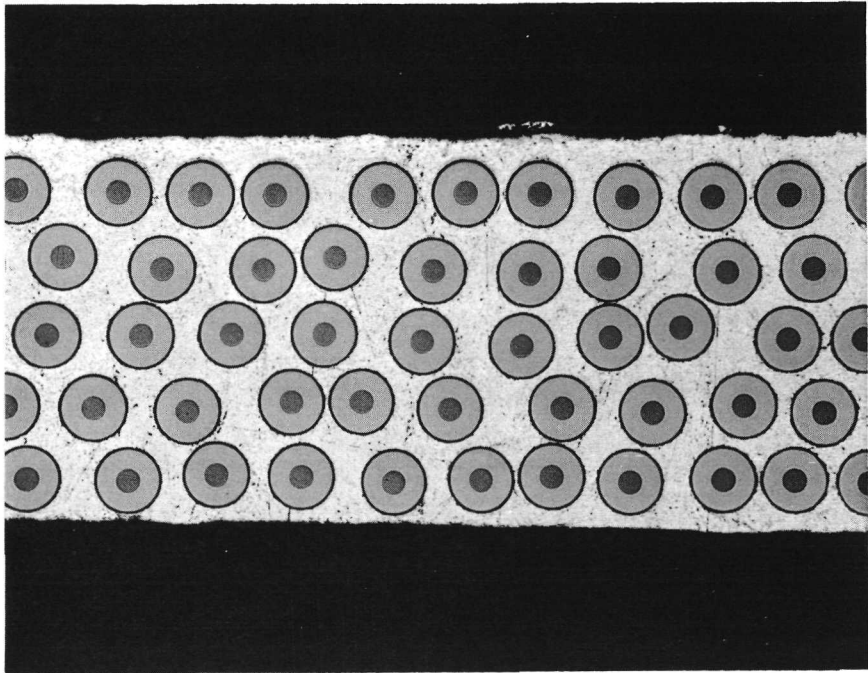
1000 CYCLES: R.T. \rightarrow 427°C
NO. 1951-2-2



THERMAL FATIGUE
CRYOGENIC TO ELEVATED TEMPERATURES



UARL/2024
COMPOSITE 1964
USED FOR THERMAL FATIGUE



although the UARL composites may have been affected to a degree. Optimum composite quality is necessary to insure resistance to thermal fatigue. Finally, the effect of filament volume fraction on composite performance appears to be minimal although higher volume fractions (>0.5) were not investigated.

5.6 Thermal Aging

5.6.1 Experimental Procedure

Thermal exposure tests were conducted at temperatures of 260°C and 427°C in a moving air environment for periods of up to 1000 hrs. Specimens were placed in an oven for the 260°C tests and a tube furnace for the 427°C tests, then removed after the desired exposure time and tested in tension at room temperature. The results were compared with base line tensile data in the same manner as with the thermal fatigue tests.

5.6.2 Results and Discussion

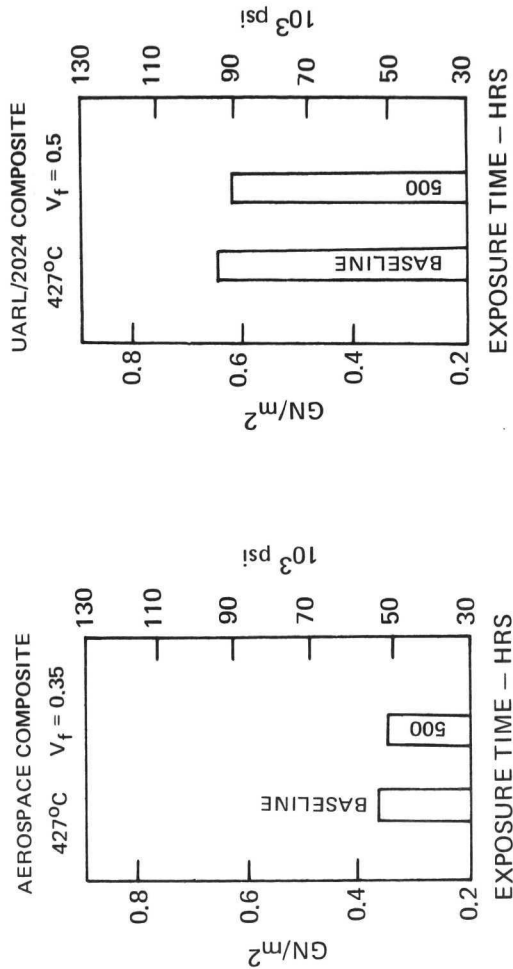
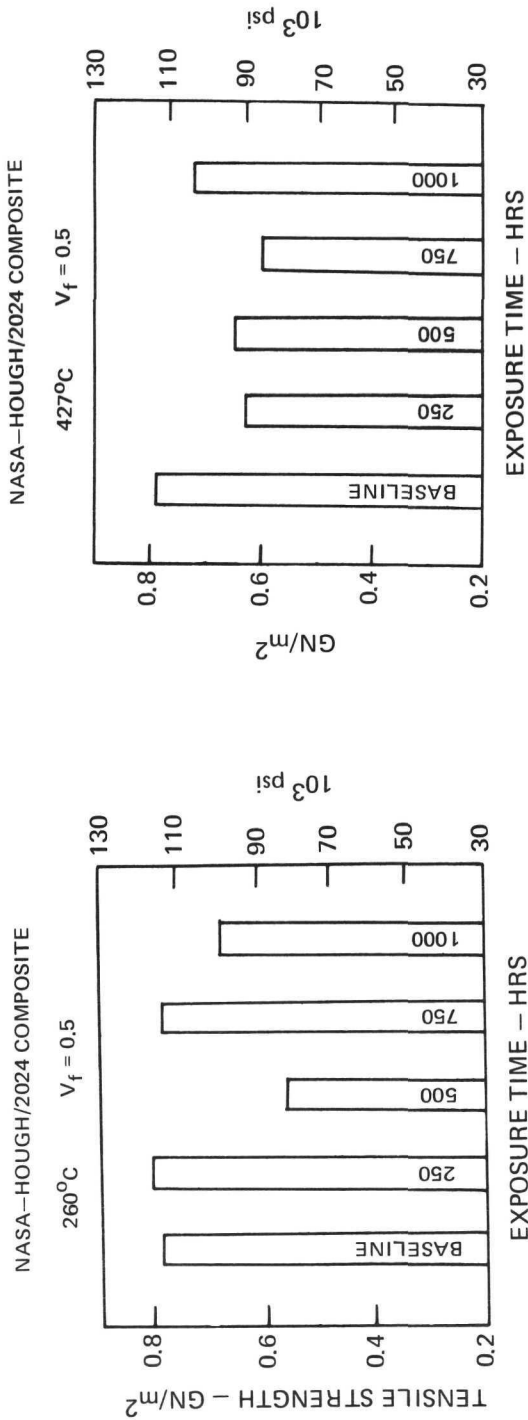
The results of thermally aging longitudinally reinforced specimens are graphically presented in Fig. 34. Two specimens were tested per condition. None of the composites was seriously affected by the exposures. The NASA-Hough materials may have lost 5-10 percent of their strength after the 427°C tests but further testing would be required to establish that definitely. The NASA-Hough specimens exposed for 500 hrs at both 260°C and 427°C were inadvertently tensile tested without aluminum doublers. This no doubt had an adverse effect on the measured strength. Figure 35 shows a cross section of a NASA-Hough composite after 1000 hrs at 427°C , and no reaction zones are evident at filament-matrix interfaces.

The same tests were performed on transversely reinforced NASA-Hough/2024 specimens and the results are shown in Fig. 36. The longer exposures at 427°C appear to have reduced the transverse tensile strength, although the base line strengths are so low that a meaningful comparison is difficult.

Similar tests have been reported on boron and BORSIC-6061 composites (Ref. 5) at a temperature of 370°C . After 1000 hrs at that temperature the room temperature longitudinal strength of boron composites dropped by 12 percent while that of BORSIC composites was unchanged. Under the same conditions the transverse tensile strength of boron composites was unchanged while the BORSIC composites suffered a 28 percent loss in strength.

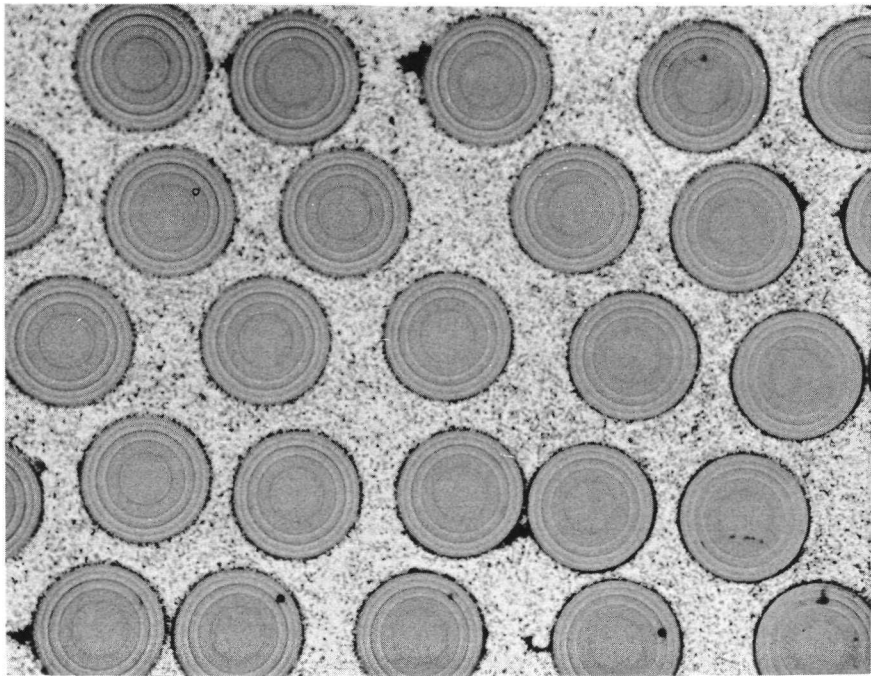
In view of those results it is felt that the NASA-Hough composites showed very good resistance to thermal aging. Had the boron-aluminum tests of Ref. 5 been conducted at 427°C as in the present study, it is quite likely that the degradation would have been more severe since the boron fiber itself suffers

THERMAL AGING
LONGITUDINAL TENSION



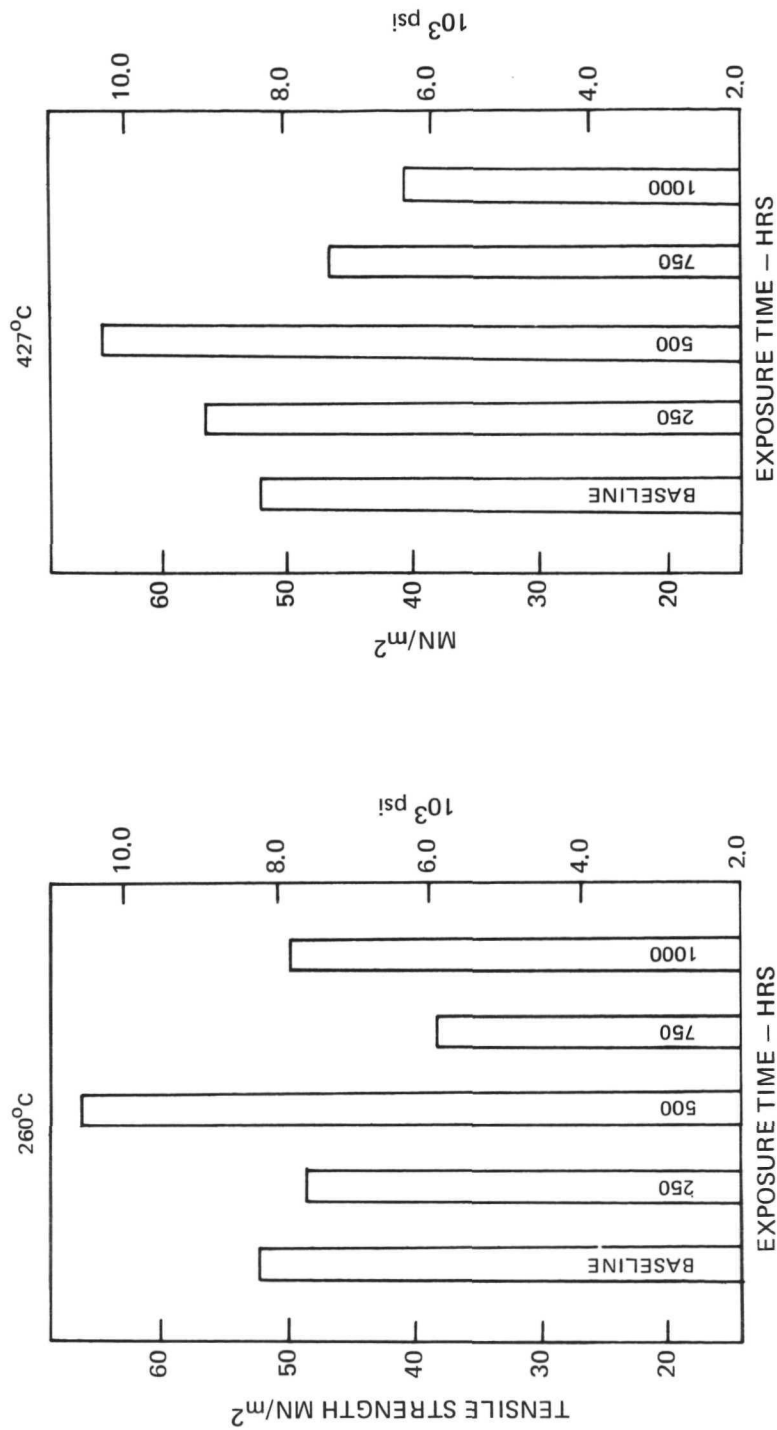
THERMAL AGING

NASA-HOUGH/2024
1000 hrs. @ 427°C



THERMAL AGING
TRANSVERSE TENSION

NASA-HOUGH/2024 COMPOSITE



strength losses at elevated temperatures (Ref. 9). Thus, the data indicate the potential of the NASA-Hough filament as a high temperature reinforcement.

5.7 Thermal Expansion

Thermal expansion tests were conducted in both the longitudinal and transverse directions on 50 v/o NASA-Hough/2024 composites. Duplicate tests were performed in both cases, and the results were identical. Figure 37 presents typical expansion data between RT and 427°C. The transverse tests were well-behaved with an average coefficient of $\alpha_T = 21 \times 10^{-6}$ cm/cm/°C. The longitudinal tests resulted in an initial high coefficient, $\alpha_{L1} = 21 \times 10^{-6}$ cm/cm/°C, up to about 120°C, then a lower coefficient in the expected range of $\alpha_{L2} = 2.1 \times 10^{-6}$ cm/cm/°C up to 427°C. The initial value may be due to relaxation of residual stress, but no thorough explanation is available.

5.8 Impact

5.8.1 Experimental Procedure

Izod impact tests were conducted on a series of NASA-Hough reinforced composites to establish base line data and to determine the effect of filament volume fraction. All specimens were "miniature" in that the thickness was reduced from that of the standard specimen. Most specimens were .19 cm (.075 in.) thick with two being .36 cm (0.143 in.). All other dimensions were standard, i.e. 6.35 cm long x 1.25 cm wide (2.5 in. x .5 in.). Notch depth was .25 cm (.1 in.). Commercial purity titanium specimens having the same thicknesses were also tested to serve as a frame of reference.

5.8.2 Results and Discussion

The data from the impact tests are summarized in Table XVI. In general, the composites fractured in two pieces under the notch and exhibited a high degree of filament pullout. Figure 38 shows a typical fracture surface just below the notch. The larger magnification shows separation between the core and the deposit which was sometimes observed. This was not observed on any static specimens.

Both specimens cut from composite 1944 behaved in a much different manner from the others. The specimens did not fracture during the test but rather twisted in the fixture when struck by the tup. Figure 39 shows one of the specimens after the impact test. This different behavior was reflected in a much higher energy being absorbed per unit area as reported in Table XVI. The reasons for the different behavior are not understood although the specimens' edges were not as flat and parallel as the others and they may have been somewhat misoriented in the fixture causing them to be struck off angle.

THERMAL EXPANSION

NASA-HOUGH CARBON/2024 ALUMINUM

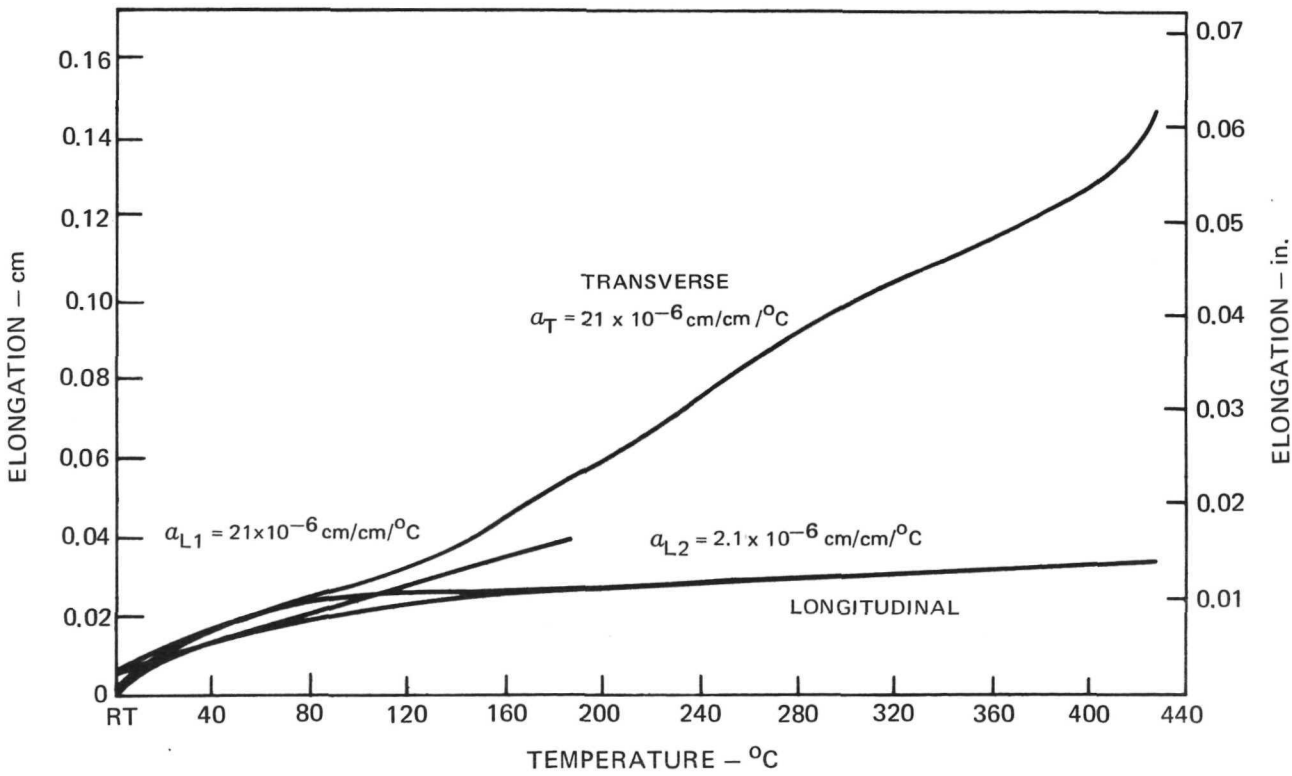


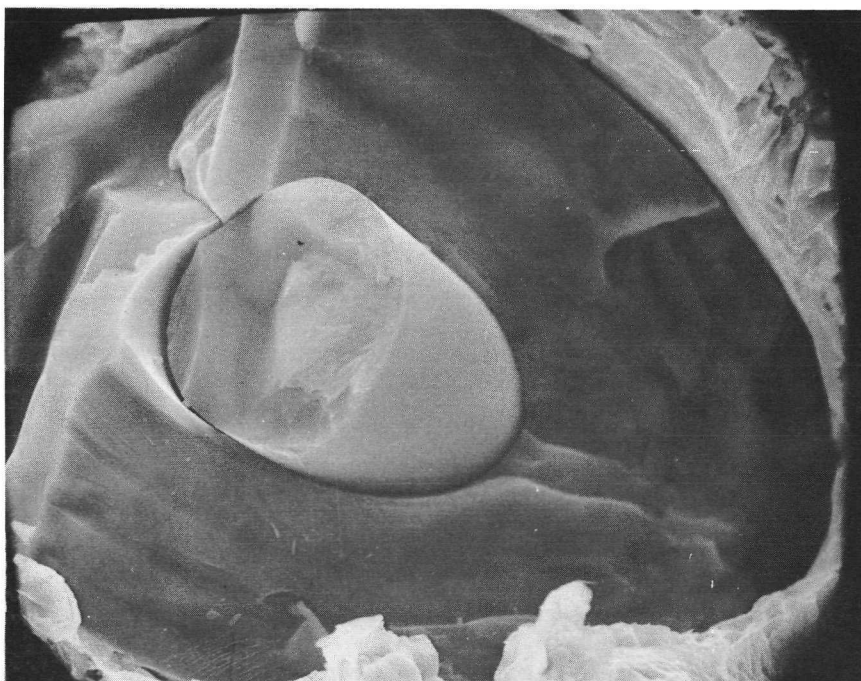
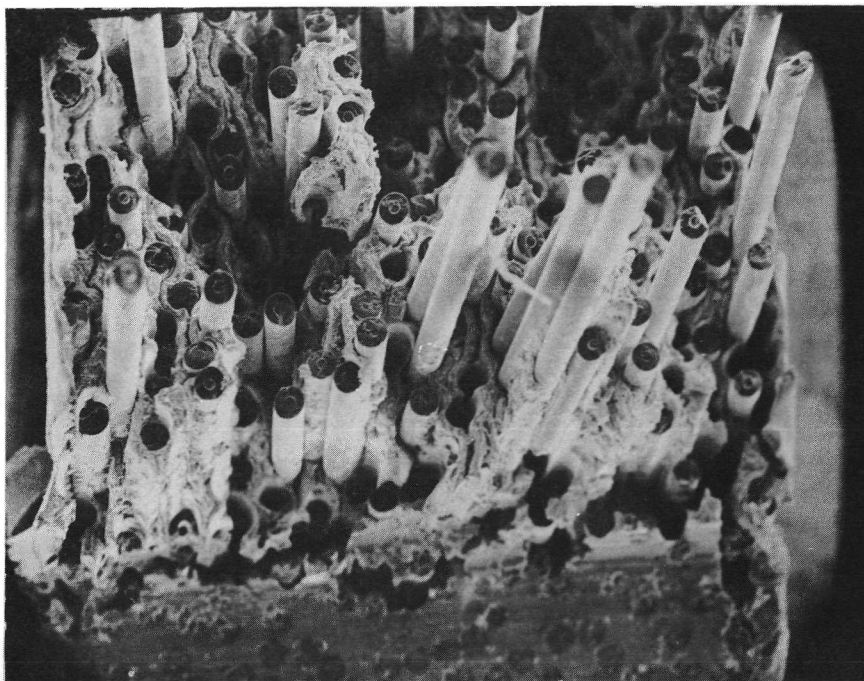
Table XVI

Izod Impact
NASA-Hough/2024

<u>Composite</u>	<u>V_f</u> <u>(%)</u>	<u>Measured Energy</u>		<u>Specimen Thickness</u>		<u>Energy per Area</u>	
		<u>joules</u>	<u>(in-lbs)</u>	<u>cm</u>	<u>(in)</u>	<u>joules/cm²</u>	<u>(in-lbs/in²)</u>
1966	55	6.4	56.9	.363	.143	17.6	995
1925-1	38	1.3	11.4	.191	.075	6.8	380
1925-2	38	1.6	14.0	.191	.075	8.3	468
1943-1	38	4.2	36.8	.188	.074	22.4	1245
1943-2	38	>2.7 ¹	>24.0	.188	.074	>14.4	>810
1944-1	54	7.1	62.8	.188	.074	37.8	2110
1944-2	54	8.8	78.0	.188	.074	46.9	2630
Titanium-1	-	10.5	102.5	.363	.143	28.9	1790
Ti-4	-	13.0	115.5	.363	.143	35.8	2010
Ti-2	-	5.5	49.2	.191	.075	28.8	1640
Ti-3	-	6.2	55.2	.191	.075	32.4	1840

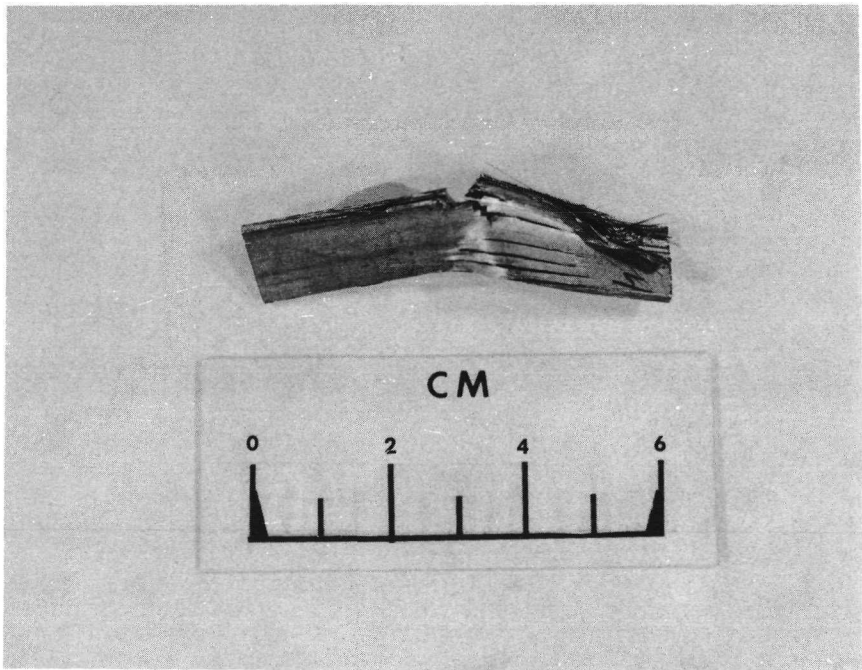
¹ Stopped impact hammer

NASA-HOUGH/2024 IZOD IMPACT SPECIMEN



IZOD IMPACT SPECIMEN

NASA-HOUGH/2024
COMPOSITE 1944
 $V_f = 0.5$



The differences in specimen thickness were judged to have no effect on the energy absorbed per unit area based on the results for the titanium samples and the findings of Ref. 5 for boron-aluminum. Therefore the data for all the specimens which fractured in the conventional manner were plotted as a function of filament volume fraction in Fig. 40. With the exception of the high value at 38 v/o, the absorbed energy is seen to increase with increasing amount of the brittle constituent (filaments). This is in agreement with the findings of Ref. 5 for aluminum matrix composites and Ref. 10 for resin matrix composites. Both literature sources found that the energy absorbed during impact could be related to composite constituent properties by the following equation:

$$\text{Energy} = \frac{V_f d_f \sigma_f^2}{24 \tau_{my}} \quad (1)$$

where V_f = filament volume fraction
 d_f = filament diameter
 σ_f = filament tensile strength
 τ_{my} = matrix shear yield strength or interfacial shear strength.

The 38 v/o composite with the high impact strength (No. 1943) did not fit the expected data trend. This composite will be discussed further in the following paragraphs.

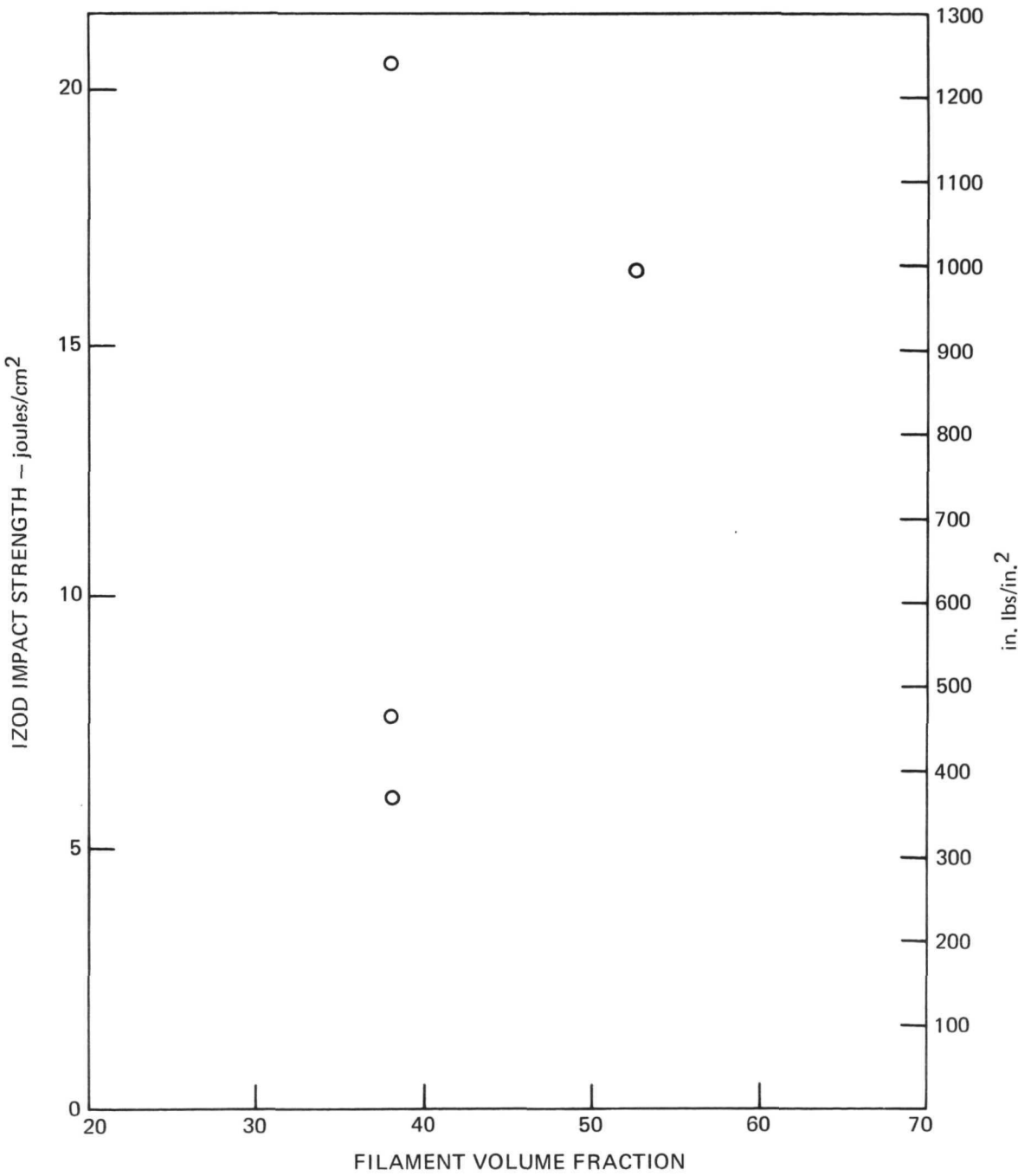
The correlation between BORSIC-aluminum composite impact strength and Eq. (1) was worked out in Ref. 5 and is shown in Fig. 41 along with the data for NASA-Hough composites 1925, 1943, and 1966. The calculations for the NASA-Hough composites were made using measured values in the numerator of Eq. (1) and a value of 31.7 MN/m² (4.6 ksi) for the interfacial shear strength. This latter value was derived by solving for τ using Eq. (1) and the measured impact energy of composite 1966. This was done rather than assuming a τ_{my} of half the matrix tensile strength as in Ref. 5 because SEM pictures of fracture surfaces showed the interface was failed in the NASA-Hough impact specimens.

Examination of Fig. 41 shows that with the exception of composite 1943, Eq. (1) correlated fairly well with the measured impact strength. Composite 1943 was intended to be high volume fraction, but the tape was wound at the wrong spacing. The result was a much more random fiber distribution than the ordered rows generally observed as shown in Fig. 42. This may have been related to the impact strength being higher than predicted, but it is not clear what role the random array would play.

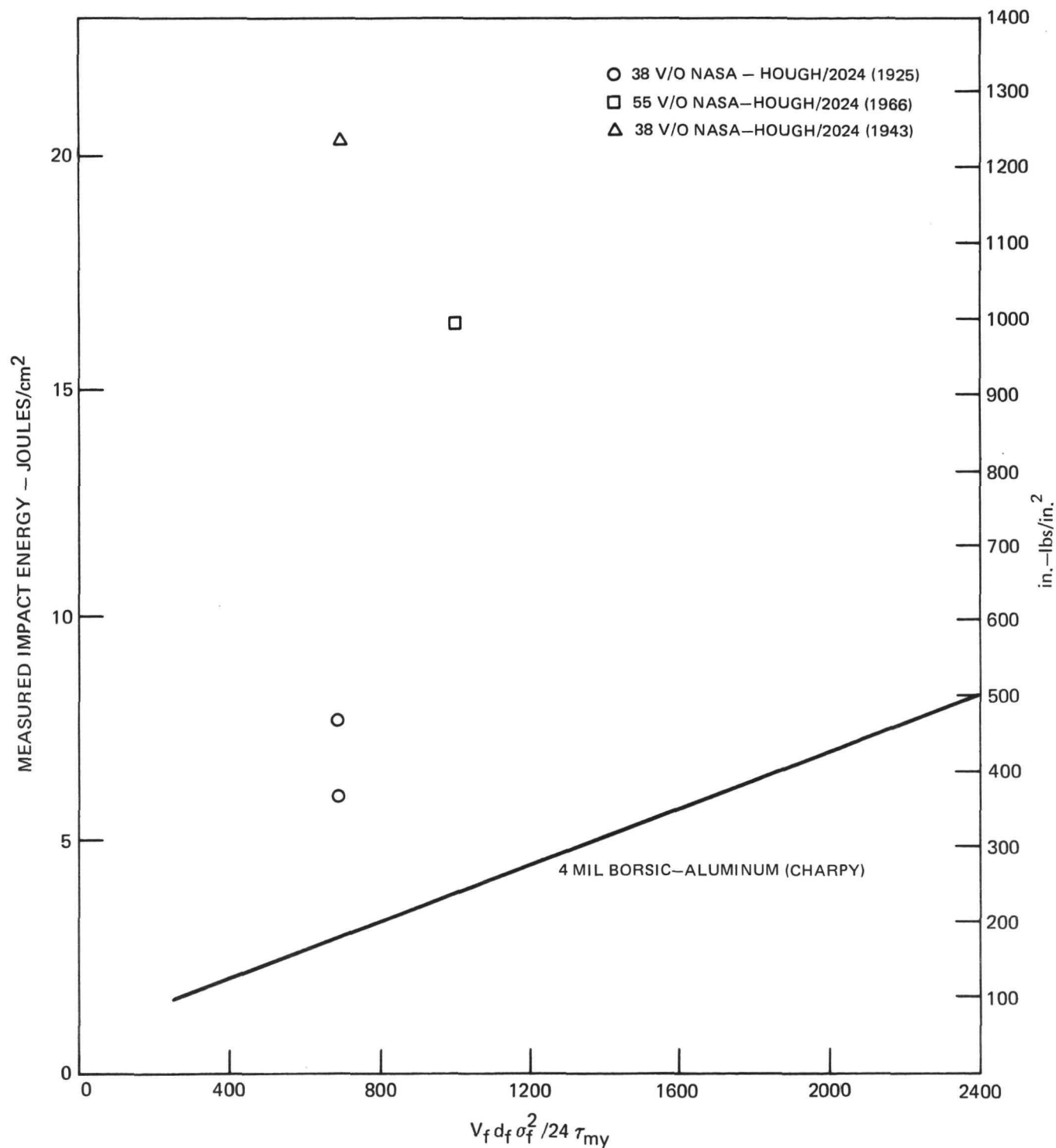
The energy per area values for NASA-Hough/2024 were much better than those of BORSIC composites, probably due to the much greater pullout lengths of the former. Unfortunately, however, the pullout mechanism only operates during fracture of the composite, and it would be more desirable to absorb energy without actually fracturing the material.

IZOD IMPACT

NASA-HOUGH CARBON/2024 ALUMINUM



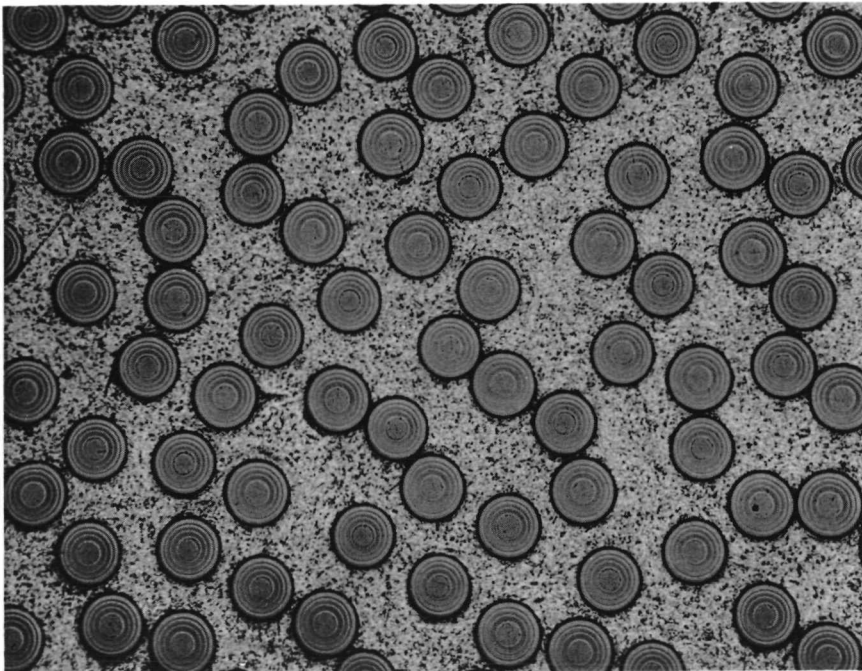
IMPACT ENERGY VS $V_f d_f \sigma_f^2 / 24 \tau_{my}$



**IZOD IMPACT
MICROSTRUCTURE OF COMPOSITE 1943**

NASA-HOUGH/2024

$V_f = 0.38$



From Eq. (1) it can be seen that there are several approaches to improving composite impact strength: increasing volume fraction, filament diameter, or filament strength, and decreasing matrix yield strength. United Aircraft Research has demonstrated that unidirectional composites of .014 cm (5.6 mil) boron of high strength in an annealed pure aluminum matrix can exhibit standard size Charpy impact strengths in excess of 28.4 joules (276 in-lbs) at a volume fraction of 50-60 percent (Ref. 11). This corresponds to an energy per area of 38 joules/cm² (2300 in-lbs/in²). In order to take advantage of the large amount of energy absorbed by the low yield strength matrix it is necessary to have a good interfacial bond so that failure does not prematurely occur at the interface before the ductile aluminum can yield. For useful filament volume fractions, the use of a compliant matrix had the largest effect of any of the variables in boron-aluminum because it could be varied over the largest range. Furthermore, invoking this mechanism does not require fracture of the composite. Rather, the yielding of the matrix results in a material which can absorb energy through plastic deformation, a much less catastrophic process. This type of behavior was observed in the boron-aluminum example cited above.

For this mechanism to be useful in carbon-aluminum it will be necessary to achieve a better interfacial strength than that obtained to date with NASA-Hough composites. The other methods of increasing impact strength, larger filaments and stronger filaments, must come through further development of the filament manufacture process.

VI. CONCLUSIONS

1. Carbon-multifilament composites, prepared by infiltrating the fiber bundle with an aluminum powder slurry then diffusion bonding, could not be fabricated without breaking fibers or inadequately consolidating the matrix. This limits the strength which can be developed in the composite.

2. Carbon-base monofilament composites were fabricated using state-of-the-art techniques. Such composites exhibit good translation of longitudinal filament properties, but composite transverse tensile properties are quite low due to a poor bond between the filaments and the aluminum matrix. Further study of the interface should be conducted in order to improve the transverse tensile strength.

3. Longitudinally reinforced NASA-Hough/2024 composites exhibit good elevated temperature capability in terms of static tensile strength, stress-rupture and creep, and thermal aging. Thermal fatigue response between room temperature and temperatures as high as 427°C was also good. Thermal cycling between -160°C and $+427^{\circ}\text{C}$ caused severe losses in composite strength.

4. Longitudinally reinforced UARL/2024 composites are similar to NASA-Hough composites in terms of strength and have a higher modulus. Elevated temperature response of the UARL composites may be somewhat poorer.

5. Impact strength of NASA-Hough composites is higher than that of state-of-the-art BORSIC composites. Further investigation should be conducted to optimize response to impact loading, however.

VII. REFERENCES

1. R. Hough, "Development of Manufacturing Process for Large Diameter Carbon-Base Monofilament by Chemical Vapor Deposition", NASA CR-72770, Nov. 1970.
2. R. Veltri, B. Jacob, "Development of Large Diameter Carbon Monofilament", NASA CR-121229 (1973).
3. R. C. Rossi, et al, "Development of Aluminum-Graphite Composites", Ceramic Bulletin, Vol. 50, No. 5 (1971).
4. W. H. Shaefer, J. L. Christian, et al, "Evaluation of the Structural Behavior of Filament Reinforced Metal Matrix Composites", Vol. III, AFML-TR-69-36, Jan. 1969.
5. K. G. Kreider, L. Dardi, K. Prewo, "Metal Matrix Composite Technology", AFML-TR-71-204, Dec. 1971.
6. D. F. Adams, et al, "Mechanical Behavior of Fiber-Reinforced Composite Materials", AFML-TR-67-96, May 1967.
7. E. M. Breinan, K. G. Kreider, "Axial Creep and Stress-Rupture of B-Al Composites", Metallurgical Transactions, Vol. 1, Jan. 1970.
8. R. C. Novak, "Torsional Fatigue Behavior of Unidirectional Resin Matrix Composites", ASTM, Third Conference on Composite Materials: Testing and Design, Mar. 1973.
9. R. Veltri, F. Galasso, Nature, Vol. 220, p 781 (1968).
10. R. C. Novak, M. DeCrescente, "Impact Behavior of Resin Matrix Composites Tested in the Fiber Direction", ASTM STP-497, Feb. 1972.
11. K. Prewo, "The Charpy Impact Energy of Boron-Aluminum", J. Comp. Mat'ls, Vol. 6, Oct. 1972.